REDUCTION OF MAGNESIUM CONTAMINATION IN ZINC CONCENTRATES FROM THE PINE POINT PRODUCING AREA, PINE POINT, N.W.T..

by Gregg S. Hill

A thesis submitted to the Faculty of Graduate Studies and Research
in partial fulfilment of the requirements
for the degree of Master of Science

Department of Mining and Metallurgical Engineering
McGill University
Montreal, Canada

ABSTRACT

High levels of magnesium (dolomite) contamination are periodically experienced in the zinc cleaning circuit of the Pine Point concentrator. In this project the response of Pine Point lead-zinc ore to flotation and sulphuric acid leaching is examined. A textural study is conducted upon a sample of rod mill feed in order to identify mineralogical textures which may contribute to variations in metallurgical performance.

It is found that Pine Point dolomite exhibits a negligible amount of entrainment and no detectable flotation response in simulated zinc cleaning circuits; however, intricate associations between dolomite and sphalerite cause locking down to particle sizes of approximately 15-25μm. It is estimated that the occurrence of variable amounts of intricate textures in Pine Point mill feeds could contribute to variations of approximately 0.1% in magnesium levels in the zinc concentrate.

RÉSUMÉ

Des niveaux élevés de contamination au magnésium (dolomite) sont périodiquement observés dans le circuit de nettoyage du zinc du concentrateur de Pine Point. Ce projet a consisté à étudier le comportement du minerai de zinc et plomb à la flotation et à la lixiviation à l'acide sulphurique. On a étudié la texture d'un échantillon de l'alimentation au broyeur à tiges afin d'identifier les textures minéralogiques pouvant favoriser les variations du rendement métallurgique.

On a constaté que la quantite de dolomite récupérée par entraînement hydraulique ou vraie flotation est négligeable en simulant plusieurs circuits de nettoyage en laboratoire. Toutefois, des associations complexes entre la dolomite et la sphalérite produisent des particules mixtes jusqu'a une finesse de 15µm a 25µm. On a estimé que la présence de ces textures complexes en quantités variables pourrait produire des variations d'environ 0.1% en magnésium dans la concentré de zinc.

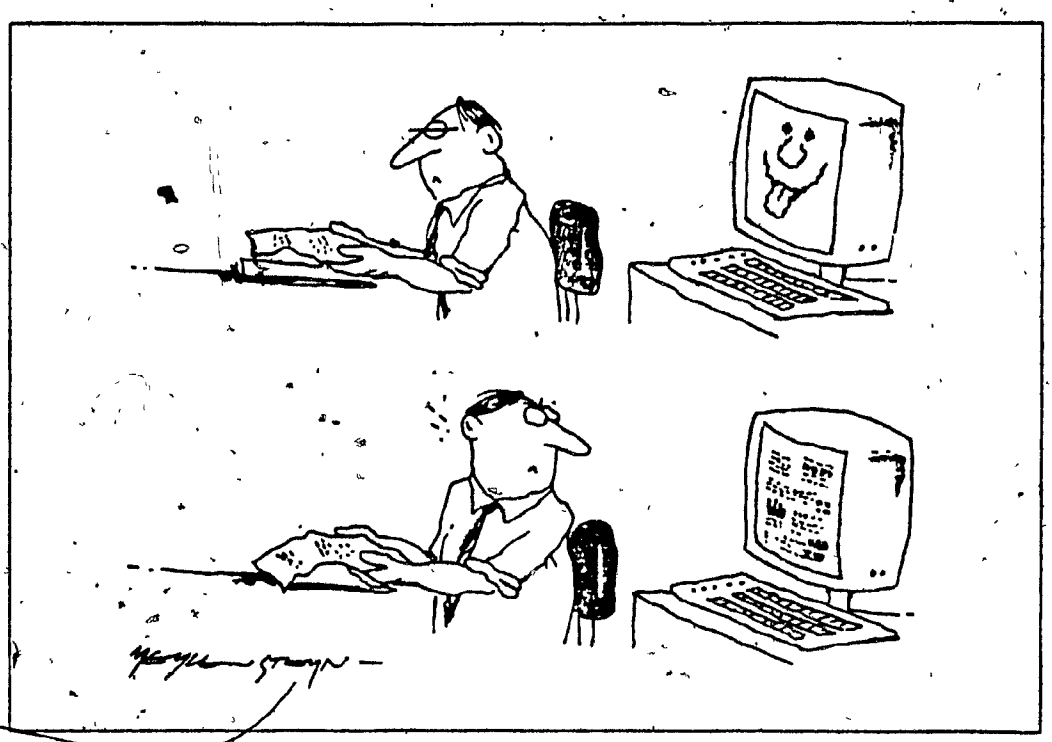

To Mom, who was with me
when I collected my first rock

ACKNOWLEDGEMENTS

It has been my privilege to work among people who not only are knowledgeable in their respective fields, but who also enjoy their work and the company of their colleagues. For this reason the past two years have been happy and memorable ones which shall undoubtedly rank among the best years of my life. I extend my deepest thanks and appreciation to all of my friends and co-workers who, in their various ways, have always made themselves available to teach me and to support me along the way.

To Neil Rowlands, for his friendship and his guidance. His door has always been open for me, both in the office and at home. Thanks for everything, Neil.

To Jim Finch, who has always made time for me, given me the benefit of his expertise and shown genuine interest in this research. Thanks, Jim.

To Michel Leroux and Glenn Dobby, who tolerated my pestering and countless questions when I first entered the department and did not know how anything worked. I couldn't have done it without you.

To Andre Laplante, who has always been around to discuss problems, suggest readings and keep an eye on my inlaws. Thanks, Andre.

To Ross, my brother, who did the locked cycle lab work with me.

To Helene, my wife, who never complained (well, not very much, anyway) when I worked too late.

To Mom, Dad, Ross and Lesley who were always there. I love you all!

The author greatly appreciates the efforts of the personnel at Pine Point Mines Ltd. who collected and shipped the ore and concentrate samples used in this research.

The author would like to acknowledge the Natural Science and Engineering Research Council (NSERC) and Les Fonds FCAC pour L'Aide et le Soutien à la Recherche, both of which provided funding for this research.

TABLE OF CONTENTS

PAGE

ABSTRACT i

ACKNOWLEDGEMENTS ii

TABLE OF CONTENTS iii

LIST OF ILLUSTRATIONS vi

LIST OF TABULATIONS ix

CHAPTER 1: INTRODUCTION

1.1 Pine Point Location and History 1
1.2 Purity Standards for Zinc Concentrates 3
1.3 Magnesium Levels in Pine Point Zinc Concentrates 5
1.4 Research Objectives 10
1.5 Development of the Pine Point Flowsheet 11
1.6 Description of the Pine Point Leach Plant . . . 16

CHAPTER 2: GEOLOGY OF THE PINE POINT AREA

2.1 Tectonic History of the Pine Point Area . . . 22
2.2 The Emplacement of Pine Point Sulphides . . . 28
2.3 Classification of the Pine Point Ore Bodies . 31
2.4 Emplacement of the Pine Point Ore Deposits . . 32

CHAPTER 3: LOCKED CYCLE FLOTATION OF PINE POINT ORE

3.0 Introduction 41
3.1 Materials and Equipment 42
3.2 Definition and Principles of Locked Cycle Flotation 45
3.3 Setting Up the Locked Cycle Test 49
3.4 Design of an Experimental Circuit 51
3.5 Incremental Flotation Tests 54
3.6 Application of the Agar Predictive Model . . . 63
3.7 Evaluation of Sources of Error in Locked Cycle Testing 68
3.8 Verification of Equilibrium and Test of the Agar Model 76
3.9 Analysis of Locked Cycle Flotation Performance 92
3.10 Effects of the Acid Leach upon Calculations . . 94

PAGE

3.11 Performance of the Rougher 98
3.12 Performance of the Scavenger 104
3.13 Performance of the First Cleaner 109
3.14 Performance of the Second Cleaner 115
3.15 Performance of the Third (Post-leach) Cleaner 122
3.16 Summary of the Locked Cycle Flotation Test . . 129
3.17 The Effects of Leaching upon Subsequent Flotation 136
3.18 Discussion 138

CHAPTER 4: RECOVERY OF CARBONATES BY FLOTATION AND BY ENTRAINMENT

4.0 Introduction 142
4.1 Recovery of Gangue Material in the Presence of Xanthates 142
4.2 Summary of Gangue Flotation 147

CHAPTER 5: LIBERATION OF FINE POINT ORE DURING GRINDING

5.0 Introduction: Goals of Comminution and Choice of Grind Sizes 148
5.1 Textural Characteristics of Fine Point Ore and Ore Mineral Distribution in the Rod Mill Feed 150
5.2 Liberation in a Sample of Fine Point Leach Plant Feed (Second Cleaner Concentrate) . . . 177
5.3 A Model for the Sectioning of Locked Particles 188
5.4 Summary of the Liberation and Textural Study . . 206

CHAPTER 6: LEACHING OF FINE POINT CONCENTRATES

6.0 Introduction 208
6.1 Leaching at Various Pulp Densities 208
6.2 Leaching Tests of Variable Duration 217
6.3 Production of Calcium Sulphate during Leaching 216
6.4 The Path of Dissolved Magnesium through the Processing Circuit 220
6.5 Summary of Acid Leaching 223

PAGE

CHAPTER 7: DISCUSSION, CONCLUSIONS AND RECOMMENDATIONS

7.1 Discussion 224
7.2 Conclusions 228
7.3 Recommendations for Further Work 233

APPENDICES

APPENDIX 1 : PROCEDURES

A1.1 Flotation Procedure 235
A1.2 Special Procedures for Locked Cycle Test . . . 236
A1.3 Analytical Procedures 237

APPENDIX 2 : CALCULATION OF MAXIMUM MAGNESIUM REMOVAL IN ACID LEACH 238

APPENDIX 3 : PROGRAM LISTING FOR PARTICLE SECTIONING MODEL 244

REFERENCES 253

LIST OF ILLUSTRATIONS

PAGE

CHAPTER 1

1.1 Location of Pine Point 2
1.2 Pine Point Flotation Circuit, 1965-1980 14
1.3 Pine Point Flotation Circuit, Post-1980 15
1.4 Residence Time in the Pine Point Leach Plant . . . 17
1.5 Leach Plant Schematic 18

CHAPTER 2

2.1 Extent of Devonian Marine Transgression 23
2.2a Initial Stages of Barrier Buildup 25
2.2b Development of the South Hinge 26
2.2c Subsidence and Development of the North Hinge . . . 27
2.2d Pine Point Area at Present 27
2.3 Cycle of Mineralization at Pine Point 33
2.4 Botryoidal Sphalerite 35
2.5 Banded Sphalerite Lining a Vug 35
2.6 Skeletal Grain of Galena in Sphalerite 37
2.7 Galena Crystals Cross-cutting Banding in Sphalerite 37
2.8 Fracture-filling Galena in Sphalerite 37
2.9 Cycle of Mineralization at West Hayden and Edgerton Ore Bodies 39

CHAPTER 3

3.1 Leeds Flotation Cell 44
3.2 Experimental Circuit for Locked Cycle Test 53
3.3 Rougher: Incremental Zinc Grade vs. Time 61
3.4 Scavenger: Incremental Zinc Grade vs. Time 61
3.5 Cleaner 1: Incremental Zinc Grade vs. Time 61
3.6 Cleaner 2: Incremental Zinc Grade vs. Time 62
3.7 Cleaner 3: Incremental Zinc Grade vs. Time 62
3.8 Real vs. Predicted Mass in Final Concentrate . . . 80
3.9 Real vs. Predicted Mass in Final Tailings 80
3.10 Real vs. Model Recovery of Mass in Concentrate . . 82
3.11 Real vs. Model Recovery of Mass in Tailings . . . 82
3.12 Real vs. Model Zinc Flow in Concentrate 86
3.13 Real vs. Model Zinc Flow in Tailings 86
3.14 Flow of -400 and +400 Mesh Zinc Units into Tailings 88
3.15 Recalculated Zinc Grade of Material Leaving System 88

		PAGE
3.16	Rougher Recoveries	99
3.17	Rougher: % Gangue Rejection per % Zinc Rejection	101
3.18	Zinc and Magnesium Distribution in Rougher Conc.	101
3.19	Zinc and Magnesium Distribution in Rougher Tailings	101
3.20	Scavenger Recoveries	106
3.21	Scavenger: % Gangue Rejection per % Zinc Rejection	108
3.22	Zinc and Magnesium Distribution in Scavenger Concentrate	108
3.23	Zinc and Magnesium Distribution in Scavenger (Final) Tailings	108
3.24	Cleaner 1 Recoveries	110
3.25	Cleaner 1: % Gangue Rejection per % Zinc Rejection	112
3.26	Zinc and Magnesium Distribution in Cleaner 1 Conc.	112
3.27	Zinc and Magnesium Distribution in Cleaner 1 Tails	112
3.28	Cleaner 2 Recoveries	116
3.29	Cleaner 2: % Gangue Rejection per % Zinc Rejection	118
3.30	Zinc and Magnesium Distribution in Cleaner 2 Conc.	118
3.31	Zinc and Magnesium Distribution in Cleaner 2 Tails	118
3.32	Cleaner 3 Recoveries	123
3.33	Cleaner 3: % Gangue Rejection per % Zinc Rejection	125
3.34	Zinc and Magnesium Distribution in Cleaner 3 Conc.	125
3.35	Zinc and Magnesium Distribution in Cleaner 3 Tails	125
3.36	Flow of +200 Mesh Zinc through Circuit	130
3.37	Flow of −200 Mesh / + 15um Zinc through Circuit	130
3.38	Flow of −15um Zinc through Circuit	130
3.39	Flow of +200 Mesh Magnesium through Circuit	131
3.40	Flow of −200 mesh / +15um Magnesium through Circuit	131
3.41	Flow of −15um Magnesium through Circuit	131

CHAPTER 4

4.1	Recovery of Water and Solids vs. Time	143
4.2	Recovery of Solids vs. Water	143
4.3	Recovery of Gangue and Silica	145

CHAPTER 5

5.1	Polished Section of Colloform Ore	154
5.2	Sphalerite Botryoid Nucleating around Galena	154
5.3	Dendritic Galena in Sphalerite (Colloform Ore)	155
5.4	Secondary Alteration in Colloform Ore	157
5.5	Secondary Alteration in Colloform Ore (×-polar)	157
5.6	Carbonate Replacement Textures in Colloform Ore	159
5.7	Secondary Electron Image (SEI) of Replacement	

PAGE

5.8 Zinc K-Alpha Emissions from Area of Fig. 5.7 . . . 162
5.9 Calcium K-Alpha Emissions from Area of Fig. 5.7 . 163
5.10 Polished Section of Disseminated Ore 165
5.11 Void-filling Variety of Disseminated Ore 166
5.12 Co-precipitated Variety of Disseminated Ore . . . 166
5.13 Polished Section of Blocky Ore 169
5.14 Micritic Variety of Dolomite Gangue 171
5.15 Sucrosic Variety of Dolomite Gangue 171
5.16 Sparry Variety of Dolomite Gangue 172
5.17 Simple Type of Locked Particle . . . . . .
5.18 Complex Type of Locked Particle 179
5.19 Abundance of Simple Locked Particles of Various Compositions 183
5.20 Abundance of Complex Locked Particles of Various Compositions 183
5.21 Type of Locking vs. Estimated Magnesium Contribution 187
5.22 Vertical Section through Locked Particle 191
5.23 Vertical Section Showing Rotated Plane of Intersection 191
5.24 Simulated Surface of Sectioned Particle 193
5.25 Amount of Free Sections Produced by Particles of Various Compositions 199
5.26 Amount of Free Gangue Observed when Free Ore is not Counted 199
5.27 Distribution of Sections Produced by Particles of Various Compositions 202
5.28 Distribution of Sections Produced by Even Distribution of Particle Compositions 203
5.29 Distribution of Sections Produced by Skewed Distribution of Particle Compositions 203

CHAPTER 6

6.1 Leaching of Fine Point Zinc Concentrates at Various Pulp Densities 210
6.2 Leaching of Fine Point Zinc Concentrates for Various Times 215
6.3 Composition of Leach Precipitate as a Function of Time 217
6.4 Mass Loss in Leach as a Function of Time 219

LIST OF TABULATIONS

PAGE

CHAPTER 1

1.1 Production Data for First Ten Years of Concentrator Operation 6

CHAPTER 3

3.1 First Incremental Rougher Flotation 57
3.2 Second Incremental Rougher Flotation 57
3.3 Third Incremental Rougher Flotation 58
3.4 Incremental Scavenger Flotation 58
3.5 Incremental Cleaner 1 Flotation 59
3.6 Incremental Cleaner 2 Flotation 59
3.7 Incremental Cleaner 3 Flotation 60
3.8 Summary of Optimum Flotation Times 60
3.9 Comparison Between Agar Predictive Model and Locked Cycle Data 66
3.10 Summary of Incremental Flotation Results 70
3.11 Split Factors for Zinc and for Mass with Standard Deviations 70
3.12 Predicted Zinc Flow through Circuit 72
3.13 Predicted Mass Flow through Circuit 72
3.14 Standard Deviation of Zinc Flow due to Experimental (External) Error 73
3.15 Standard Deviation of Mass Flow due to Experimental (External) Error 73
3.16 Zinc Assays Predicted by Model 75
3.17 Mass Recovery in Locked Cycle Test 78
3.18 Adjusted Mass Recovery vs. Model Predictions . . . 78
3.19 Zinc Assays and Calculated Zinc Flow 85
3.20 Assay Data for Rougher Flotation 99
3.21 Calculations for Rougher 100
3.22 Assay Data for Scavenger Flotation 106
3.23 Calculations for Scavenger 107
3.24 Assay Data for First Cleaner Flotation 110
3.25 Calculations for First Cleaner 111
3.26 Assay Data for Second Cleaner Flotation 116
3.27 Calculations for Second Cleaner 117
3.28 Assay Data for Third Cleaner Flotation 123
3.29 Calculations for Third Cleaner

PAGE

CHAPTER 4

4.1 Recoveries of Solids and Water during Flotation . 143
4.2 Recoveries of Solids and Water during Flotation (previous work) 146

CHAPTER 5

5.1 Assay Data for Second Cleaner Concentrate 177
5.2 Liberation of -64#/+100# Particles 181
5.3 Liberation of -100#/+150# Particles 181
5.4 Liberation of -150#/+200# Particles 182
5.5 Liberation of -200#/+270# Particles 182
5.6 Contribution of Simple and Complex Locked Particles to Magnesium Contamination 187
5.7 Matrix Produced by Simulation Program 196
5.8 Abridged Matrix from Simulation 205
5.9 Inverse of Abridged Matrix 205
5.10 Recalculated Particle Assemblage 205

CHAPTER 6

6.1 Acid Leaching at Various Pulp Densities 211
6.2 Effect of Time upon Acid Leaching 214

APPENDIX 2

A2.1 Maximum Amount of Magnesium in Pre-Leach Cleaner 2 Concentrate 239
A2.2 Magnesium Levels in Cleaner Concentrates 242
A2.3 Effects of the Leach upon Recalculated Recoveries and Separation Efficiencies 242

CHAPTER 1

INTRODUCTION

CHAPTER 1: INTRODUCTION.

1.1 Pine Point Location and History

The Pine Point mining district is situated on the south shore of Great Slave Lake, N.W.T. at latitude 61°40'N, longitude 114°30'W (Figure 1.1). The district is 960 km almost due North of Edmonton, the nearest large city, and 80 km east of the Great Slave Lake railway terminus at Hay River. The region contains over 40 individual ore bodies in various stages of development with estimated tonnages ranging from a few hundred thousand to over 15 million tonnes. Average grades are approximately 7% zinc and 2% lead.

Exposed lead and zinc deposits were first staked in 1898; however, the area was explored only intermittently for the next 50 years. In 1948 Cominco Ltd. initiated a major exploration program which, by 1955, had delineated a large mineralized belt. The area was developed over the years 1963-1964 and mine production commenced late in 1964. The early development of the Pine Point properties is summarized by Baranger (1964) and by Campbell (1966, 1967).

From 1964 to 1968 over a million tons of direct-shipping ore were produced at grades of 18.0% to 22.5% lead and 25.0% to 29.1% zinc. The concentrator commenced production in November of 1965 at a designed throughput of 5000 STPD and by the end of 1968 a total of over 5 million tons of ore were produced at average head grades of 4.3% lead and 8.5% zinc. In 1968 Cominco Ltd. acquired mining rights to a large ore body located to the east of the Pine Point claims and the

FIG. 1.1.

PINE POINT LOCATION AND REGIONAL GEOLOGY

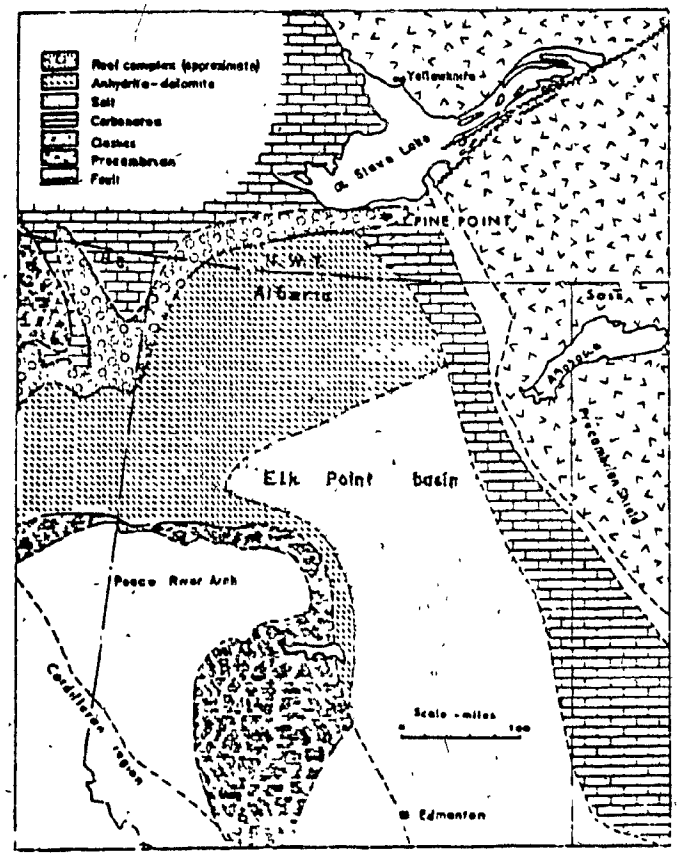

(from CAMPBELL 1967)

concentrator was expanded to 8000 STPD throughput. Current milling capacity is over 11,000 STPD.

The Pine Point district has developed into one of the richest producing areas of the world. By the end of 1981 over 54 million tons of ore had been produced at an average grade of 10.9% zinc and 2.5% lead, and exploration is still active in the area. Production and reserves data are taken from Jackson and Folinsbee (1969), Cormode (1977) and the Canadian Mines Handbook (1982/83).

1.2 Purity Standards for Zinc Concentrates

The refinery specifications for zinc concentrates depend highly upon the refining process being used. Until the early 1960's horizontal zinc retorting was the standard method of refining zinc. In this process zinc concentrates were roasted, mixed with carbon (coal or coke), placed in a clay retort and heated to approximately 1150°C in a gas-fired furnace to produce zinc oxide. The zinc oxide reacted with carbon to produce carbon monoxide and zinc vapour, which was precipitated into condensers at the open end of the retort. Impurities were collected into a slag which was periodically bled out of the retort.

The principal advantage of retorting was its ability to accept high levels of impurities in the incoming concentrates. However, it was clear by the early 1960's that horizontal retorting could not compete with roast-leach-electrowinning of

zinc. Labour and fuel costs were excessive and metal purity was sometimes unacceptable. The last remaining zinc retort furnace was retired in 1976 in Bartlesville, Oklahoma. The history and eventual obsolescence of zinc retorting are summarized by Dutrizac (1983).

Roast-leach-electrowinning is now the standard process used to refine zinc concentrates. Concentrates are roasted to form zinc oxide and zinc ferrites which are then dissolved in a two-stage sulphuric acid leach to form zinc sulphate. The sulphate is electrolytically refined using a zinc cathode, upon which the zinc in solution is electroplated. Sulphates of contaminating metals do not plate out; rather, they concentrate in the electrolyte up to their saturation points and subsequently precipitate out as a sludge which can be removed by filtration.

In zinc concentrates from dolomitic ores such as Pine Point the principal contaminants in the concentrate are calcium and magnesium. Calcium poses little problem, since its solubility in the electrolyte is only about 2 grams per litre; however, magnesium sulphate, with a solubility of about 350 grams per litre, does not readily precipitate out from the electrolyte. The consequent magnesium buildup causes the following problems (Gorman and Nenninger, 1976):

1) Increase of the specific gravity of the electrolyte, which causes poorer settling and filtration.
2) Reduced electrical current efficiency in the cells

due to resistive heating.

3) Environmental problems in treating or disposing of the purged electrolyte.

Thus, the changeover from retorting to roast-leach-electrowinning which occurred in the 1960's and early 1970's has resulted in an increase in the purity requirements for zinc concentrates. Depending upon the specific operation, tolerable magnesium levels in zinc concentrates may range from 0.10 to 0.25 mass percent. Penalties are levied against concentrates up to about 0.40% magnesium, and concentrates with Mg levels above 0.40 mass percent are essentially unsaleable. These requirements are much stricter than the requirements of retorting operations which would accept up to 0.40 to 0.50 mass percent magnesium without penalty.

1.3 Magnesium Levels in Pine Point Zinc Concentrates

The major constituents of Pine Point ore include the ore minerals galena (PbS) sphalerite (ZnS) and the non-ore mineral pyrite (FeS_2), hosted in dolomite ($CaMg(CO_3)_2$) and calcite ($CaCO_3$). The presence of large amounts of carbonate in the ore is advantageous in one respect due to the high acid-neutralizing potential of the waste rock and mill tailings; however, the abundance of magnesium in the ore presents considerable milling problems, particularly during zinc beneficiation.

A typical sample of Pine Point mill feed contains 8-11%

magnesium and 5-10% zinc. It is readily calculated that in order to meet the 0.10% Mg requirement over 99.9% of the magnesium must be rejected. Moreover, this feat must be accomplished without bringing the zinc recovery below about 90-95%. It is not surprising, therefore, that the benefication of zinc at Pine Point is a technologically complex process which requires precise control and great efficiency.

Table 1.1 presents production data for the first ten years of concentrator operation. Data on magnesium levels in the zinc concentrate was collected only for 1972 and 1976; however, data on total carbonate (dolomite and calcite) contamination can be used to obtain an estimate of magnesium contamination in the concentrate, assuming a dolomite:calcite ratio of about 4 to 1.

TABLE 1.1: PRODUCTION DATA FOR FIRST TEN YEARS OF CONCENTRATOR OPERATION

YEAR	TONS MILLED X 10^6	TONS ZN CON X 10^5	% CARBONATE GANGUE	%MG (ESTIMATED)	%ZINC RECOVERY
1966	1.46	2.41	2.54	(0.23)	92.70
1967	1.52	2.33	2.84	(0.26)	94.10
1968 *	2.14	2.23	3.24	(0.29)	93.70
1969	3.60	4.31	3.06	(0.28)	92.20
1970	3.86	4.51	4.42	(0.40)	92.10
1971	3.89	4.17	4.98	(0.45)	92.90
1972	3.81	3.91	4.69	0.45	92.00
1973 **	3.90	3.71	3.35	(0.30)	91.70
1974	4.14	3.57	3.86	(0.35)	92.80
1975	3.90	3.03	3.50	(0.32)	92.20
1976	3.77	3.26	2.87	0.22	93.50

* MILL UPGRADED BY ADDITION OF THE SPHYNX (X) CIRCUIT
** IMPLEMENTATION OF PROGRAM TO CONTROL MG CONTAMINATION

(from CORMODE, 1977)

During the initial years of production zinc head grades were high and magnesium levels in the concentrate were acceptable (1966 estimate approximately 0.2?%) though close to the acceptable limit. Over subsequent years head grades fell and dolomite rejection did not increase. The net result of this situation was a continuous rise in magnesium levels in the zinc concentrate to the point at which the concentrates produced were virtually unsaleable. The year 197? marked the beginning of an intensive effort to reduce magnesium contamination in the concentrate. Various measures were implemented including the following:

1) Careful ore blending to provide more constant head grades to the zinc circuit and a closer control of reagent levels.
2) Installation of two additional cleaners in the zinc flotation circuit.
3) Construction of a sulphuric acid leach circuit to treat part of the concentrate.

The dolomite rejection program experienced mixed success. Between 197? and 1976 magnesium contamination was reduced from the 1972 level of 0.45% Mg to a much better (but still only barely acceptable) level of 0.22% Mg. Ores which were difficult to treat were routed to the acid leach circuit for further Mg reduction. The leach plant was also used to build up stockpiles of high-purity concentrates for offshore sales.

One of the principal problems experienced at Pine Point after 1973 was the high cost of operating and maintaining the zinc circuit. At this point in time the zinc circuit contained a total of 244 small flotation cells in 15 banks with individual cell volumes ranging from 40 to 200 cubic feet. The leach plant, unlike the flotation circuit, was easy to maintain and operate; however, acid consumption was very high (between 45 and 55 kg. of 93% H_2SO_4 per tonne of concentrate treated) and reagent costs were excessive.

The next major renovation of the zinc circuit occurred in 1979-1980, at which time many of the small-volume cells were replaced by 1300 cubic foot units and the leach plant was changed from an auxiliary operation into a part of the regular processing stream. Zinc concentrate grades and recoveries both rose and acid addition to the leach was cut back to approximately 22 to 27 kg. per tonne of concentrate treated.

The development of the Pine Point zinc circuit is summarized by Cormode (1977) and by Jones (1982). Additional information was provided by K. Tietz of Pine Point Mines Ltd..

Magnesium contamination of the zinc concentrate continues to be a problem at Pine Point. Several aspects of the problem can be noted:

1) Magnesium levels are not constant; rather, they tend to rise in ores from specific "difficult" pits.
2) Magnesium contamination is not caused solely by low head grades or by high levels of magnesium in the

feed. High-grade ores often prove to be more difficult to treat than low-grade ores.

3) At the present time almost all of the ore must be treated in the leach plant, even though the zinc circuit contains what would normally be considered as a large amount of cleaning flotation capacity.

4) The zinc cleaning and leach stages of the zinc circuit seem to be working rather inefficiently with respect to magnesium, despite close control by the Pine Point operators and much plant research over the past fifteen years. At times it is difficult to meet smelter requirements even with the acid leach in the circuit. The precise factors which are responsible for the occurrence of "difficult" ores are still not known.

5) The leach plant is very expensive to operate. Acid consumption can cost up to 6% of the value of the concentrate treated and additional costs are incurred due to difficulties in disposing of leach plant effluents. Moreover, the acid plant must be periodically shut down due to high H_2S emissions caused by the partial dissolution of sulphides.

The problem of magnesium contamination in zinc concentrates from dolomite-hosted ore bodies is not specific to Pine Point. Problems similar to those at Pine Point have been encountered in some Tennessee operations (Gorman, Pagel

and Nenninger, 1976), at Cominco Ltd.'s Magmont operation in Missouri (Schweitzer, 1983), and at Cominco Ltd's Polaris operation in the Northwest Territories (J. Finch, personal communication).

1.4 Research Objectives

The previous discussion has established that Pine Point experiences difficulties in reducing magnesium levels to tolerable levels. It was also indicated that the problem at Pine Point is a general problem associated with many dolomite-hosted zinc deposits in Canada and the United States. The amount of time, resources and personnel invested by various operations in an attempt to solve the "dolomite problem" is not to be underestimated. Pine Point itself has produced copious internal reports over the past fifteen years dealing specifically with the possible causes of dolomite contamination in the zinc circuit and possible solutions to the problem.

The aim of this research, therefore, is to continue the ongoing effort to identify mechanisms of dolomite contamination in zinc concentrates, with specific reference to the ores and to the zinc circuit of Pine Point, N.W.T.. The topic is of technological interest, since the required degree of magnesium rejection in Pine Point zinc concentrates is so high as to push flotation technology to its limits. The topic is also of practical interest since dolomite contamination in

zinc concentrates is still an imperfectly understood phenomenon, the solutions to which have proven both costly and, in some cases, ineffective.

In this project experimental simulations of Pine Point zinc flotation and acid leaching have been undertaken with the goal of characterizing the following:

1) Mechanisms by which dolomite reports to the concentrate during cleaning flotation.
2) Factors which affect magnesium recovery during flotation.
3) Factors which affect zinc recovery and sphalerite kinetics during flotation.
4) Factors which affect leach efficiency, and the kinetics of sulphuric acid leaching.
5) The effects of acid leaching upon subsequent stages of flotation.

Experiments have been designed to simulate Pine Point operating conditions as closely as possible in order to elucidate the factors which are responsible for magnesium contamination in Pine Point zinc concentrates.

1.5 Development of the Pine Point Flowsheet

The zinc circuit at Pine Point has undergone several radical changes since mill startup in 1965. The following is an elaboration upon the brief circuit description of the

previous section, and is drawn from Cormode (1977), Jones (1982) and information provided by K. Tietz of Pine Point Ltd..

The original Pine Point circuit was designed for a throughput of 5000 STPD. Four banks of lead roughers were followed by one bank of lead cleaners and two banks of recleaners. The lead tailings were routed to the zinc circuit, which consisted of five banks of roughers, two banks of cleaners and two banks of recleaners. The cells were all 40 cubic foot Galigher Agitair model #48 units.

In 1968 Pine Point acquired mining rights to the Pyramid ore bodies located 54 km east of the Pine Point concentrator. At this time mill capacity was upgraded to 8000 STPD by installing an independent processing circuit (the Sphynx, or "X" circuit) parallel to the existing Pine Point circuit. The Sphynx circuit had independent grinding and flotation capacity and merged with the Pine Point circuit only at the thickening and filtration stages of processing. The Sphynx circuit consisted of one bank of lead roughers (100 cubic foot Denver 30DR's), one bank of lead cleaners and one bank of lead recleaners/supercleaners (both Agitair #48 units), followed by three banks of zinc roughers and one bank of zinc cleaners/recleaners/supercleaners (all Denver 30DR's).

As part of the 1972 program to increase dolomite rejection additional cleaning capacity was added to the zinc circuit. The zinc concentrates from the Pine Point and Sphynx

circuits were combined and fed to two banks of 200 cubic foot Denver #200V cells, which were partitioned into a third cleaner (one bank), a fourth, and a fifth cleaner (1/2 bank each).

The post-1972 flotation circuit at the Pine Point concentrator is illustrated in Figure 1.2. In total the circuit consisted of 266 flotation cells in the Pine Point circuit, 108 cells in the Sphynx circuit and 16 cells in the added zinc cleaning circuit. Of these, 174 cells with a combined volume of 10,200 cubic feet were used for zinc roughing and 68 cells with a combined volume of 6440 cubic feet were used for zinc cleaning. The circuit was a rather unwieldy one which posed several problems:

1) Process flows could not be evenly balanced amongst the separate banks. Thus, it was almost impossible to achieve optimum metallurgical performance and zinc recovery.
2) The Pine Point and Sphynx rougher circuits exhibited different retention times (17.9 minutes in Pine Point vs. 22.8 in Sphynx) and this adversely affected metallurgical performance.
3) As time progressed the Agitair cells reached the end of their useful operating lives. Many needed rebuilding, and the necessary overhauls were both lengthy and expensive.
4) Automated process control was impossible due to the

FIG. 1.2.

PINE POINT FLOWSHEET (1964 - 1980)

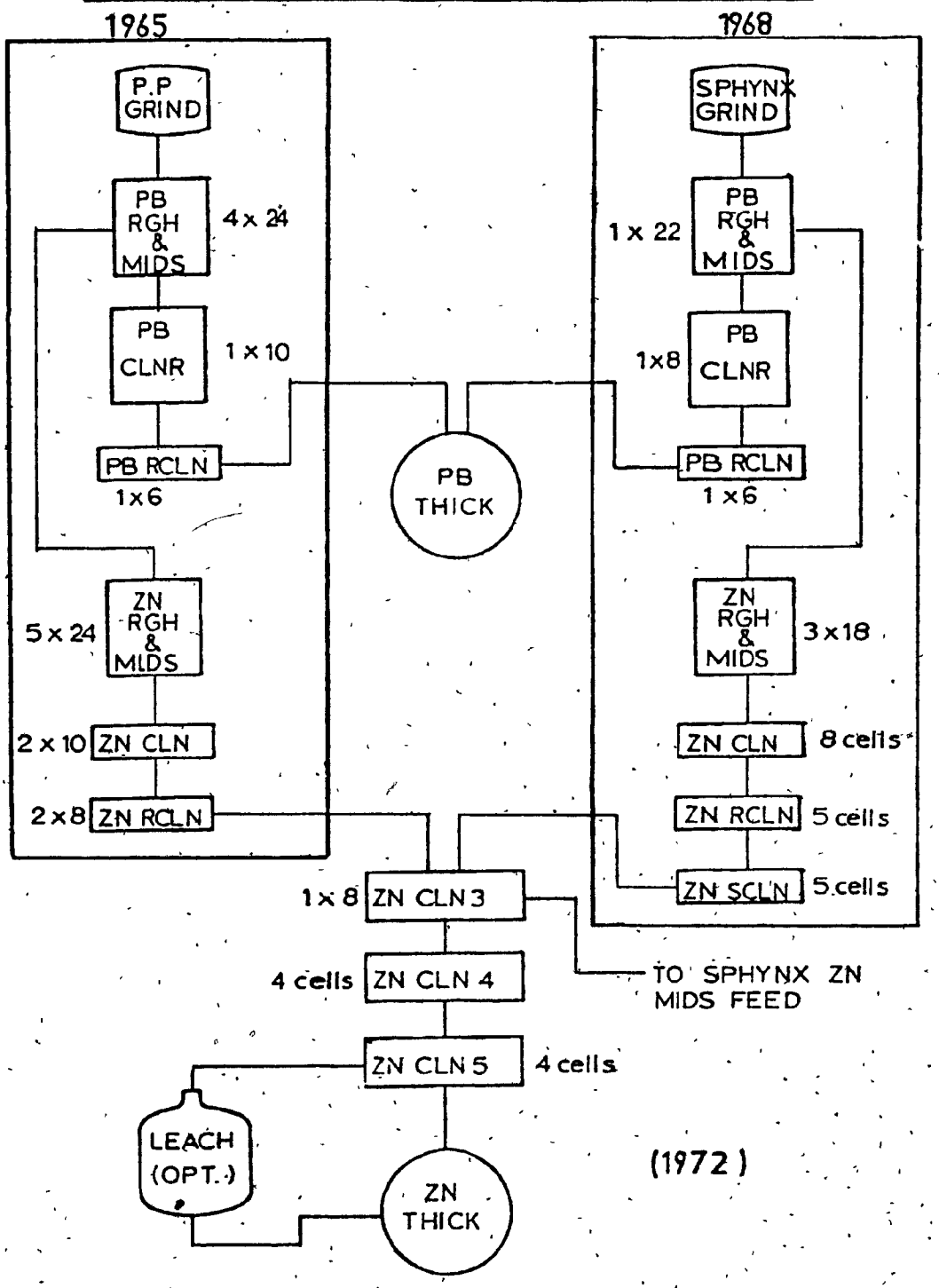

FIG. 1.3

NEW (1980) CIRCUIT

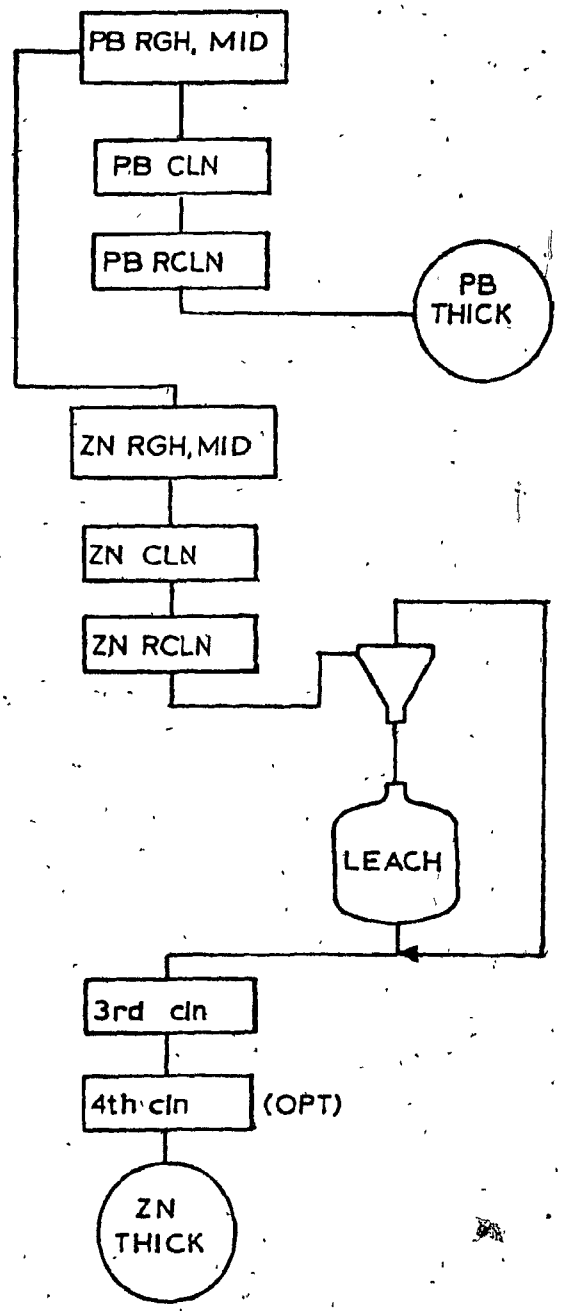

multitude of flotation cells and process streams in the two circuits.

By the mid-seventies it was evident that further changes needed to be effected. In 1980-81 the entire flotation section of the concentrator was dismantled and the small-volume cells were replaced by 600 cubic foot OK-16 and 1350 cubic foot OK-38 flotation cells. The new flotation circuit (shown in Figure 1.3) has a capacity of 11,000 STPD and is now in operation. After consolidation of the Pine Point and Sphynx circuits an increase in the zinc concentrate of 0.6 grade units and 0.2 recovery units was realized. The circuit is now amenable to on-stream analysis and process control, both of which are being considered.

1.6 Description of the Pine Point Leach Plant

The Pine Point leach plant was put into operation late in 1972 as part of the program at that time to reduce magnesium levels in the zinc concentrate. Test work had established that magnesium could be effectively removed from zinc concentrates according to the reaction:

$$2H_2SO_4 + MgCa(CO_3)_2 \rightarrow Mg^{++} + Ca^{++} + 2H_2O + 2CO_2$$

The plant consisted of four wood-staved tanks in series and was designed to reduce magnesium levels in the concentrate from approximately 0.25% to below 0.10%, operating continuously at a design capacity of 1000 STPD. It was soon

discovered, however, that the incoming concentrate magnesium levels were closer to 0.35%, and it was necessary to add a fifth leach tank to the plant in order to provide longer retention of the concentrate. The current mean residence time in the leach circuit is approximately two hours (Figure 1.4).

A schematic of the leach plant is shown in Figure 1.5. Sulphuric acid is added to the first and second tanks, which act as acidifiers. The third and fourth tanks act as holding tanks, or digesters, and liquid ammonia is added to the fifth tank, which serves as a neutralizer. The neutralizer is necessary in order to consume excess acid since the post-leach flotation cells and the thickener are not acid proof. The neutralizer also reduces soluble zinc to a metallurgicaly insignificant level (although still high from an environmental standpoint). Typical pH levels in the tanks are 1.0 to 1.5 in the acidifiers, 2.0 to 2.5 in the first digester, 2.5 to 3.5 in the second digester, and 7.0 to 8.0 in the neutralizer. Acid addition in 1973 was 45 to 55 kg per tonne of concentrate, but is presently about 22 to 27 kg per tonne. Ammonia consumption varies at up to 7 kg per tonne.

The layout of the leach plant has remained the same from 1973 to present; however, its position in the processing circuit was changed during the 1980-81 plant renovations. From 1973 to 1980 the plant was used as an auxiliary post-flotation operation to treat "difficult" ores and to provide stockpiles of low-Mg zinc concentrate for concentrate blending and for

FIG. 1.4

RESIDENCE TIME IN THE PINE POINT LEACH PLANT

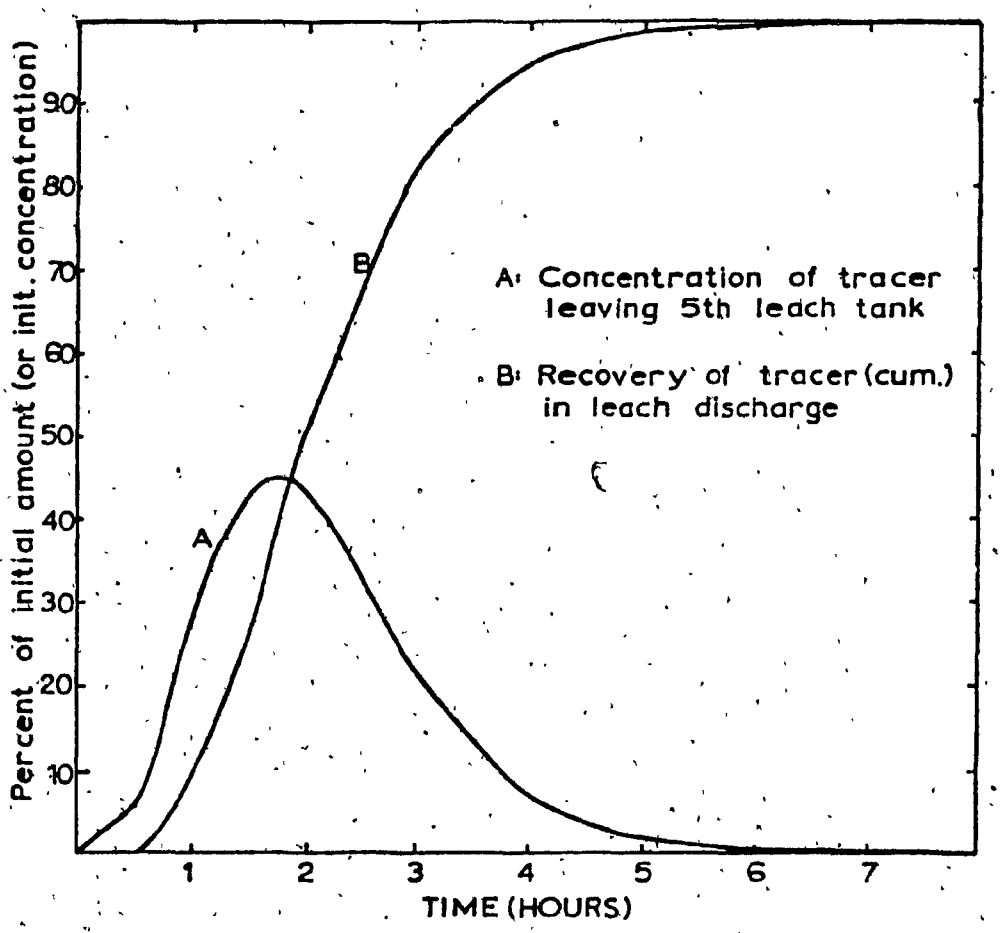

(from Pine Point circuit survey June 7 1978)

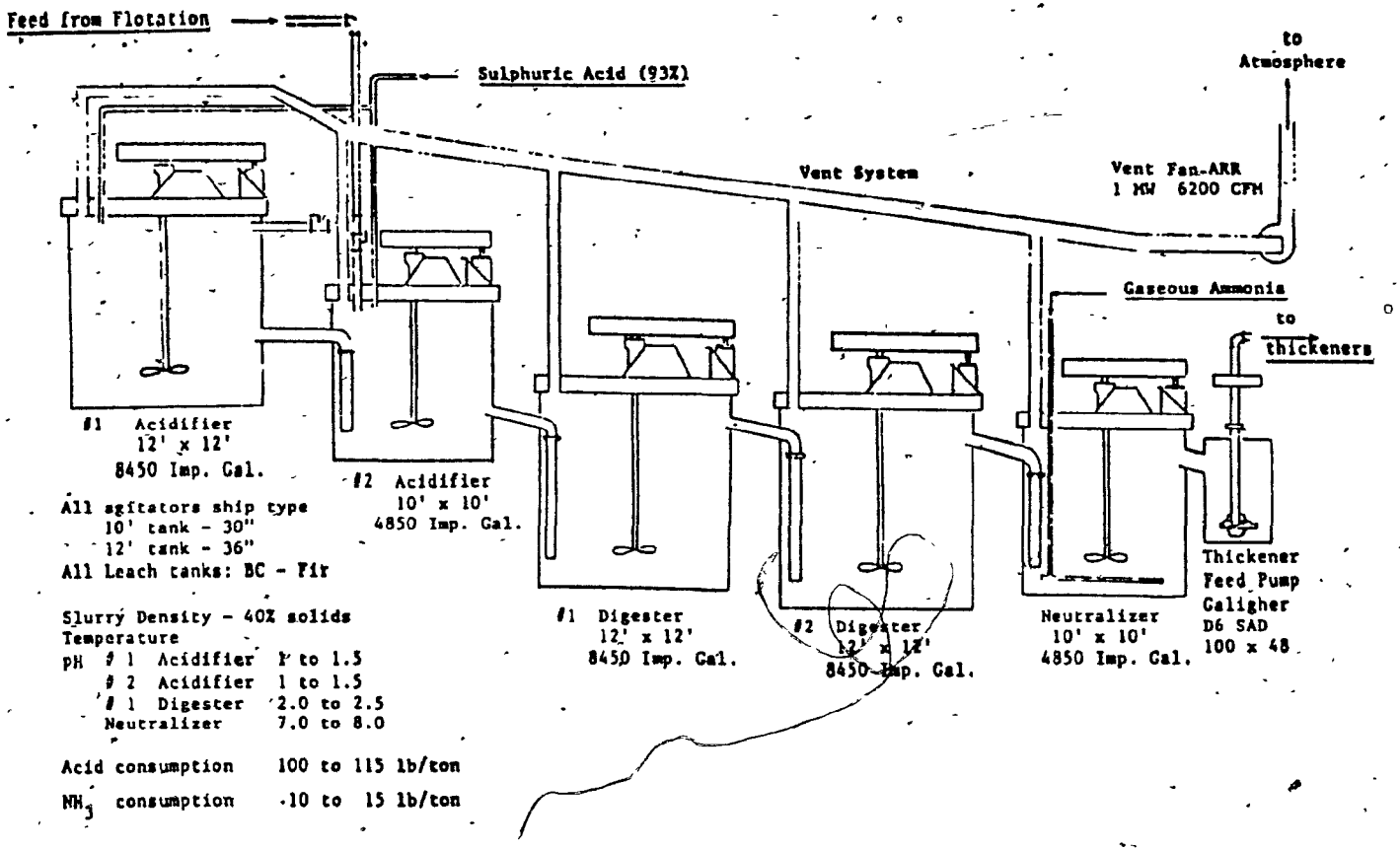

FIG. 1.5 PINE POINT LEACH PLANT SCHEMATIC

(from Jones 1982)

offshore sales. The position of the leach plant in the 1973 circuit is shown in Figure 1.2.

Following the 1980-81 plant renovations the leach plant was incorporated into the regular processing stream. Concentrate from the #2 zinc cleaner is cycloned, and the underflow (at 60 to 70% solids) is pumped to the leach plant (Figure 1.3). The leach plant discharge and cyclone overflow are combined and constitute the feed to a third (and optional fourth) bank of cleaning cells. Tails from the third and fourth cleaners are routed back to the head of the zinc cleaning circuit. When unusually high magnesium levels are encountered in the cleaner 2 concentrate the pre-leach cyclone is bypassed and all of the concentrate is thickened and leached.

There are several operational and environmental problems associated with the Pine Point leach plant. The reaction between acid and dolomite releases copious amounts of carbon dioxide gas, and foaming is a common problem. In order to control this, wash water is added to the tops of the tanks and all tanks are well agitated. Occasionally there is a problem with H_2S emissions (usually when the pH of the acidifiers falls below 1.0 to 1.5) and the plant must be temporarily closed down, despite the fact that the tanks are all vented to the atmosphere. Water from the zinc thickener cannot be recycled due to ammonia evolution if it is used in the flotation circuit and disposal of this water causes

environmental problems due to its high content of dissolved metals.

The leach plant has proved to be a successful method of reducing magnesium contamination in Pine Point zinc concentrates; however, the costs incurred in its operation are very high. The quoted (1973) acid consumption of approximately 50 kg per tonne of concentrate translates into about 7000 tonnes of H_2SO_4 which must be purchased and shipped to Pine Point each year, even if only half the concentrate is treated. This ultimately results in about 7000 tonnes of sulphate ions and a comparable mass of metal ions which must be disposed of in tailings ponds, as well as nitrates from neutralization and H_2S from sulphide dissolution. Fortunately for Pine Point, Trail B.C. the major consumer of Pine Point zinc, accepts magnesium levels of up to 0.25% in the zinc concentrate without penalty. For this reason acid addition can often be kept low; however, as head grades fall and as more "difficult" ore is treated the leach plant is becoming more heavily relied upon in the effort to produce satisfactory zinc concentrates.

CHAPTER 2

GEOLOGY OF THE PINE POINT AREA

CHAPTER 2: GEOLOGY OF THE PINE POINT AREA

2.1 Tectonic History of the Pine Point Region

The location of Pine Point in relation to major geological features was shown in Figure 1.1. An understanding of the general tectonics of the Pine Point area and the petrogenesis of the ore deposits is useful to the geologist, who uses such information to direct exploration. Petrogenetic information is less commonly used in mineral processing, although it can be of great value in determining the types and variability of mineral textures which exist in the ore deposits and the potential processing problems which may arise in ore mined from various pits.

Pine Point is located on the eastern flank of the Western Canada Sedimentary Basin in the Central Plains province (Figure 1.1). It is part of a broad reef-like barrier complex which extends to the southwest from near the Precambrian Shield, passes north of the Peace River Arch in subsurface and continues to the southwest (Figure 2.1). The barrier complex developed in Devonian times (345 to 395 million years ago) and influenced sedimentation over much of Western Canada. The complex is located directly over a major NE/SW trending fault system in the Precambrian basement rocks which can be traced for many miles both to the northeast and to the southwest of Pine Point. The stratigraphy of the Pine Point region is well documented by Skall (1975), Campbell (1966,67) and Jackson and Folinsbee (1967).

Prior to Devonian times the Pine Point region was a

NNW/SSE trending clastic sedimentary basin which accumulated quartz sandstones from the uplands to the east and west. Restricted marine conditions existed in the area and some evaporites were deposited. Emergence took place in the early Devonian, causing a break in sedimentation. This was followed by a widespread marine transgression which quickly shifted conditions from restricted to open marine. The ocean transgressed over much of Western Canada and as far into the interior as North Dakota (Figure 2.1). At this time dolomite was deposited in the Pine Point area. The quartz sandstones, evaporites and dolomite referred to so far are named the Old Fort Island formation, the Chinchaga formation and the Keg River formation respectively, and these form the base upon which the Pine Point group was deposited.

Gentle arching of the Pine Point area in the middle Devonian lifted the sediments close enough to sea level so that reef-building organisms could establish themselves. The arch developed parallel to the underlying fault system in the Precambrian basement and established the shape and the location of the barrier complex. Figure 2.2a shows the general appearance of the complex at this point with the right-hand side of the diagram facing open marine conditions. The barrier at this point consisted of a buildup of reefal organisms flanked on the seaward side by reef detritus and on the landward side by tidal-flat carbonates. Away from the reef on the seaward side deep-water shales were deposited. All of

FIGURE 2.2A: INITIAL STAGES OF BARRIER BUILDUP

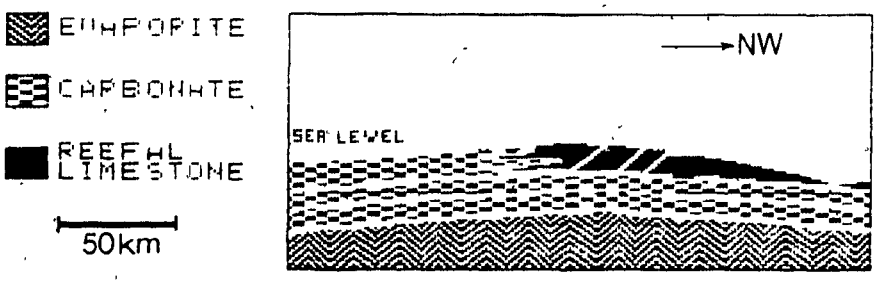

(adapted from SHALL, 1975)

these facies were deposited upon the Keg River formation. The barrier was not fully developed at this time; it contained several gaps which allowed circulation of brine between the inland and open marine areas. Conditions behind the barrier were very similar to the conditions which existed during the deposition of the Keg River formation; consequently, the back-reef strata are referred to as the Upper Keg River formation.

The next sequence of events included increased subsidence to the south. The fault system under Pine Point acted similarly to a hinge and caused vertical faulting of the overlying sediments (Figure 2.2b). By this time the barrier was well established and circulation of water around and across it was very restricted. Much of the Canadian interior including most of Alberta and Saskatchewan became analogous to a huge evaporating pan. There existed a continuous flow of

FIGURE 2.2B: DEVELOPMENT OF THE SOUTH HINGE

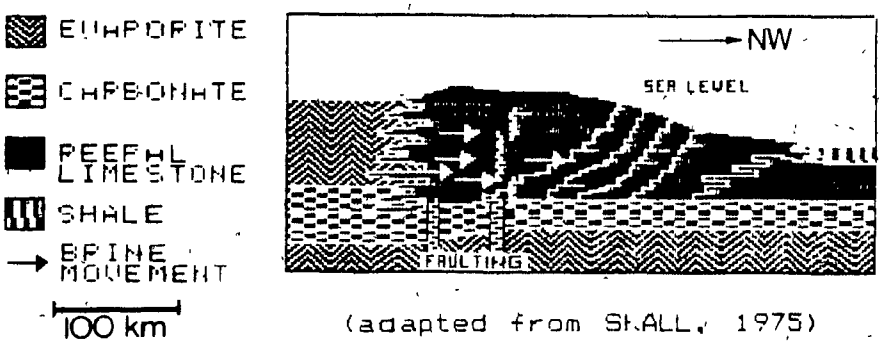

(adapted from SHALL, 1975)

water inland over the Pine Point barrier; however, due to the restriction of circulation the rate of flow inland was less than the rate of evaporation on the continent. Marine salts with low solubilities precipitated closest to the barrier, while the more soluble salts were carried inland. For this reason there are vast occurrences of halite and potash in southern Saskatchawan, and comparably large occurrences of anhydrite and gypsum (of the Muskeg formation) in the Pine Point area. A high osmotic gradient existed between the extremely saline waters trapped in the Muskeg sediments and the seawater on the marine side of the barrier. Large volumes of brine refluxed through the barrier, and in passing changed the reefal limestones to dolomite (Figure 2.2b).

Continued subsidence in the South eventually caused increased movement of the faulted area under the Pine Point barrier complex and two more hinge zones developed (the Main

FIGURE 2.2C: SUBSIDENCE AND DEVELOPMENT OF THE NORTH HINGE

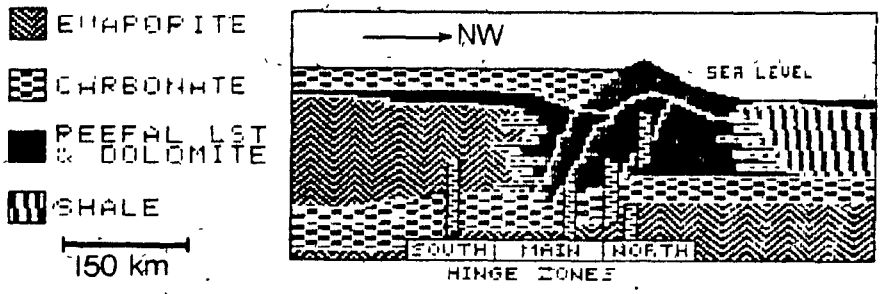

(adapted from SHALL, 1975)

Hinge in the centre of Figure 2.2c, and the North Hinge to the right of it). Movement along these hinges overtook the rate of growth of the barrier, thereby drowning it. All that remained of the organic barrier was a small buildup over the North Hinge. Since circulation was no longer restricted evaporite deposition to the south was terminated and a shallow marine limestone was deposited. With the end of evaporite deposition

FIGURE 2.2D: PINE POINT AREA AT PRESENT

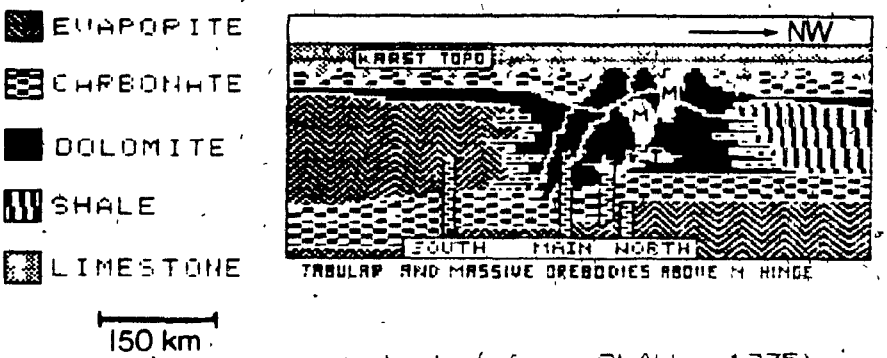

(adapted from SHALL, 1975)

came the end of refluxing brines through the barrier complex and the end of dolomitization. The carbonates directly over the three hinges were faulted by the hinge movements which occurred.

Several subsequent events altered the appearance and the stratigraphy of the complex. A widespread marine regression exposed the Pine Point area some time in the Late Middle Devonian. The area was elevated approximately 30 meters above sea level and erosion formed extensive areas of karst topography and solution brecchiation. Increased subsidence followed and resulted in the deposition of limestones of the Watt Mountain formation, which constitute the last formations in the sedimentary sequence. Near the end of the Paleozoic era (approximately 250 million years ago) the whole barrier system was deformed, and it now plunges gently westward. Outcrops of the barrier are found only in the Pine Point region; however, drillhole and geophysical data indicate that the complex extends as far as northeastern British Columbia at depths of 1700 to 2500 meters.

2.2 The Emplacement of Pine Point Sulphides

The rocks forming the Pine Point area and hosting the Pine Point deposits are very porous. Part of this porosity is a result of the biogenic origin of the barrier complex, and part is the result of the karst topography and the solution brecchiation which developed in the area. In addition to

porosity in the rocks there exists an extensive network of fracture and fault systems over the three hinge zones, as previously discussed and shown in Figure 2.2d. The barrier rocks therefore served as an excellent conduit for fluids (ore-bearing and otherwise) which moved in the subsurface through the area. Skall (1975) described the complex as a huge "plumbing system" for moving fluids.

The first significant episode of fluid movement in the area occurred in the Late Devonian, at which time warm magnesian brines moved up through the fractured rocks overlying the Main and North Hinge zones. Much of the limestone in the area was transformed to a coarse, crystalline dolomite referred to as the Presqu'ile dolomite, and it is this dolomite which hosts many of the Pine Point ore bodies. The circulation of magnesian brines through the complex may have been convectively driven by an exothermic reaction between anhydrite and hydrocarbons which formed hydrogen sulphide, carbon dioxide and water (Dunsmore, 1977). This dolomitization predated ore emplacement.

Ore genesis at Pine Point occurred some time during or after the Late Devonian, approximately 345 million years ago. The origin of the ore-forming fluids and the precise mechanism of deposition are sources of debate; however, it is evident that metal-bearing solutions moved up through the faulted zones over the Main and North Hinges and deposited their metals in the pores and cavities in the Pine Point carbonates.

Much of the mineralization occurs in the Presqu'ile dolomite, although about half of the Pine Point ore bodies extend beyond or occur outside of the dolomitized regions.

Typical relationships between the Pine Point ore bodies and surrounding strata are shown in Figure 2.2d. Emplacement of the ore bodies was closely controlled by the faulted and karst regions in the area. The ore bodies are concentrated over the North and Main Hinges, and are elongated parallel to them. The margins of the ore bodies are typically very sharp and lack disseminated fringes at the outer edges even though the wallrock porosity continues.

The Pine Point orebodies are subdivided into massive and tabular varieties. Massive orebodies are vertically elongated with little horizontal extension and occur in the upper levels of the Presqu'ile dolomite, sometimes even penetrating the Watt Mountain carbonates and shales. Tabular ore bodies are thin and horizontally extended and occur in deeper strata. The two types of ore bodies exhibit different lead/zinc ratios, with an average of 1:1.6 for massive and 1:2.6 or greater for tabular ore bodies. It can be interpreted that these two types represent two different episodes of mineralization (Skall, 1975). Most of the ore reserves in production at Pine Point are of the massive variety since their proximity to the surface makes them easier to explore and to produce than the deeper-seated tabular ore bodies.

2.3 Classification of the Pine Point Ore Bodies

Ore deposits can be classified into one of several types based upon such factors as mineralogy, mode of origin, textures, type of host rock and a variety of other factors. Deposits of the same type often exhibit very similar characteristics and this allows inferences to be made about an ore deposit based upon geological information or operating experience from another deposit of the same type.

The Pine Point ore bodies belong to a group called Mississippi Valley-type deposits. Many such deposits occur in North America including deposits in Mississippi, Missouri, Oklahoma, Kansas, Tennessee, Pennsylvania, Montana, Wisconsin and in Canada's Northwest Territories, including not only Pine Point but also Polaris and Nanasivik. Mississippi Valley-type ore deposits have the following features in common:

1) The deposits contain lead, zinc and often copper and barium. Silver values are low.
2) The ore minerals are epigenetic (ie. emplaced after formation of the host rocks rather than with them).
3) The host rocks are carbonates.
4) The deposits are strata-bound or stratiform.
5) The deposits were emplaced at low temperatures and caused little to no alteration of the country rock.
6) Sphalerite often exhibits banded or botryoidal (colloform) textures.

The Pine Point deposits are typical Mississippi Valley-type deposits in all respects except for their lack of copper and barium.

2.4 Paragenesis of the Pine Point Ore Deposits

The host rocks of the Pine Point deposits are dolomite and calcite with trace amounts of gypsum. During ore deposition sphalerite and galena were introduced along with small amounts of marcasite and pyrrhotite. Rare celestite, sulphur, bitumen and fluorite have also been reported in the area (Small, 1975; Jackson and Folinsbee, 1969). Thus, the deposits exhibit simple mineralogy, although the textural relationships between minerals tend to be complex. An understanding of the paragenetic sequence at Pine Point is of use in determining the factors which control textures and textural variations in the ore bodies.

As part of an isotopic study of Pine Point carbonates Fritz (1969) developed a paragenetic sequence for the deposition of hydrothermal minerals during ore genesis. Temperatures of formation were extrapolated from O(18)/O(16) isotopic ratios of the carbonates, which decrease as the temperature of formation rises. Some of his results and petrogenetic interpretations are presented below and in Figure 2.3.

FIGURE 2.3: CYCLE OF MINERALIZATION AT PINE POINT

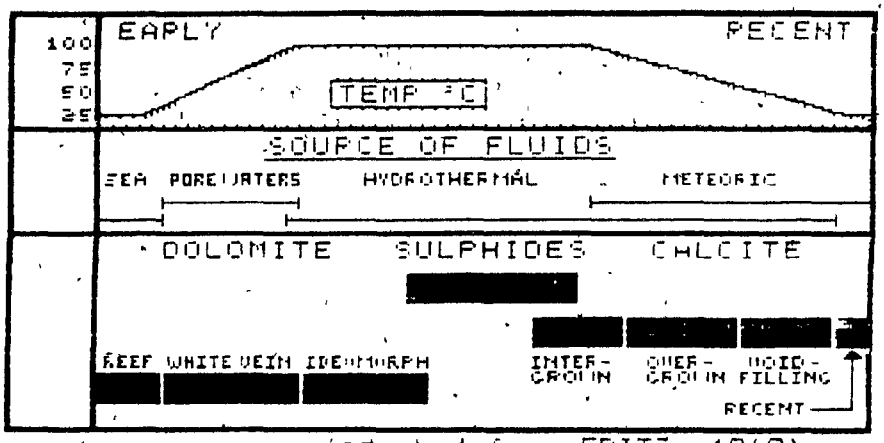

(adapted from FRITZ, 1969)

Prior to the onset of ore deposition a period of low-temperature hydrothermal activity (50° to 70°C) caused the recrystallization of some of the Fresqu'ile dolomite into a white, sparry dolomite (white vein dolomite) which crosscuts and overgrows the Fresqu'ile. As hydrothermal activity increased the white vein dolomite was overgrown by clear, well-crystalline dolomite which lined or filled cavities (ideomorphic dolomite). The temperature of formation of the ideomorphic dolomite was approximately 100°C and this temperature was sustained during the onset of ore deposition. A short period of coprecipitation of dolomite and ore occurred; however, during the principal episode of ore deposition the hydrothermal fluids were undersaturated with carbonate and dolomite dissolution occurred.

The principal stage of ore deposition was characterized by the precipitation of sphalerite, galena and

pyrite/marcasite. All of these minerals precipitated concurrently in several repeated episodes of precipitation and dissolution. The major occurrences and textures of the ore minerals are described below.

Sphalerite is the major ore mineral and was deposited mostly in thin layers on vugs and pores in the host rock, often completely occluding cavities. Due to this mode of deposition the sphalerite exhibits thin bands which vary from about 10μm to a few millimeters in thickness. Hundreds of these bands may be deposited one upon another in radial arrangement, so that the overall appearance of the sphalerite varies from banded botryoids to laminated crusts (Figures 2.4 and 2.5). The overall texture of the sphalerite is referred to as "colloform" (Small, 1975); however, this may be an unfortunate choice of terms since it suggests that the sphalerite was precipitated as a gel. In reality, much evidence exists that the sphalerite was directly precipitated from solution as fine crystalline layers (Roedder, 1968). The term "colloform" is used in this discussion as a descriptive rather than as a genetic term.

Individual sphalerite bands exhibit different colours varying from white through a series of yellows, reddish-browns and browns to a very dark brown which appears black in hand specimens. Although there has been some controversy (Roedder, 1968) it appears that the colour of the sphalerite is directly related to its iron content (McLimans et. al., 1980).

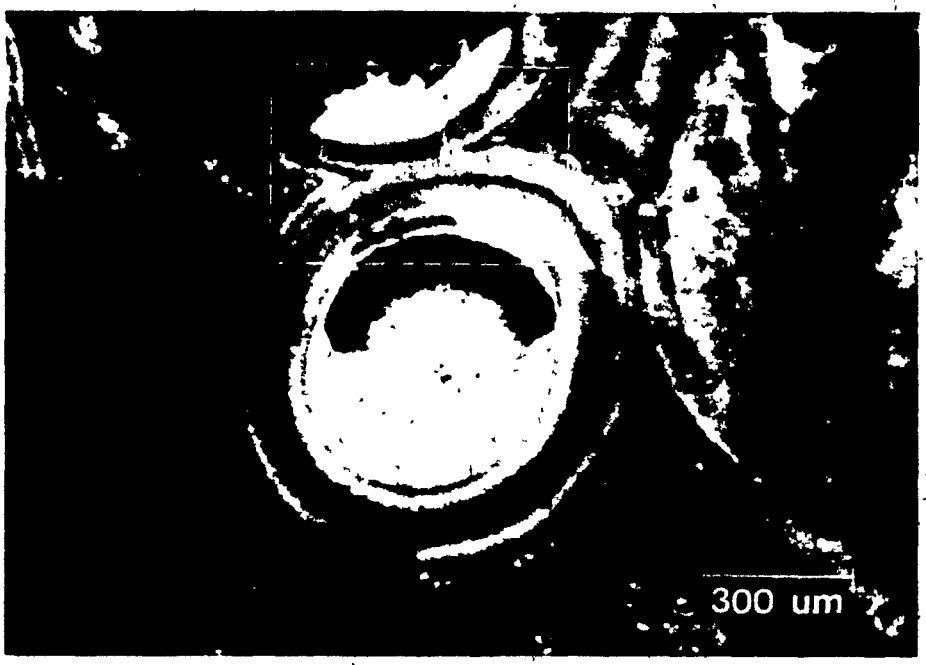

FIGURE 2.4: BOTRYOIDAL SPHALERITE
(Boxed area shows interface between botryoids)

FIGURE 2.5: BANDED SPHALERITE LINING A VUG
(Galena can be seen at centre of the vug)

Sphalerite from Pine Point has iron contents which range from 0.2 mole percent to over 14 mole percent and the colour of the sphalerite varies from white at 0.2 mole percent iron to opaque at about 4 or more mole percent.

Not all of the sphalerite at Pine Point is colloform. In some areas the sphalerite forms ideomorphic or blocky crystals which occur as vug-linings or intergrowths with sparry calcite. Skall (1975) reports that colloform sphalerite is common in massive ore bodies but rare in the tabular variety.

Pine Point galena is found in three principal varieties which are described by Roedder (1968). These are:

1) Large, skeletal crystals, mainly in the centres of sphalerite botryoids, which transect the sphalerite bands.
2) Elongated crystal blebs which are radially arranged in the sphalerite botryoids. The galena crystals are often faceted at their leading edges, with the (111) crystallographic direction (the fastest-growth direction) pointing outwards.
3) Coarsely crystalline veinlets which cross the sample in part randomly but which tend to be concentrated between individual botryoids on their interference surfaces.

The three types of galena are illustrated in Figures 2.6, 2.7 and 2.8.

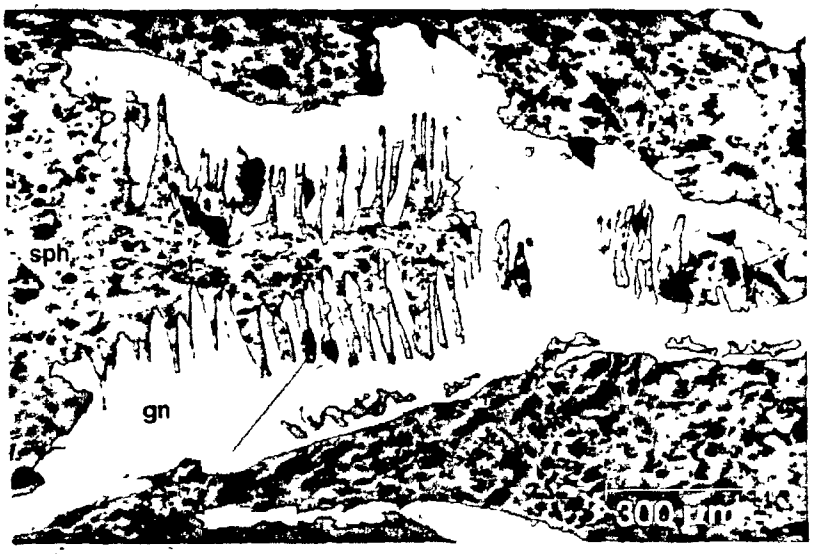

FIGURE 2.6:

SKELETAL GRAIN OF GALENA IN SPHALERITE

FIGURE 2.7:

GALENA CRYSTALS CROSS-CUTTING BANDING IN SPHALERITE

FIGURE 2.8:

FRACTURE-FILLING GALENA IN SPHALERITE

Pyrite and marcasite at Pine Point are found in two principal forms. The first is a primary stage of syngenetic pyrite which occurs as small disseminated blebs in the dolomite, often concentrated along bedding planes. This type of pyrite forms only a tiny volume of the total ore but is so widely disseminated as to be present in almost any sample of the country rock. It is interpreted that this pyrite was formed in the soft sea-floor sediments during decomposition and reduction of organic matter.

The second and major occurrence of pyrite and marcasite is as a hydrothermal mineral deposited with the sphalerite and the galena. Crystals are usually ragged and disseminated and form only a small fraction of the ore volume, although Small (1975) reports that some sulphide deposits at Pine Point are composed almost totally of iron sulphides with only traces of lead and zinc.

Close to the end of ore deposition the chemical composition of the hydrothermal fluids underwent changes which favoured the precipitation of calcite. The calcite precipitated concurrently with the ore and gave rise to intimate associations of ore minerals (especially sphalerite) and calcite gangue. Calcite precipitation persisted after the termination of ore deposition, and this late calcite can be observed as overgrowths on the ore and as vug fillings on dolomite. Calculated temperatures of formation of the calcite vary from 100° to 25°C and record the termination of

hydrothermal activity. A secondary, non-hydrothermal calcite is found as overgrowths on all of the hydrothermal carbonates and ore minerals and represents an episode of ongoing calcite precipitation under the influence of meteoric waters.

The described paragenetic sequence is very similar to the sequence described by McLimans, Barnes and Ohmoto (1980) for the West Hayden and Edgerton ore bodies in Southwest Wisconsin. Figure 2.9 summarizes the depositional sequence proposed by these authors. It is interesting to note that ore deposition was preceded by a period of dolomite deposition and followed by a period of calcite deposition; however, unlike Pine Point there was no coprecipitation of dolomite and ore. The features and mineralogical textures of ores from this

FIGURE 2.9: CYCLE OF MINERALIZATION AT WEST HAYDEN AND EDGERTON ORE BODIES

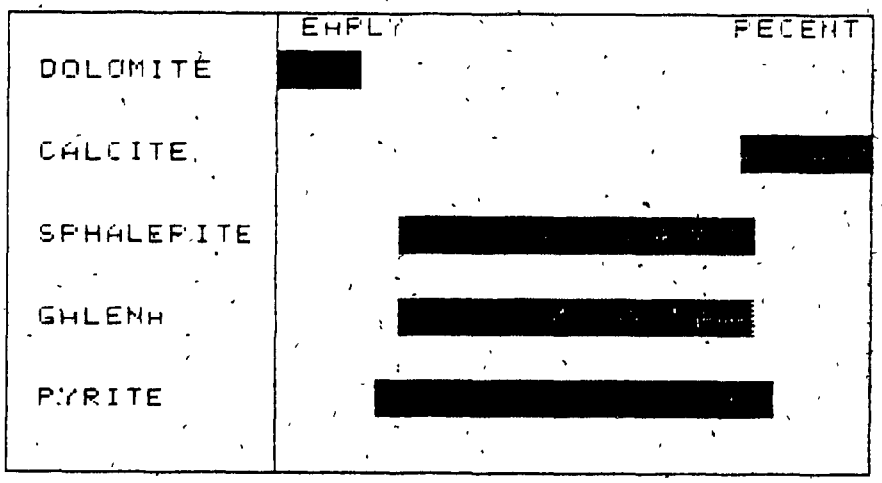

(adapted from BARNES and OHMOTO, 1980)

region are remarkably similar to those of the Pine Point ore bodies and reflect a common mode of origin. Ores of the Mississippi Valley region (called the Vibernum Trend) are discussed in detail by Gerdemann and Myers (1971), Sverjensky (1981) and by McLimans, Barnes and Ohmoto (1980).

CHAPTER 3

LOCKED CYCLE FLOTATION OF TIME POINT ORE

CHAPTER 3: LOCKED CYCLE FLOTATION OF FINE POINT ORE

3.0 Introduction

The fundamental goal of laboratory-based test work is to provide a simulation of full-scale plant operating conditions, yet in a closely controlled and measurable environment. The advantages and the disadvantages of laboratory work are well known. Bench scale tests are much more controllable than plant tests and the researcher has a much greater choice and range of operating variables than he does in the plant. Unfortunately, however, laboratory test results are often difficult to apply to "real life" situations.

This project is exclusively a laboratory project, since the Fine Point mill was shut down over most of the period during which this research was conducted. Thus, much care had to be exercised in choosing laboratory experiments whose results could reasonably be applied to a "real" situation without directly correlating them with plant data. It was also desirable to simulate the widest possible variety of contamination mechanisms by which magnesium could enter the Fine Point concentrate.

The data collected in this experimental work is largely, in the form of assay data, recoveries, metal distributions and the like. Since it is not possible to make a direct correlation between observed laboratory results and anticipated plant performance the presentation of numerical data has been kept to a minimum. It is believed, however, that a qualitative analysis of laboratory flotation performance can

provide insight into the range and magnitude of possible flotation problems at the Pine Point mill. In accordance with this approach experimental results have been presented graphically wherever possible. All experimental results which are not tabulated in the text can be found in the appendices at the end of this thesis.

Plant data from Pine Point was available on a limited basis for most of the plant operations, and for a time period spanning most of the life of the mill. Unfortunately the vast majority of the plant data was collected prior to the installation of the new (1980) flotation circuit, so that the data may no longer be applicable to Pine Point operating conditions. A limited comparison between plant and laboratory results has been carried out upon the assumption that the magnesium problem prior to 1980 probably has the same or a similar cause as the current magnesium problem.

3.1 Materials and Equipment

The material which was obtained for this and for all subsequent flotation tests was a sample of Pine Point ore which was considered by the mill operators to be a difficult ore to process. The sample (about 100 kg) was cut from the rod mill feed and sent from Pine Point in sealed buckets. This material had a size of about 60% passing 3 mesh, and was reduced at McGill to about 70% passing 200 mesh using two-stage jaw and cone crushing. The sample was split

repeatedly to produce about 80 sub-samples of 1200g which were put into paper bags and stored in a sealed plastic bucket. The sample was moist upon receipt and was not dried prior to storage. The ore samples were prepared in October of 1982 and were used over the period October 1982 to February 1984. It is hoped that the surface characteristics of the ore underwent no drastic changes during storage.

Size reduction prior to flotation was accomplished using a 24cm (length) by 18cm (diameter) steel rod mill charged with nineteen 1.5cm by 22cm steel rods. It was determined that a seven minute grind at 65% pulp density would reduce the feed to the Pine Point grind size of 50% -200 mesh. It is expected that this batch grinding method should produce more coarse (+100 mesh), and more fine (-400 mesh) material than the Pine Point grinding circuit, which employs closed-circuit grinding and classification.

The flotation cell used in this test was a Leeds cell (Fig. 3.1). The cell features a bottom-driven impeller, which allows free access to the top of the flotation cell and unimpeded collection of the concentrate. The impeller is hooked up to a digital tachometer and air flow is metered through a precision flow guage. Pulp level is automatically controlled via a pressure transducer at the back of the cell. Tailings can be purged (with difficulty) via a spigot at the bottom left-hand side of the cell. The Leeds cell was found to

FIG. 3.1

LEEDS FLOTATION CELL

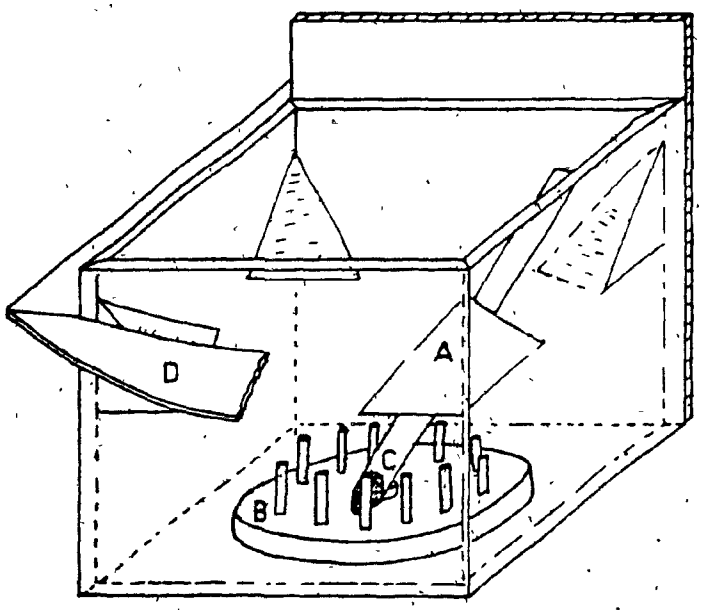

A: Baffle
B: Impeller
C Air supply
D: Collection collar (cut away)

give very uniform and reproducable operating conditions and flotation performance.

Reagents used in flotation tests came from Cyanamid Inc. (Xanthate), the Dow Chemical Co. (Dowfroth 250), and Fisher Ltd. (metal salts such as NaCN, CaO etc.). Stock solutions of the metal salts were kept for several months, while organic reagents were prepared just prior to the experiments.

3.2 Definition and Principles of Locked Cycle Flotation

Simulation of plant flotation conditions can be effected in a variety of ways, ranging from a single batch test to the construction of a miniature pilot plant. In this project it was not feasible to conduct continuous flotation tests , so that a flotation procedure had to be found using batch tests which would simulate plant conditions. One such method is locked cycle flotation, in which a continuous flotation circuit can be simulated by performing multiple batch flotations and by recirculating middlings from early flotation stages to the feeds of subsequent stages. The principles of this method are that:

1) A batch test must be conducted for every flotation stage (called a node) which is to be simulated.
2) The individual stages are performed in a chronological order corresponding to the normal (plant) processing sequence.
3) The middlings collected at each node are retained.

4) When all nodes have been simulated (ie. when one cycle of the test has been performed), the entire procedure is repeated using fresh feed and middlings from the first cycle are added at appropriate points within the circuit.

5) Sufficient cycles of the experiment are performed so that the system reaches equilibrium. Equilibrium can be recognized in several ways, two of which are: a) The summed compositions of the concentrate and the tailings become equal to the composition of the fresh feed (ie. what comes out = what goes in). This condition is not true in the first cycle, for example, since part of the feed is retained as middlings. b) The assays and the masses of all streams stabilize.

In order to effectively use the locked cycle procedure, one must determine several operating parameters before the test is started, including the following:

1) The optimum flotation times must be established for each node in the experimental circuit. (It is assumed that the physical and chemical conditions at each node are predetermined according to plant practice and are constant throughout the test).

2) A prediction must be made concerning the cycle at which the test can be terminated. This is necessary

due to the fact that equilibrium is not visually observable.

The only alternative batch procedure to locked cycle flotation is open cycle testing. This is the "conventional" method for performing laboratory flotation tests. For the purposes of this project a locked cycle test was chosen, although both locked and open cycle procedures have their advantages and disadvantages, as summarized below.

Open Cycle Flotation:

Advantages:

1) The procedure is fast, since each node is simulated only once, and flotation times are usually established by "eyeballing" the concentrate which comes up.
2) As a direct result of the speed of the procedure a very complex circuit can be simulated in a reasonable amount of time.

Disadvantages:

1) The procedure reveals almost nothing about plant flotation since nothing is known about the ultimate destination of middling particles.
2) In order to be confident with the results the experiment must be performed more than once. Since this requires almost as much effort as performing the locked cycle test, some of the time advantage is lost.

Locked Cycle Flotation:

Advantages:

1) This is the form of batch test which provides the closest approach to plant testing.
2) The effects of recirculating loads and the ultimate destinations of middlings can be examined.
3) The test is self-verifying, since the establishment of an equilibrium situation requires that at least three identical cycles be performed in succession.

Disadvantages:

1) The procedure requires 10 to 20 times as much time as an open cycle test. This is largely due to the amount of preliminary work which must be carried out before the locked cycle test is undertaken. The procedure also requires 15-20 times the amount of feed, reagents etc. as an open cycle test.
2) In most cases several cycles are needed to reach equilibrium. This means that in, say, a circuit with 5 nodes a total of 30-40 individual flotations must be performed in order to adequately establish equilibrium. The middlings cannot be saved overnight due to possible changes in their surface properties; thus, there is a limit to the amount of nodes which can be simulated. The experimental circuit must be kept simple.
3) The procedure requires two operators and the

availability of some fast dewatering equipment. The dewatering procedure should not lose any fines, nor should it use any reagents such as flocculants. The dewatering needs are caused by the large amounts of water which are recirculated back to the small, fixed-volume batch cell.

It was decided that for the purpose of this project it was more advantageous to perform a locked cycle test. The test was limited to a simple circuit; however, it was believed that this disadvantage would be more than offset by the greater applicability of the experimental results.

3.3 Setting Up the Locked Cycle Test

Work prior to locked cycle testing involves the establishment of flotation times at each node and the prediction of the best end-point for the experiment. The experimental procedures used here are those described by Agar (1980).

Agar defines three criteria for choosing the optimum flotation time at a node. Since the goal of flotation is the upgrading of a feed, no material should be collected during flotation which is lower in grade than the feed to that stage. In other words, flotation should continue until the incremental grade of the concentrate equals the feed grade. This is Agar's first criterion. If the recovery of metal is unacceptably low, Agar reasons that it is better to add a

second flotation stage than to continue the first.

Since the object of flotation is the recovery of an ore mineral and the rejection of gangue minerals, the difference in recovery between the ore and gangue minerals should be maximized . If it is assumed that the recoveries of ore and gangue can be treated as first order rate processes it can be shown that the difference in recovery between ore and gangue is at a maximum when the two minerals are being recovered at an equal rate. As long as any mineral "A" is being recovered faster than any mineral "B", the absolute difference in recovery "R(A)-R(B)" must be increasing with time. It follows that the difference in recovery is at a maximum when "R(A)-R(B)" equals zero, or when "R(A)" equals "R(B)". This is Agar's second criterion.

Agar's third criterion states that the separaton efficiency should be maximized . Since the separation efficiency is defined as the difference in recovery between the ore mineral and the gangue, there is no discernable difference between the second and the third criteria. Agar shows that the separation efficiency is at a maximum when the incremental concentrate grade equals the feed grade. This conclusion is logical if one considers the following:

- By bypassing flotation altogether the difference in recovery between ore and gangue is zero. (Ie. both are "recovered" at 100%).
- If the concentrate which is being collected has a

higher metal assay than the feed, separation is taking place and the recovery of metal is higher than the recovery of gangue. The separation efficienc, is therefore positive.

- If flotation progresses to the point where the concentrate assay is less than the feed assay a negative separation is taking place. Mass for mass, adding this material to the concentrate lowers the grade faster than bypassing flotation and adding fresh feed to the concentrate. Since bypassing flotation altogether corresponds to a separation efficiency of zero, the "worse" situation corresponds to a separation efficiency which is negative.

Thus, the three criteria defined by Agar are all statements of the same basic principle, namely that flotation should continue until the incremental grade of concentrate being collected equals the feed grade.

3.4 Design of an Experimental Circuit

The complexity of locked cycle testing required that the maximum amount of separation stages in this experiment be limited to four or five. It was therefore decided that lead roughing would be omitted and that the test would employ bulk lead/zinc flotation. It was hoped that the presence of galena in the zinc circuit would not affect the flotation behaviour of the other minerals.

The chosen experimental circuit is illustrated in Figure 3.2. The circuit was designed to simulate the following:

1) Zinc roughing/scavenging.

2) Recirculation between the rougher and the cleaners.

3) Recirculation between two cleaners.

4) Flotation after leaching.

Most of the circuit design is conventional and self-explanatory. The routing of third cleaner tails to the head of the first cleaner, however, is not a standard practice. The rationale behind this is as follows:

- It is not desirable to have large recirculating loads going through the leach, since this results in high acid consumption and large soluble zinc loss.
- It is not desirable to let material escape from the circuit too easily if it has reached the third cleaner. Thus, the material is not sent directly back to the roughers.

At Pine Point the post-leach tailings are sent all the way back to roughing. Material in the roughers, however, has a mean residence time of about 27 minutes. This allows for greater recovery of slow-floating zinc than the relatively short flotation times used in laboratory test work. It was decided that in this case it was better not to emulate the Pine Point circuit.

FIG. 3.2

EXPERIMENTAL CIRCUIT FOR LOCKED CYCLE TEST

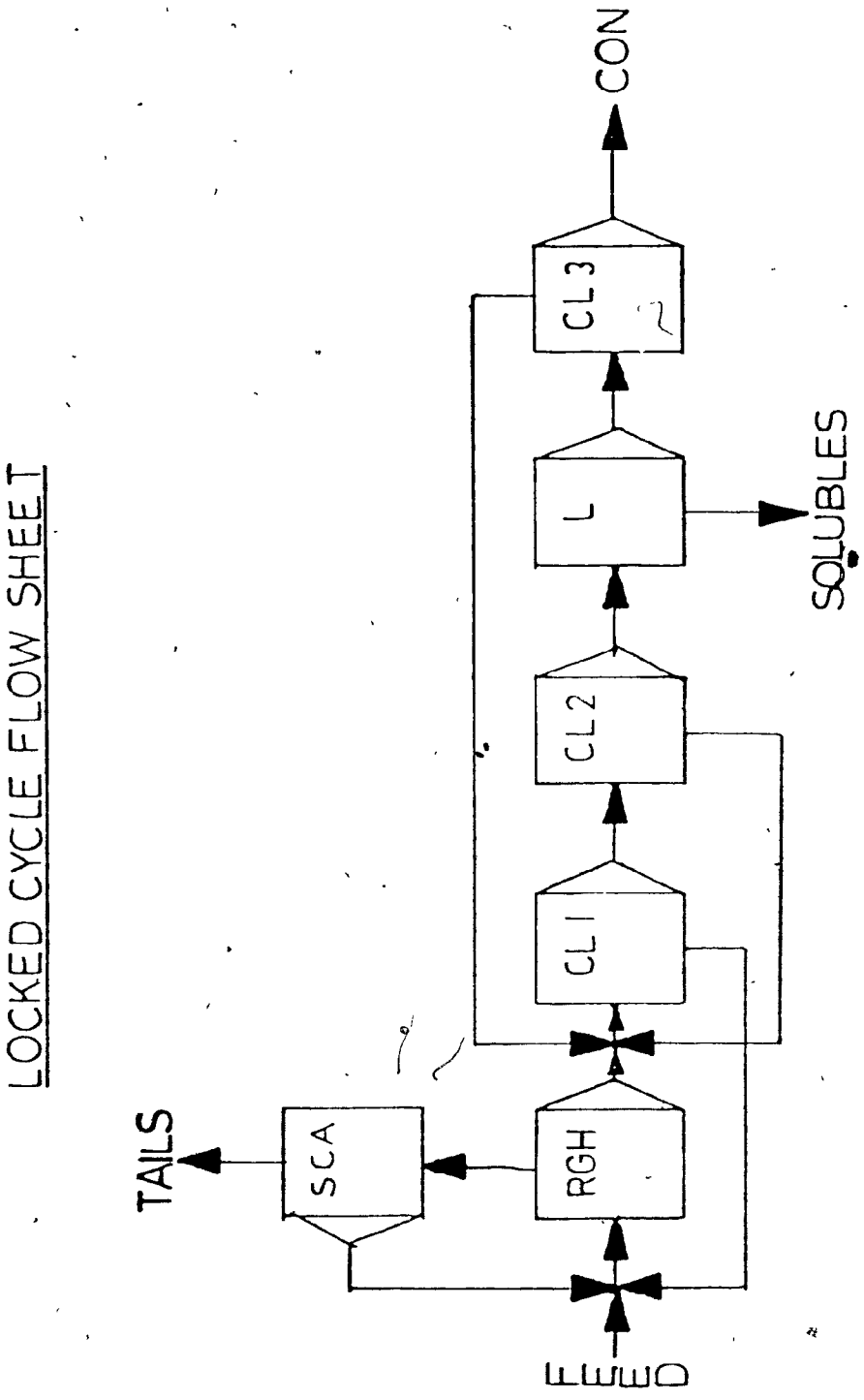

Flotation conditions in the individual flotation stages were chosen to simulate Fine Point conditions as closely as possible, and are outlined in Appendix 1. Likewise, the leach was chosen to simulate Fine Point leach conditions. A plastic pail with a magnetic stirrer was used as the leach vessel, and an acid addition corresponding to 22kg tonne was used. The leach time was only 45 minutes, but this short time was unavoidable since seven batches of concentrate had to be leached during the test. There is evidence presented in Chapter 5 that within 45 minutes the dissolution reaction is close to completion.

7.5 Incremental Flotation Tests

A total of seven incremental flotation tests were used to establish the appropriate flotation times for the five nodes in the locked cycle test. The average of three flotation tests was used to determine the correct rougher flotation time, since the rougher performance has an overwhelming effect upon the performance of subsequent flotation stages.

The incremental flotation tests are straightforward and need little explanation. Results of the three rougher tests are presented Fig.7.3, and in Tables 7.1 to 7.3. Once the rougher flotation time was established, scavenger and cleaner 1 incremental flotations could be performed. Results of these tests are presented in Figures 7.4 and 7.5, and in Tables 7.4 and 7.5. In a similar manner, once the flotation time of the

first cleaner had been established, an incremental second cleaner flotation could be performed (Figure I.6 and Table I.6), and finally a third cleaner flotation (Figure I.7 and Table I.7). The optimum flotation times can be read off Figures I.I to I.7 by finding the time at which the incremental zinc grade intersects the back calculated feed grade to that separation stage. The optimum flotation times are summarized in Table I.8.

Some notes can be pointed out concerning the incremental flotation tests. In the scavenger test the Agar cutoff criterion was never reached. Mass recovery quickly dropped to almost nothing at just over 1 minute. A relatively short flotation time of 5 minutes was chosen. This was considered to be adequate, since in the incremental tests it corresponded to an overall zinc recovery in the circuit of over 99.5%. In the other stages of flotation the Agar criterion was reached without problem. In fact, the criterion was reached so quickly in the cleaners that it was difficult to assign a correct flotation time. The point of time-zero in flotation tests is difficult to estimate accurately, and in cases where very short flotation times are required small errors in the estimation of time-zero can represent a significant proportion of the total flotation time. For example, in the second cleaner (Fig. I.6) it can be seen that a 10 second error in the estimation of the time-zero point could cause the concentrate incremental zinc grade to differ by + - 2% zinc.

In the laboratory cell the recovery rate of zinc in the cleaners was governed not by the flotability of the zinc, but by the ability of the froth to support the huge mass of floats which were collected in the froth layer within the first minute of the test. It was decided, therefore, that a small amount of time (15 to 30 seconds) should be added to the "optimum" times. The additional time is meant to help compensate for possible errors in the estimation of time-zero and for the rather unpredictable effects of operating at maximum bubble-loading and froth-collecting capacity. The optimum flotation times indicated by Figures 7.1 through 7.7 were rounded up to the nearest half minute, and are presented in Table 7.8.

TABLE 3.1: FIRST INCREMENTAL ROUGHER FLOTATION

TEST 1: ROUGHER FLOTATION

	MASS (G)	MASS%	CUM. MASS	ASSAY ZINC%	REC. ZINC	CUM. REC.	CUM. GRADE
0-1 MIN.	217.40	16.64	16.64	44.00	62.62	62.62	44.00
1-2 MIN.	74.30	5.69	22.32	37.20	18.09	80.72	42.27
2-4 MIN.	68.40	5.23	27.56	29.10	13.03	93.75	39.77
4-6 MIN.	21.80	1.67	29.23	16.00	2.28	96.03	38.41
6-8 MIN.	14.40	1.10	30.33	9.70	0.91	96.94	37.37
8-10 MIN.	16.00	1.22	31.55	5.00	0.52	97.47	36.11
SCAVENGER (4 MIN.)	18.30	1.40		6.60	0.79		
TAILS:	876.10	67.05		0.30	1.74		
RECALCULATED HEAD GRADE:				11.69			

TABLE 3.2: SECOND INCREMENTAL ROUGHER FLOTATION

TEST 2: ROUGHER FLOTATION

	MASS (G)	MASS%	CUM. MASS	ASSAY ZINC%	REC. ZINC	CUM. REC.	CUM. GRADE
0-1 MIN.	234.00	19.51	19.51	42.30	70.52	70.52	42.30
1-2 MIN.	56.80	4.73	24.24	33.20	13.44	83.96	40.52
2-4 MIN.	38.10	3.18	27.42	27.10	7.36	91.32	38.97
4-6 MIN.	32.40	2.70	30.12	20.00	4.62	95.93	37.27
6-8 MIN.	11.70	0.98	31.09	10.50	0.88	96.81	36.43
8-10 MIN.	12.00	1.00	32.09	4.40	0.38	97.18	35.43
SCAVENGER (4 MIN.)	22.30	1.86		9.20	1.46		
TAILS:	792.30	66.05		0.24	1.34		
RECALCULATED HEAD GRADE:				11.70			

TABLE 3.3: THIRD INCREMENTAL ROUGHER FLOTATION

TEST 3: ROUGHER FLOTATION

	MASS (G)	MASS%	CUM. MASS	ASSAY ZINC%	REC. ZINC	CUM. REC.	CUM. GRADE
0-1 MIN.	234.80	20.19	20.19	41.50	73.12	73.12	41.50
1-2 MIN.	64.60	5.56	25.75	33.10	16.04	89.16	39.69
2-4 MIN.	31.60	2.72	28.46	22.00	5.22	94.38	38.00
4-6 MIN.	17.30	1.49	29.95	15.00	1.95	96.33	36.80
6-8 MIN.	9.30	0.80	30.75	10.00	0.70	97.02	36.16
8-10 MIN.	4.70	0.40	31.15	4.40	0.16	97.18	35.75
SCAVENGER (4 MIN.)	10.30	0.89		13.20	1.02		
TAILS:	789.80	67.92		0.30	1.80		
RECALCULATED HEAD GRADE:				11.46			

TABLE 3.4: INCREMENTAL SCAVENGER FLOTATION

TEST 4: SCAVENGER FLOTATION

	MASS (G)	MASS%	CUM. MASS	ASSAY ZINC%	REC. ZINC	CUM. REC.	CUM. GRADE
ROUGHER:	355.20	30.19		36.10	(93.8)		
SCAV.FEED	821.50	69.81		1.03	(6.2)		
SCAV. CON	52.40	4.44		12.92	(4.9)		
0-1 MIN.	27.30	3.32	3.32	20.10	64.72	64.72	20.10
1-2 MIN.	7.20	0.88	4.20	6.60	5.61	70.33	17.28
2-3 MIN.	4.40	0.54	4.74	5.50	2.85	73.18	15.95
3-5 MIN.	8.70	1.06	5.79	4.10	4.21	77.39	13.78
5-7 MIN.	4.80	0.58	6.38	4.40	2.49	79.88	12.92
TAILS:	769.60	65.37		0.23	27.60 (1.3)		
RECALCULATED HEAD GRADE:				11.62			

TABLE 3.5: INCREMENTAL CLEANER 1 FLOTATION

TEST 5: CLEANER 1 FLOTATION

	MASS (G)	MASS%	CUM. MASS	ASSAY ZINC%	REC. ZINC	CUM. REC.	CUM. GRADE
ROUGHER:	345.50	(29.65)		37.56	(94.87)		
SCAV. :	68.30	(5.86)		7.81	(3.90)		
0-1 MIN.	258.50	74.82	74.82	44.40	88.44	88.44	44.40
1-2 MIN.	20.80	6.02	80.84	42.00	6.73	95.18	44.22
2-4 MIN.	6.90	2.00	82.84	36.70	1.95	97.13	44.04
4-6 MIN.	2.00	0.58	83.42	32.80	0.51	97.63	43.96
CLNR1 TLS	57.30	16.58		5.45		2.37	
FINAL TLS	731.60	(64.49)		0.22	(1.23)		
RECALCULATED HEAD GRADE				11.74			

TABLE 3.6: INCREMENTAL CLEANER 2 FLOTATION

TEST 6: CLEANER 2 FLOTATION

	MASS (G)	MASS%	CUM. MASS	ASSAY ZINC%	REC. ZINC	CUM. REC.	CUM. GRADE
ROUGHER:	342.55	(30.26)		37.56	(96.44)		
SCAV. :	24.62	(2.17)		7.81	(2.32)		
CLNR1 CON	315.45	(27.87)		41.00	(94.44)		
CLNR1 TLS	27.10	(2.39)		9.08	(2.00)		
0-1 MIN.	281.69	89.30	89.30	42.10	91.69	91.69	42.10
1-2 MIN.	25.84	8.19	97.49	36.00	7.19	98.89	41.59
2-4 MIN.	3.64	1.15	98.64	27.80	0.78	99.67	41.43
4-6 MIN.	0.40	0.13	98.77	-----	0.00	99.67	41.37
CLNR2 TLS	3.88	1.23		11.50	0.33		
FINAL TLS	765.10	(67.59)		0.22	(1.23)		
RECALCULATED HEAD GRADE				12.07			

TABLE 3.7: INCREMENTAL CLEANER 3 FLOTATION

TEST 7: CLEANER 3 FLOTATION

	MASS (G)	MASS%	CUM. MASS	ASSAY ZINC%	REC. ZINC	CUM. REC.	CUM. GRADE
ROUGHER:	418.27	(34.29)		33.15	(96.83)		
CLNR1 CON	357.65	(29.32)		37.76	(94.30)		
CLNR2 CON	326.42	(26.76)		38.91	(88.70)		
CLNR2 TLS	31.20	(2.56)		25.66	(5.60)		
CLNR1 TLS	60.60	(4.97)		5.98	(1.80)		
0-1 MIN.	241.10	73.86	73.86	40.28	76.46	76.46	40.28
1-2 MIN.	50.30	15.41	89.27	39.59	15.68	92.14	40.16
2-4 MIN.	18.70	5.73	95.00	36.33	5.35	97.49	39.93
4-6 MIN.	4.60	1.41	96.41	21.36	0.77	98.26	39.66
CLNR3 TLS	11.50	3,69		18.64	1.74		
FINAL TLS	801,70	(65.72)		0.56	(1.23)		
RECALCULATED HEAD GRADE				11.74			

TABLE 3.8: SUMMARY OF OPTIMUM FLOTATION TIMES

FLOTATION STAGE	OPTIMUM TIME	CORRESPONDING RECOVERY
ROUGHER :	7.0 MIN	95.9 PERCENT
SCAVENGER	5.0 MIN	56.8 "
CLEANER 1	2.5 MIN	96.9 "
CLEANER 2	1.0 MIN	93.0 "
CLEANER 3	2.5 MIN	92.1 "

FIGURE 3.3

ROUGHER: INCR. ZN GRADE VS. TIME

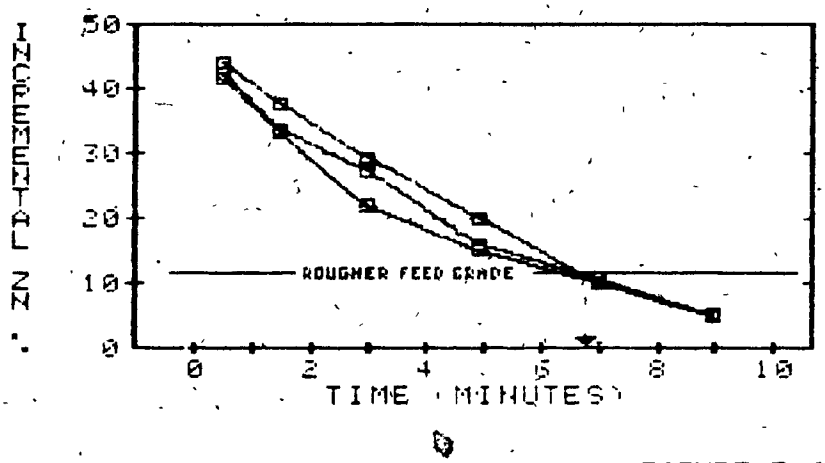

FIGURE 3.4

SCAVENGER: INCR. GRADE VS. TIME

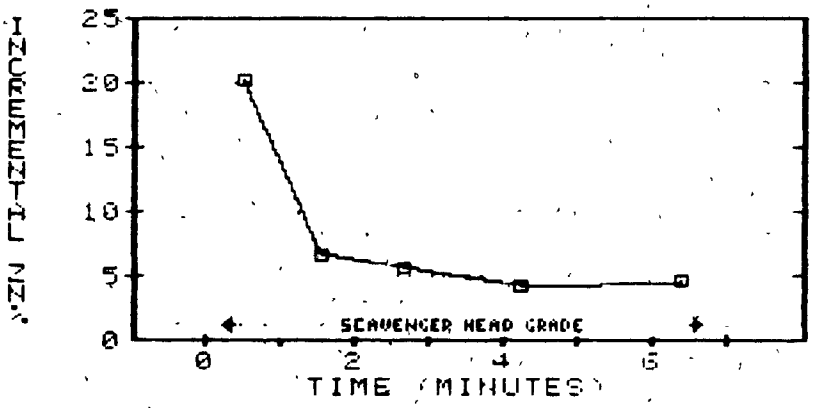

FIGURE 3.5

CLEANER 1: INCR GRADE VS. TIME

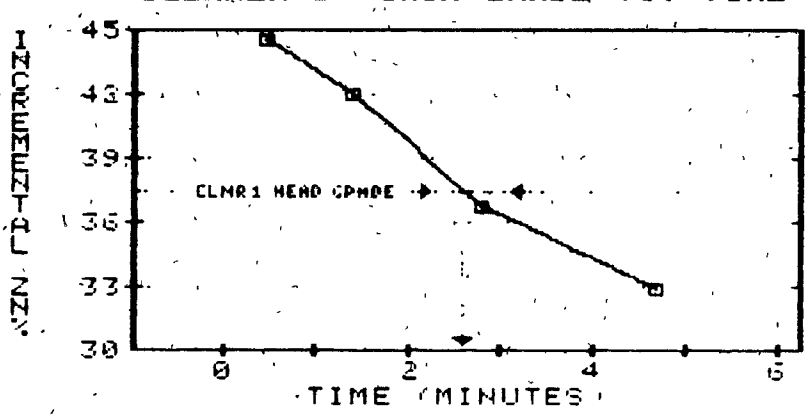

FIGURE 3.6

CLEANER 2: INCR. GRADE VS. TIME

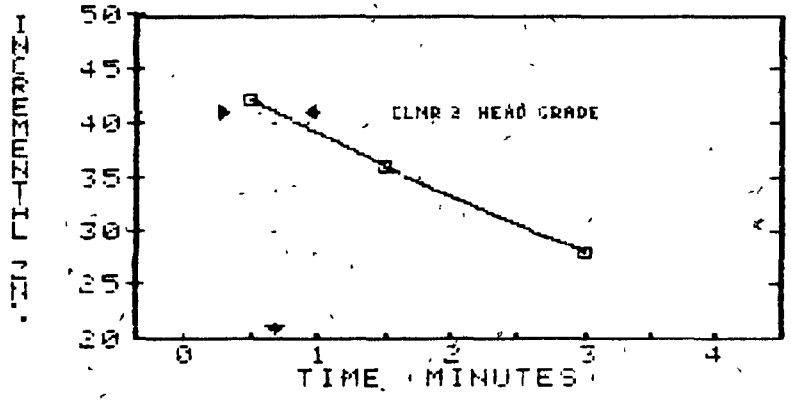

FIGURE 3.7

CLEANER 3: INCR. GRADE VS. TIME

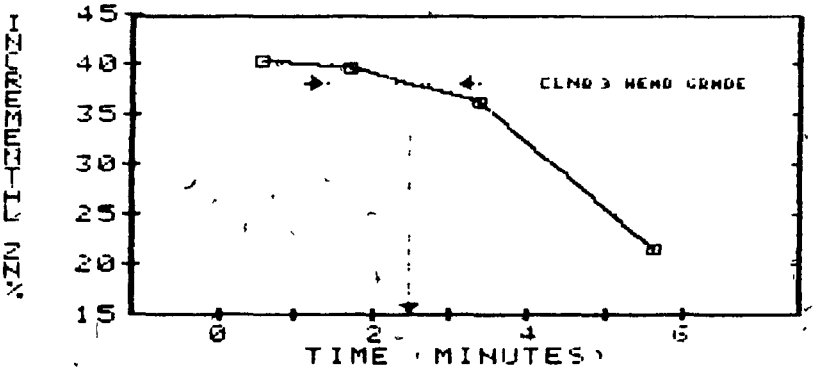

7.6 Application of the Agar Predictive Model

Agar (1978) published a mathematical model which uses the results of open cycle tests to predict the results of a locked cycle test. The development of this model became necessary when Agar wished to make predictions about plant performance using samples which were too small to use in a locked cycle test. It has been mentioned that the locked cycle procedure yields a better estimation of plant performance than does open cycle testing; however, the locked cycle procedure requires about 10-15 times as much sample as an open cycle test. It was therefore highly desirable to develop a method by which open cycle test results could be extrapolated to yield a prediction of locked cycle behaviour.

Incremental flotation tests which are performed under identical physical and chemical conditions should define fixed grade/recovery curves for each mineral in the feed. Consequently, the flotation time used at any node within a circuit should ideally have associated with it a fixed recovery for each mineral. This recovery is referred to as a split factor. In the Agar model the split factors which are calculated at each node are used to predict the cycle at which equilibrium will be reached, and the conditions which will exist at that equilibrium. A mathematical simulation of the flotation procedure is carried out by using the split factors to calculate the amount of middlings expected at each node

during the first cycle of the test. The calculations are then repeated, with the middlings inserted at appropriate points in the circuit, and the simulation is continued until the results converge upon "equilibrium" values.

It is assumed during these calculations that the split factors obtained from incremental flotation tests are fixed values, and that they are not affected by the buildup of recirculating middlings during locked cycle testing. This assumption is a fundamental (but unavoidable) weakness in the predictive power of the Agar model. For example, zinc which is found in the middlings is less flotable, on average, than zinc which reports directly to the concentrate. When this material is recirculated back to the head of a separation stage there is an inevitable lowering of the zinc split factor. Since this translates into an increased backwards flow of zinc in the circuit, zinc losses into the tailings are almost always higher than the model predicts. In a similar manner, magnesium which reaches the cleaners is more flotable, on average, than magnesium which is rejected straight away in the roughers. (The precise reason for this, "increased flotability", be it locking or whatever, is irrelevant). Thus, when middlings streams are recirculated there is a general <u>increase</u> in the magnesium split factor. Since this represents an increased forward flow of magnesium in the circuit, magnesium levels in the concentrate are usually higher than the model predicts. Thus, the Agar model predictions are generally optimistic in

grades and recoveries of concentrates, and tend to predict recirculating loads which are too low. The significance of these deviations depends highly upon the material being tested. Agar suggested the calculation of separate split factors for the recirculating streams in cases where they are significant mass.

The model developed by Agar has potential value if it can be used to accurately predict the cycle at which equilibrium will occur in a locked cycle test or, better still, if it can be used as a replacement for the test itself. In tests involving copper-nickel sulphides and a silver ore Agar evaluated the agreement between results obtained by open cycle prediction and results obtained by conducting locked cycle tests (Table 2.9). In the six tests reported by Agar the relative error in the predicted concentrate assay (defined as 100*(observed/predicted)) averaged 17%; the relative error in the tailings assay averaged 19%, and the relative error in eleven middlings assays averaged 29%. The relative errors for metal distributions in the same six tests averaged 4%, 17% and 30% for the concentrate, tailings and middlings, respectively. These results indicate that the predictive model can be used with fair accuracy to predict the final concentrate produced from a locked cycle test, but that accuracy is considerably less for the tailings and especially for the middling streams. It is likely that in cases where locked cycle testing cannot be performed it is more advantageous to use results of the

TABLE 3.9: COMPARISON BETWEEN AGAR PREDICTIVE MODEL AND LOCKED CYCLE DATA

TYPE OF ORE	STREAM	PREDICTED DIST.	OBSERVED DIST.	PERCENT DIFFERENCE	GRADE PREDICTED	GRADE OBSERVED	PERCENT DIFFERENCE
NI/CU SULPHIDE	MIDDLINGS	19.00	18.40	-3	0.46	0.34	-35
	MIDDLINGS	35.60	27.10	-31	3.82	2.23	-71
	CONC.	84.30	75.70	-11	4.97	5.81	14
	TAILS	15.60	21.20	26	0.07	0.09	22
NI/CU SULPHIDE	MIDDLINGS	23.00	34.70	34	0.63	0.66	5
	CONC.	81.10	80.80	0	6.60	4.98	-33
	TAILS	18.80	18.80	0	0.09	0.09	0
NI/CU SULPHIDE	MIDDLINGS	6.40	11.00	42	0.61	0.37	-65
	MIDDLINGS	15.60	14.90	-5	0.29	0.21	-38
	CONC.	77.70	80.00	3	4.40	4.90	10
	TAILS	22.30	19.10	-17	0.11	0.09	-22
NI/CU SULPHIDE	MIDDLINGS	2.10	3.70	43	0.25	0.41	39
	MIDDLINGS	1.20	1.60	25	0.58	0.62	6
	CONC.	94.80	91.60	-3	3.33	3.56	6
	TAILS	5.20	8.40	38	0.08	0.12	33
NI/CU SULPHIDE	MIDDLINGS	3.30	7.70	57	0.50	0.82	39
	MIDDLINGS	2.20	5.90	63	1.34	1.61	17
	CONC.	90.00	86.70	-1	3.85	3.40	-13
	TAILS	9.90	11.30	12	0.15	0.18	17
AG EXPLORATION SAMPLE	MIDDLINGS	3.20	3.40	6	(AG) 123	(AG) 128	4
	MIDDLINGS	11.90	9.80	-21	(PPM) 391	(PPM) 360	-3
	CONC.	84.40	85.60	1	40	39	-3
	TAILS	15.60	14.40	-8	11100	13700	19

(after AGAR, 1978)

Agar predictive model than to use the unadjusted results of open cycle testing; however, for many applications deviations such as those observed in the tests performed by Agar are too high to merit the abandonment of locked cycle testing in cases where there exists sufficient material for the locked cycle procedure to be performed.

Agar sought to improve the predictive value of his model by generating secondary split factors for a nickel-copper ore such as that used in the experiments of Table 3.9. The middling streams were floated and assigned their own split factors. It was found that the secondary split factors were almost identical to the primary split factors, and that no significant improvements were made over the initial prediction. This result suggests that the difference between predicted and observed results was caused by a sensitivity of the material to small changes in the operating procedure rather than by a fundamental weakness in the predictive model.

3.7 Evaluation of Sources of Error in Locked Cycle Testing

There are two distinct types of error which can contribute to deviations between predictions of the Agar model and actual locked cycle results. These are external errors caused by slight changes in the air flow rate, impeller speed etc., and intrinsic errors generated by variable flotation of the feed under absolutely identical operating conditions. In a single flotation test there is no deviation caused by intrinsic errors; however, in locked cycle flotation where the nature of the feed to any one stage changes from cycle to cycle one cannot make this assumption. The Agar model is potentially useful as a model to predict locked cycle behaviour so long as any one of the following conditions are met:

a) The intrinsic errors are small or constant for a wide variety of ores, thus allowing for some type of empirical correction factor to be established.
b) The intrinsic errors can be quantified by the generation of secondary split factors.
c) The intrinsic errors are within the confidence limits which are desired in the prediction.

In order to evaluate the intrinsic errors associated with the application of locked cycle predictions to Pine Point ore it is necessary to develop some sort of range within which the results could vary due to experimental procedure alone. Any

variation beyond this range can be attributed to intrinsic sources of variation. There is a limited amount of replicate data from the incremental flotation tests which can be used to establish a rough estimate of the reproducability of flotation results during locked cycle testing.

The results of the seven incremental flotation tests are summarized in Table 3.10. Four pieces of information are provided for each flotation stage. These are recovery of zinc at the optimum flotation time (ie. the split factor), cumulative grade of the concentrate collected up to the optimum flotation time, the percent mass recovery associated with this cutoff time (expressed as a percent of the initial feed mass), and the recalculated zinc head grade going into the separation stage.

The information in Table 3.10 was used to calculate the average split factors and the standard deviations of split factors for zinc and for mass at each node. These results are presented in Table 3.11. The number of trials upon which each split factor/standard deviation were based varied from seven for the rougher flotation (which had to be performed in each of the seven tests) to only one for the third cleaner flotation (which was performed only in the last test). The standard deviations of the split factors for the second and third cleaners could not be calculated due to an insufficient amount of replicate tests, and were therefore estimated using the calculated standard deviation of the rougher split factor

TABLE 3.10 SUMMARY OF INCREMENTAL FLOTATION RESULTS

		TEST1	TEST2	TEST3	TEST4	TEST5	TEST6	TEST7
CLNR 3:	RECOVERY:	-----	-----	-----	-----	-----	-----	81.70
------	GRADE:	-----	-----	-----	-----	-----	-----	40.20
	%MASS REC	-----	-----	-----	-----	-----	-----	23.80
	HEAD:	-----	-----	-----	-----	-----	-----	37.80
CLNR 2:	RECOVERY:	-----	-----	-----	-----	-----	86.80	88.70
------	GRADE:	-----	-----	-----	-----	-----	42.10	38.90
	%MASS REC	-----	-----	-----	-----	-----	24.90	26.70
	HEAD:	-----	-----	-----	-----	-----	41.00	37.80
CLNR 1:	RECOVERY:	-----	-----	-----	-----	90.60	94.40	94.30
------	GRADE:	-----	-----	-----	-----	44.20	41.00	37.80
	%MASS REC	-----	-----	-----	-----	25.70	24.90	29.30
	HEAD:	-----	-----	-----	-----	37.60	38.54	33.20
ROUGHER:	RECOVERY:	96.50	96.40	96.60	93.80	94.87	96.44	96.80
-------	GRADE:	37.90	36.90	36.50	36.10	37.55	38.54	33.15
	%MASS REC	29.80	30.60	30.40	30.19	29.65	30.25	34.29
	HEAD:	11.69	11.70	11.46	11.62	11.74	12.07	11.74
SCAV.:	RECOVERY:	32.00	54.00	36.00	77.00	77.00	65.00	-----
-----	GRADE:	6.60	9.20	13.20	13.80	7.80	12.90	-----
	%MASS REC	1.40	1.90	0.90	4.00	5.90	2.20	-----
	HEAD:	0.58	0.61	0.56	1.03	0.80	0.62	0.56
TAILS:	RECOVERY:	1.70	1.30	1.80	1.50	1.20	1.20	-----
-----	GRADE:	0.30	0.24	0.30	0.26	0.22	0.22	-----

TABLE 3.11 SPLIT FACTORS FOR ZINC AND FOR MASS WITH STANDARD DEVIATIONS

STREAM	NUMBER OF TRIALS	%ZN FLOATS (SPLT FCTR)	STANDARD DEVIATION	%MASS FLTS (SPLT FCTR)	STANDARD DEVIATION
ROUGHER	7	0.959	0.011	0.308	0.016
SCAVENGER	6	0.568	0.197	0.036	0.021
CLEANER 1	3	0.969	0.013	0.881	0.036
CLEANER 2	2	0.930	(0.015)	0.902	(0.015)
CLEANER 3	1	0.921	(0.015)	0.891	(0.015)

(the most confident value available).

The zinc split factors were used according to the Agar procedure to calculate the expected amount of recirculating zinc in each middlings stream and in the concentrate and tails (Table 3.12). A similar set of calculations was performed for mass (Table 3.13). It can be seen from either of the tables that equilibrium should be reached in the fourth cycle of the locked cycle test. It was decided to perform the test for seven cycles in the hope of obtaining three sets of replicate data.

Tables 3.14 and 3.15 present the standard deviations of the predicted zinc and mass flow rates, calculated from the data of Tables 3.11, 3.12 and 3.13. At junctions where two or more streams are merged (such as the feed to the first cleaner) the variance of the flow rate is equal to the sum of the flow rate variances of the component streams. At the five separation stages the variances of the concentrate and tailings flow rates can be obtained by applying a Taylor series expansion as follows:

For the concentrate:

$$CON = FEED * SF \quad (SF = \text{split factor})$$

$$VAR(CON) = (VAR(FEED)^2 * SF) + (VAR(SF)^2 * FEED)$$

TABLE 3.12 PREDICTED ZINC FLOW THROUGH CIRCUIT

UNITS OF ZINC, WHERE 100 UNITS ARE ADDED TO THE ROUGHER EACH CYCLE

STREAM	CYCLE1	CYCLE2	CYCLE3	CYCLE4	CYCLE5	CYCLE6	CYCLE7	CYCLE8
RGHR FEED	100.00	105.30	106.00	106.11	106.13	106.14	106.14	106.14
RGHR FLTS	95.90	100.98	101.65	101.76	101.78	101.78	101.78	101.78
RGHR TLS	4.10	4.32	4.35	4.35	4.35	4.35	4.35	4.35
SCAV FEED	4.10	4.32	4.35	4.35	4.35	4.35	4.35	4.35
SCAV FLTS	2.33	2.45	2.47	2.47	2.47	2.47	2.47	2.47
SCAV TLS	1.77	1.87	1.88	1.88	1.88	1.88	1.88	1.88
CLN1 FEED	95.90	114.32	117.54	118.10	118.20	118.22	118.22	118.22
CLN1 FLTS	92.93	110.77	113.90	114.44	114.54	114.55	114.55	114.56
CLN1 TLS	2.97	3.54	3.64	3.66	3.66	3.66	3.66	3.66
CLN2 FEED	92.93	110.77	113.90	114.44	114.54	114.55	114.55	114.56
CLN2 FLTS	86.42	103.02	105.93	106.43	106.52	106.53	106.54	106.54
CLN2 TLS	6.50	7.75	7.97	8.01	8.02	8.02	8.02	8.02
CLN3 FEED	86.42	103.02	105.93	106.43	106.52	106.53	106.54	106.54
CLN3 FLTS	79.59	94.88	97.56	98.02	98.10	98.12	98.12	98.12
CLN3 TLS	6.83	8.14	8.37	8.41	8.41	8.42	8.42	8.42

TABLE 3.13 PREDICTED MASS FLOW THROUGH CIRCUIT

UNITS OF MASS, WHERE 100 UNITS ARE ADDED TO THE ROUGHER EACH CYCLE

STREAM	CYCLE1	CYCLE2	CYCLE3	CYCLE4	CYCLE5	CYCLE6	CYCLE7	CYCLE8
RGHR FEED	100.00	106.16	107.17	107.38	107.42	107.44	107.44	107.44
RGHR FLTS	30.80	32.70	33.01	33.07	33.09	33.09	33.09	33.09
RGHR TLS	69.20	73.46	74.16	74.31	74.34	74.35	74.35	74.35
SCAV FEED	69.20	73.46	74.16	74.31	74.34	74.35	74.35	74.35
SCAV FLTS	2.49	2.64	2.67	2.68	2.68	2.68	2.68	2.68
SCAV TLS	66.71	70.82	71.49	71.63	71.66	71.67	71.67	71.67
CLN1 FEED	30.80	38.02	39.58	39.92	39.99	40.01	40.01	40.01
CLN1 FLTS	27.13	33.50	34.87	35.17	35.23	35.25	35.25	35.25
CLN1 TLS	3.67	4.52	4.71	4.75	4.76	4.76	4.76	4.76
CLN2 FEED	27.13	33.50	34.87	35.17	35.23	35.25	35.25	35.25
CLN2 FLTS	24.48	30.22	31.46	31.72	31.78	31.79	31.79	31.80
CLN2 TLS	2.66	3.28	3.42	3.45	3.45	3.45	3.45	3.45
CLN3 FEED	24.48	30.22	31.46	31.72	31.78	31.79	31.79	31.80
CLN3 FLTS	21.81	26.92	28.03	28.26	28.32	28.33	28.33	28.33
CLN3 TLS	2.67	3.29	3.43	3.46	3.46	3.47	3.47	3.47

TABLE 3.14 STD. DEVIATION OF ZINC FLOW DUE TO EXPERIMENTAL (EXTERNAL) VARIATION

RELATIVE STANDARD DEVIATION OF PREDICTED ZINC FLOW PERCENT)

STREAM	CYCLE1	CYCLE2	CYCLE3	CYCLE4	CYCLE5	CYCLE6	CYCLE7	CYCLE8
RGHR FEED	1.54	2.12	2.26	2.29	2.29	2.29	2.29	2.29
RGHR FLTS	1.92	2.41	2.54	2.56	2.56	2.56	2.56	2.56
RGHR TLS	26.87	26.91	26.92	26.93	26.93	26.93	26.93	26.93
SCAV FEED	26.87	26.91	26.92	26.93	26.93	26.93	26.93	26.93
SCAV FLTS	43.88	43.90	43.91	43.91	43.91	43.91	43.91	43.91
SCAV TLS	52.93	52.95	52.96	52.96	52.96	52.96	52.96	52.96
CLN1 FEED	1.92	2.71	2.94	2.98	2.99	2.99	2.99	2.99
CLN1 FLTS	2.34	3.02	3.23	3.27	3.27	3.27	3.28	3.28
CLN1 TLS	41.98	42.02	42.04	42.04	42.04	42.04	42.04	42.04
CLN2 FEED	2.34	3.02	3.23	3.27	3.27	3.27	3.28	3.28
CLN2 FLTS	2.84	3.43	3.61	3.64	3.65	3.65	3.65	3.65
CLN2 TLS	21.56	21.64	21.67	21.68	21.68	21.68	21.68	21.68
CLN3 FEED	2.84	3.43	3.61	3.64	3.65	3.65	3.65	3.65
CLN3 FLTS	3.28	3.79	3.96	3.99	4.00	4.00	4.00	4.00
CLN3 TLS	19.20	19.29	19.33	19.33	19.33	19.34	19.34	19.34

TABLE 3.15 STD. DEVIATION OF MASS FLOW DUE TO EXPERIMENTAL (EXTERNAL) VARIATION

RELATIVE STANDARD DEVIATION OF PREDICTED MASS FLOW (PERCENT)

STREAM	CYCLE1	CYCLE2	CYCLE3	CYCLE4	CYCLE5	CYCLE6	CYCLE7	CYCLE8
RGHR FEED	0.00	1.73	1.94	1.98	1.99	1.99	1.99	1.99
RGHR FLTS	5.19	5.48	5.54	5.56	5.56	5.56	5.56	5.56
RGHR TLS	2.31	2.89	3.02	3.04	3.05	3.05	3.05	3.05
SCAV FEED	2.31	2.89	3.02	3.04	3.05	3.05	3.05	3.05
SCAV FLTS	58.38	58.40	58.41	58.41	58.41	58.41	58.41	58.41
SCAV TLS	3.18	3.62	3.72	3.74	3.75	3.75	3.75	3.75
CLN1 FEED	5.19	4.97	4.99	5.00	5.00	5.00	5.00	5.00
CLN1 FLTS	6.60	6.43	6.44	6.45	6.45	6.45	6.45	6.45
CLN1 TLS	30.63	30.59	30.59	30.59	30.59	30.59	30.59	30.59
CLN2 FEED	6.60	6.43	6.44	6.45	6.45	6.45	6.45	6.45
CLN2 FLTS	6.81	6.64	6.65	6.66	6.66	6.66	6.66	6.66
CLN2 TLS	16.67	16.60	16.61	16.61	16.61	16.61	16.61	16.61
CLN3 FEED	6.81	6.64	6.65	6.66	6.66	6.66	6.66	6.66
CLN3 FLTS	7.01	6.85	6.86	6.87	6.87	6.87	6.87	6.87
CLN3 TLS	15.35	15.28	15.29	15.29	15.29	15.29	15.29	15.29

and for the tailings:

$$TAILS = FEED * (1-SF)$$

$$VAR(TAILS) = [VAR(FEED) * (1-SF)^2] + [VAR(1-SF) * FEED^2]$$

Table 3.16 presents predicted assays of the various streams at equilibrium. Confidence intervals for the assay predictions cannot be calculated from the available data since the assays are predicted as:

Assay = 11.71% * (zinc flow / mass flow)

Zinc flow and mass flow exhibit an unknown degree of covariance, thereby rendering uncertain any calculated confidence intervals. Thus, the Agar model must be tested in terms of zinc and mass flows rather than in terms of assays.

The confidence intervals reported in Tables 3.14 and 3.15 are crude, in that they ignore much of the fundamental nature of the flotation process. In a case where several replicate flotation tests are performed there will always be slight variations in individual cell performances between tests. These variations usually cause compensating adjustments in subsequent flotation stages. For example, if the rougher entrains a little more gangue than normal in one of the flotation tests then the first cleaner is expected to reject it. If the rougher floats less zinc then the scavenger should recover it. The statistical confidence intervals which are presented do not take covariance into account. The omission is

TABLE 3.16 ZINC ASSAYS PREDICTED BY MODEL

PREDICTED ZINC ASSAYS, AS PERCENT ZINC METAL BY MASS.

STREAM	CYCLE1	CYCLE2	CYCLE3	CYCLE4	CYCLE5	CYCLE6	CYCLE7	CYCLE8
RGHR FEED	11.72	11.63	11.59	11.58	11.58	11.58	11.58	11.58
RGHR FLTS	36.49	36.20	36.09	36.06	36.05	36.05	36.05	36.05
RGHR TLS	0.69	0.69	0.69	0.69	0.69	0.69	0.69	0.69
SCAV FEED	0.69	0.69	0.69	0.69	0.69	0.69	0.69	0.69
SCAV FLTS	10.96	10.87	10.84	10.83	10.82	10.82	10.82	10.82
SCAV TLS	0.31	0.31	0.31	0.31	0.31	0.31	0.31	0.31
CLN1 FEED	36.49	35.24	34.80	34.67	34.64	34.63	34.63	34.63
CLN1 FLTS	40.14	38.76	38.28	38.14	38.10	38.09	38.09	38.09
CLN1 TLS	9.51	9.18	9.07	9.03	9.02	9.02	9.02	9.02
CLN2 FEED	40.14	38.76	38.28	38.14	38.10	38.09	38.09	38.09
CLN2 FLTS	41.38	39.96	39.47	39.32	39.28	39.27	39.27	39.27
CLN2 TLS	28.67	27.68	27.34	27.24	27.21	27.21	27.21	27.21
CLN3 FEED	41.38	39.96	39.47	39.32	39.28	39.27	39.27	39.27
CLN3 FLTS	42.78	41.30	40.79	40.65	40.61	40.60	40.59	40.59
CLN3 TLS	29.99	28.96	28.60	28.50	28.47	28.46	28.46	28.46

unavoidable since the covariances cannot be determined without lengthy experimentation. The estimated confidence intervals are therefore large compared to the actual variation which is expected. For example, zinc recovery in the rougher was found by experimentation to be 96% +/- 2%; however, the overall recovery of the circuit (calculated by the sum-of-variances method) has a confidence interval of 98% +/- 8%. (Tables 7.12, 7.14). Since the amount of variance contributed by external error is overestimated, results which fall outside of the calculated confidence intervals are likely to reveal significant amounts of intrinsic error.

7.8 Verification of Equilibrium Conditions and Test of the Agar Model

The primary objective of this section is to introduce some of the results of the locked cycle test and to verify that equilibrium conditions were reached within the seven cycle duration of the test. These results are compared with the Agar predictions made for mass and zinc flow in the circuit, with the object of determining the confidence with which the model can be used to predict performance during locked cycle flotation of this material. The following streams were collected during the test:

- Concentrates for cycles 1 through 7.
- Tailings for cycles 1 through 7.
- Middlings for cycle 7 scavenger and for the three

cleaners.

Details of the procedure used in the locked cycle test are summarized in Appendix I. The concentrates and middlings were screened so that size-by-size performance of the circuit could be evaluated. An unknown amount of mass was lost from the cycle 4 concentrate during screening and caused some anomalous data points pertaining to that cycle in the figures which follow.

The masses of material collected from each of the streams are shown in Table I.17. The overall mass recovery in the test was 97.45%, with the 2.55% mass loss distributed in unknown proportions between mass loss in the leach and mass loss during handling and filtration of the samples. In order to compare observed recoveries with those predicted by the model all data was scaled up by (1/0.9745) in Table I.18.

The occurrence of equilibrium can be detected using any of several criteria, two of which have been previously discussed. Equilibrium can be detected by any of the following:

- Mass flow in any one stream becomes constant.
- Zinc flow in any one stream becomes constant.
- The wieghted sum of the concentrate and tailings assays equals the feed grade.
- Assays in any one stream become constant.

TABLE 3.17 MASS RECOVERY IN LOCKED CYCLE TEST

CYCLE #	TOTAL G OF FEED	TOTAL G RECOVRD	MASS RECOVERED IN GRAMS CON+400	CON-400	TLS+400	TLS-400
CYCLE 1	1168	1009	170.1	60.6	519.6	258.9
CYCLE 2	1161	1080	208.8	74.7	532.6	264.0
CYCLE 3	1145	1084	223.3	63.8	527.4	269.6
CYCLE 4	1163	1097	233.7	54.2	525.6	283.0
CYCLE 5	1149	1111	228.1	59.9	528.4	294.8
CYCLE 6	1155	1131	223.8	78.0	530.1	299.2
CYCLE 7	1165	1114	227.9	71.7	545.2	269.0
SCAV.CON:		30.4	14.92	15.48		
CLN1 TLS:		146.8	11.48	135.32		
CLN2 TLS:		33.8	4.20	29.60		
CLN3 TLS:		62.5	8.26	54.24		

TOTALS:	MASS IN	MASS OUT	MASS RECOVERY
	8106	7900	97.45%

TABLE 3.18 ADJUSTED MASS RECOVERY VS. MODEL PREDICTIONS

CYCLE #	TOTAL G OF FEED	TOTAL G RECOVRD	RECOVRY INTO IN. CON	MODEL ZINC CONC.	RECOVRY INTO TAILS	MODEL TAILS	TOTAL RECOVRY CON+TLS	MODEL RECOVRY CON+TLS
CYCLE 1	1168	1036	20.28	21.81	68.43	66.71	88.70	88.52
CYCLE 2	1161	1108	25.06	26.92	70.40	70.82	95.46	97.74
CYCLE 3	1145	1112	25.73	28.03	71.42	71.49	97.14	99.52
CYCLE 4	1163	1125	25.40	28.26	71.33	71.63	96.73	99.89
CYCLE 5	1149	1140	25.72	28.32	73.52	71.66	99.24	99.98
CYCLE 6	1155	1161	26.82	28.33	73.69	71.67	100.50	100.00
CYCLE 7	1165	1143	26.39	28.33	71.70	71.67	98.09	100.00

	MASS RECOVERED	MODEL PREDICT.	MODEL STD.DEV	STD. DEV. DIFFERENCE (OBSERVED VS. MODEL)
SCAV CON	31.20	31.11	18.30	0.08
CLNR1 TLS	150.64	55.46	16.97	5.61
CLNR2 TLS	34.68	40.20	6.68	-0.83
CLNR3 TLS	64.14	40.32	6.16	3.86

Determination of Equilibrium by Mass Recovery:

Figure 3.8 shows the mass of concentrate recovered in cycles 1 through 7. It can be seen that the concentrate mass stabilized at the third cycle, but that this equilibrium mass was significantly lower than the mass recovery predicted by the model. The equilibrium recovery of mass into the concentrate was 26.0% +/- 0.8%, as compared to the predicted recovery of 28.4% +/- 1.6%.

Figure 3.9 presents similar data for the mass of tailings leaving the system. Five of the seven cycles showed tailings masses which closely followed the predicted mass recovery of 71.6%; however, the fifth and sixth cycles showed an increase in tailings mass to approximately 2% over the predicted value. This increase lies within the statistical confidence limit of the prediction.

Variations in mass flow within the circuit can be clarified by examining the separate behaviour of coarse and fine particles. Individual coarse (+400 mesh) and fine (-400 mesh) size fractions should not necessarily exhibit mass recoveries which are identical to those predicted for total mass recovery, since the split factors calculated for each node are equivalent to the weighted sum of split factors from individual size classes, each of which can respond to flotation in a different manner.

It is common experience that fines are recovered at a slower rate than coarse size fractions. The difference in

FIGURE 3.8

REAL VS. PREDICTED MASS IN FINAL CON

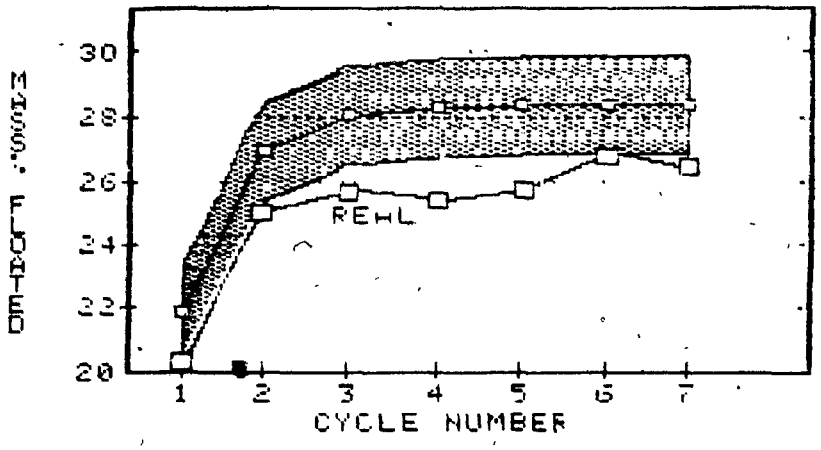

FIGURE 3.9

REAL VS. PREDICTED MASS IN FINAL TAILS

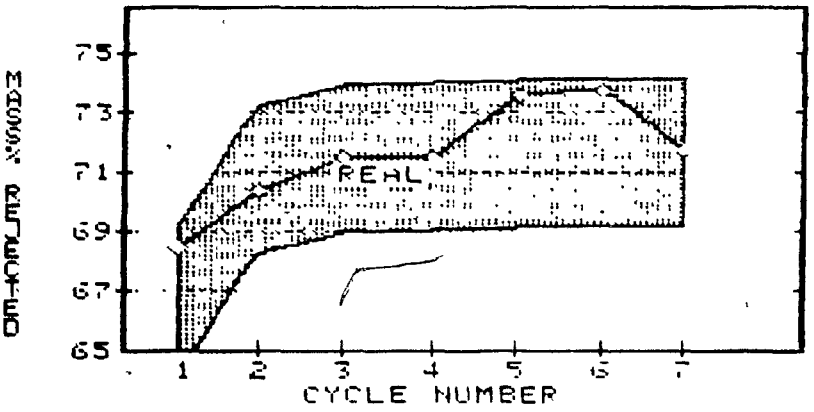

SHADED AREAS SHOW CONFIDENCE INTERVALS CALCULATED IN PREVIOUS SECTION

recovery is especially evident in circuits such as this experimental circuit where short flotation times are used. Thus, the split factors of the coarse size classes are usually higher than the overall split factor while the split factors of the fine material usually fall below it. A buildup of fine recirtulating loads in the circuit usually lowers the overall split factor below the predicted value.

Figures 3.10 and 3.11 show the masses of sized concentrate and tailings, respectively, which were recovered in cycles 1 through 7. It can be seen in both figures that the coarse material followed the predicted mass recoveries fairly closely, while the partitioning of fine material between the concentrate and the tailings tended to fluctuate. The coarse material appeared to reach equilibrium at about the third or fourth cycle of the test, while the fine material seemed not to equilibrate at all. The fluctuations in mass partitioning which can be seen in Figures 3.8 and 3.9 are caused almost exclusively by the variable behaviour of the -400 mesh size classes.

There were no changes in operating conditions during the test which could explain the variable behaviour observed in the fine sizes. It is possible that the -400 mesh particles were sensitive to subtle changes in operating parameters at a level finer than that to which the experiment could be controlled. It is the opinion of the author that the fluctuations could be caused by slight changes either in

FIG. 3.10 REAL VS. MODEL RECOVERY OF MASS IN CONCENTRATE

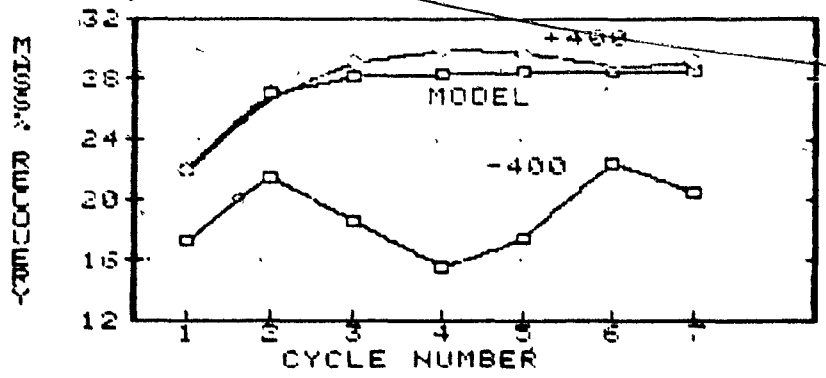

FIG. 3.11 REAL VS. MODEL RECOVERY OF MASS IN TAILINGS

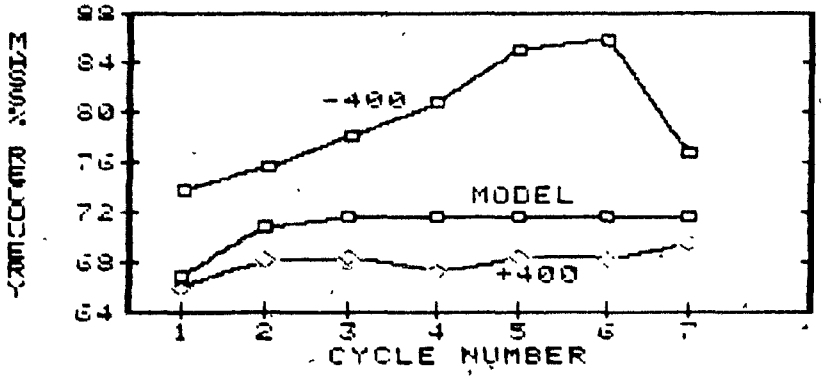

flotation time or in frother concentration in the cell. The difficulties in establishing exact flotation times have been previously mentioned. Frother concentration in the flotation cell represents a second potential source of variation since a certain amount of frother is recirculated with the middlings. The exact amount of recirculating frother varies with the amount of water in the middlings pulp.

The masses found in the recirculating loads at the end of Cycle 7 are reported at the bottom of Table 3.18. It can be seen that the masses of middlings found in the scavenger concentrate and in the second cleaner tailings were both very close to the predicted values. The first and third cleaner tailings, however, both contained masses well in excess of those which were expected. The first cleaner tailings had almost three times the expected mass (5.6 standard deviations over the prediction) while the third cleaner tailings contained over 1.5 times the expected mass (3.9 standard deviations away from the prediction). Examination of Table 3.17 shows that the vast majority of the recirculating material was of a size less than 400 mesh; thus it can be concluded that performance of the -400 mesh material caused statistically significant departures from predicted mass flows not only in the concentrate but also in the first and third cleaner tailings. Fine particle flotation performance therefore contributed a significant amount of intrinsic error which caused departures from the model predictions.

Determination of Equilibrium by Zinc Flow:

Table 3.19 presents assay data for the various streams in the test. These assays were combined with the mass recovery data of Table 3.17 to calculate zinc flow through the system.

Figure 3.12 shows the flow of zinc into the concentrate. It can be seen that the zinc flow stabilizes at about the third cycle, indicating that equilibrium was attained by that point. The small dip in zinc recovery which can be seen in the fourth cycle is undoubtedly due to the loss of part of the concentrate which occurred during screening.

The overall recovery of zinc in the circuit was lower than expected. Since 100 "zinc units" were added to the cell in each cycle, the amount of units found in the concentrate is equivalent to the zinc recovery. Recovery was low in the first few cycles due to retention of zinc in the recirculating loads. After equilibrium was reached zinc recovery stabilized at about 94.3%. This is well below the recovery of 98.1% predicted by the model though still within the calculated confidence interval.

Figure 3.13 illustrates zinc flow in the tailings. The zinc losses experienced in the circuit fluctuated from about 2% to 5%, with three of the data points showing zinc losses which were significantly higher than predicted. Zinc flow into the tailings seemed not to reach equilibrium, but varied in an unpredictable manner.

The separate contributions of +400 mesh and -400 mesh

TABLE 3.19 ZINC ASSAYS AND CALCULATED ZINC FLOW

	PERCENTAGE ZINC IN CON AND TAILS				ZINC FLOW IN CON AND TAILS			
	+400 ZN CON	-400 ZN CON	+400 TAILS	-400 TAILS	+400 ZN CON	-400 ZN CON	+400 TAILS	-400 TAILS
CYCLE 1	42.58	37.34	0.63	0.92	15.34	6.00	51.49	27.17
CYCLE 2	41.84	38.72	0.30	0.73	19.33	6.92	49.31	24.44
CYCLE 3	43.78	39.60	0.16	0.68	20.60	5.89	48.65	24.87
CYCLE 4	43.31	39.31	0.23	0.75	20.40	4.94	47.93	26.72
CYCLE 5	44.04	38.91	0.31	1.22	20.53	5.39	47.55	26.53
CYCLE 6	42.57	37.19	0.17	1.98	19.79	6.90	46.87	26.45

	TOTAL ZN CON ASSAY	TOTAL TAILS ASSAY	TOTAL FLOW IN ZN CON	MODEL FLOW IN ZN CON	TOTAL FLOW IN TAILS	MODEL FLOW IN TAILS
CYCLE 1	41.11	0.73	71.17	79.59	4.26	1.77
CYCLE 2	41.02	0.44	87.77	94.88	2.65	1.87
CYCLE 3	42.85	0.34	94.14	97.56	2.07	1.88
CYCLE 4	42.53	0.42	94.24	98.02	2.56	1.88
CYCLE 5	42.97	0.64	94.39	98.10	4.02	1.88
CYCLE 6	41.18	0.82	94.30	98.12	5.16	1.88

	TOTAL ASSAY	+400 FLOW IN ZN CON	-400 FLOW IN ZN CON	+400 FLOW IN TAILS	-400 FLOW IN TAILS
CYCLE 1	38.83				
CYCLE 2	39.83	55.76	19.15	2.77	2.13
CYCLE 3	41.94	69.07	22.87	1.26	1.52
CYCLE 4	41.82	77.01	19.90	0.66	1.44
CYCLE 5	41.24	75.46	16.59	0.94	1.71
CYCLE 6	39.09	77.20	17.91	1.26	2.76
		71.93	21.90	0.68	4.47

FIG. 3.12 REAL VS. MODEL ZINC FLOW IN CONCENTRATE

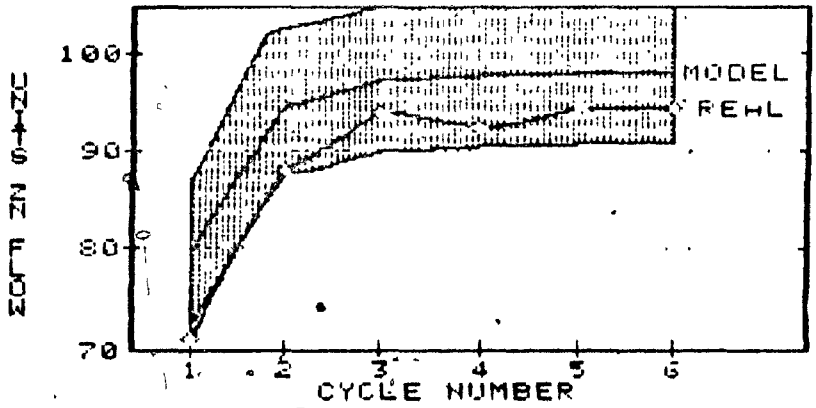

FIG. 3.13 REAL VS MODEL ZINC FLOW IN TAILINGS

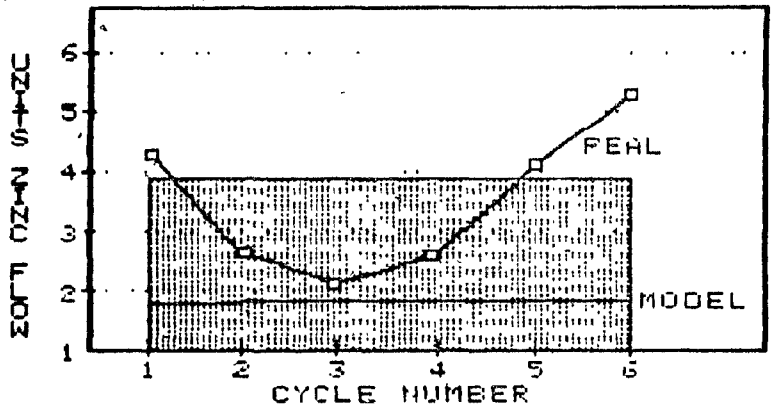

zinc to total zinc flow in the tailings are presented in Table 3.19 and illustrated in Figure 3.14. The figure reveals variability in both coarse and fine zinc loss; however, the most significant variations and the most significant zinc losses were experienced in the fine sizes. Fine (-400 mesh) material made up only about one third of the tailings; however the fine tailings contained an average of two thirds of the total unrecovered zinc.

Determination of Equilibrium by Recalculated Assays:

A final test for equilibrium can be conducted by using the weighted sums of the concentrate and tailings assays to recalculate the assays of material leaving the circuit. The recalculated head assay is expected to equal the feed assay when the recirculating loads have attained an equilibrium mass and composition.

The weighted sums of the concentrate and tailings assays are calculated in Table 3.19, and are presented in Figure 3.15. It can be seen that the recalculated head assay quickly reached the feed grade by the third cycle. Apart from the "bump" caused by the loss of mass from the cycle 4 concentrate, the recalculated grade of material leaving the system remained almost exactly equal to the feed grade after the third cycle of the test. The recalculated grades of material leaving cycles 3, 5, and 6 were 11.60%, 11.61% and 11.59% zinc respectively, as compared the feed grade of 11.72%

FIG. 3.14 FLOW OF -400 AND +400 MESH ZINC UNITS INTO TAILINGS

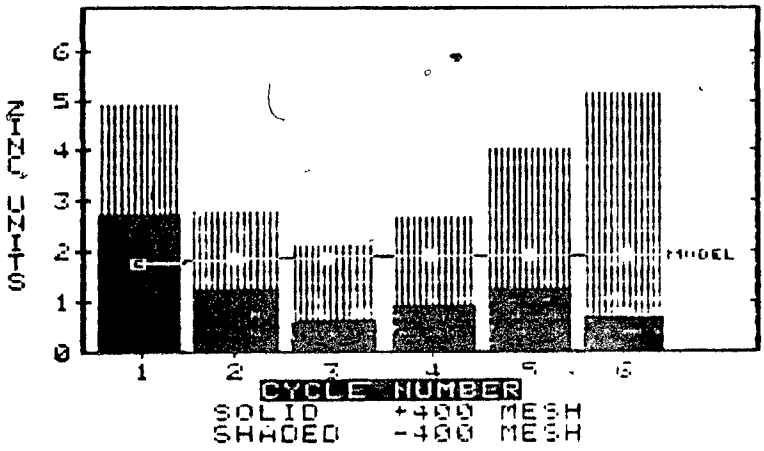

FIG. 3.15 RECALCULATED ZN GRADE OF MATERIAL LEAVING SYSTEM

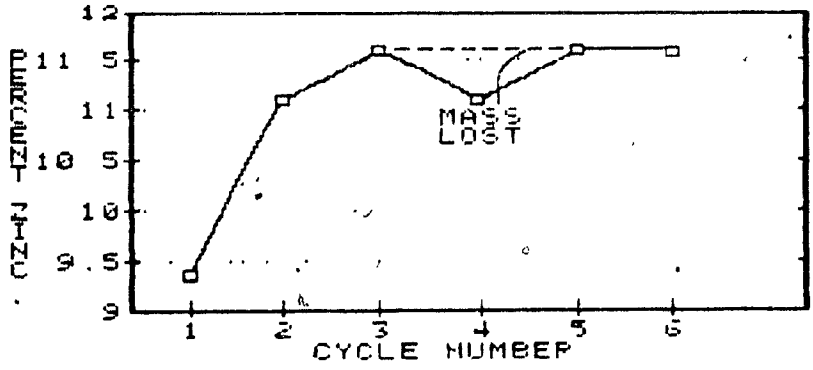

11.72% +/- 0.20% which was calculated during the incremental flotation tests.

One of the objectives of this test is the examination of the recirculating loads around the cleaners; however, it has been observed that the recirculating loads consist almost entirely of fine (-400 mesh) material, which showed erratic recoveries. One can consider the following possibilities:

1) The recirculating loads randomly recharge and discharge fines, thereby causing fluctuations in not only the concentrate and tailing assays, but also in the composition of the recirculating loads themselves.
2) The recirculating loads have an essentially constant composition, but the rougher shows variable performance and experiences variable zinc loss.

Of these two possibilities the former makes interpretation of the locked cycle results difficult, while the latter does not significantly affect the analysis.

Considering the circuit arrangement in the locked cycle test, one can see that if material is rejected in the cleaners (ie. if a "surplus" is built up in the recirculating loads) it can not leave the circuit until at least the following cycle. Similarly, if material is discharged for some reason from the cleaners then this material cannot be recharged until the next

cycle of the test is performed. The result of the first situation is that zinc "disappears" from the concentrate for one cycle and reappears in either the concentrate or in the tailings during subsequent cycles. Thus, the recalculated head grade should show a dip below the actual feed grade during the cycle in which the recirculating load is charged, and an increase over the actual feed grade during the cycle in which the recirculating loads discharge back to their equilibrium masses and compositions. Similarly, in the second situation discharged material should cause a rise in the recalculated feed grade, then in the following cycle the recharge of the recirculating loads should cause a drop in the recalculated feed grade for that cycle.

The data presented in Figure 3.15 reveals no fluctuations such as those just described. Since it is impossible for the recirculating loads to vary significantly without causing this "hill and trough" effect, it can be concluded that the erratic behaviour of the fines was caused by variable rougher performance. Material which passed the rougher can be assumed to have followed the "normal" processing route without causing any significant recharge or discharge of the recirculating loads.

Summary of Equilibrium Conditions and the Agar Model:

Data on the flow rates of mass and zinc into the concentrate and tailings was used to determine the cycle of

the locked cycle test in which equilibrium was attained. The Agar model predicted that equilibrium would be reached in the third or fourth cycle of the test. This prediction was confirmed by data on the mass recovery of +400 mesh concentrate (Fig. 3.10), on the mass recovery of +400 mesh tailings (Fig. 3.11), and on the flow of zinc in the concentrate (Fig. 3.12), all of which reached equilibrium in the third cycle of the test. The weighted sum of zinc grades in the concentrate and tailing streams reached the feed grade in the third cycle of the test (Fig. 3.13), thereby confirming that at this point the recirculating loads were fully established.

The mass and zinc flows of -400 mesh particles were unpredictable, and showed little evidence of reaching equilibrium (Figures 3.10 and 3.11). Fine zinc losses to the tailings proved to be variable and were generally higher than expected (Fig. 3.14). It was believed that the unpredictable behaviour of fine particles was largely due to variable rougher performance, and had little effect upon the equilibria reached by the recirculating loads.

The Agar model proved to be useful in predicting the behaviour of coarse particles during locked cycle flotation and in predicting the cycle at which the locked cycle test would equilibrate. The model was less successful in predicting the behaviour of fine (-400 mesh) particles. There is evidence that fine particles in this ore behaved in a different manner

from the coarse particles. The use of single, "average" split factors for the ore therefore resulted in the generation of significant intrinsic errors which caused departures from the model predictions in several of the streams. It is possible that the predictive power of the model with respect to this ore could be improved significantly by the implementation of separate coarse (+400 mesh) and fine (-400 mesh) split factors during modeling or by the implementation of secondary split factors for the middling streams as described by Agar (1978).

7.9 Analysis of Locked Cycle Flotation Performance

The following sections discuss flotation performance at the various nodes in the locked cycle test. Data is presented in the form of recoveries and distributions of zinc, magnesium and iron, the three elements of principal importance in Pine Point zinc flotation. It is assumed that zinc occurs only as ZnS and that magnesium occurs only as $MgCa(CO_3)_2$. Thus, zinc flow represents sphalerite flow and magnesium flow represents dolomite flow in the circuit. Iron occurs in any one of a number of forms, including pyrite (FeS_2), pyrrhotite ($Fe_{(1-x)}S$), marcasite (FeS_2) and in solid solution with zinc in sphalerite. Sphalerite at Pine Point exhibits variable iron composition, so that the amount of iron in the zinc concentrate due to solid solution cannot be directly evaluated.

A variable which the author has termed "separation

efficiency" is used during analysis of flotation performance. This variable is analogous to but not identical to the separation efficiency which is defined by Agar (1980). Agar defines the separation efficiency as the difference in recovery between the desired mineral and the gangue. For the purposes of this discussion the separation efficiency is redefined as:

$$\frac{\text{(\% GANGUE MINERAL REJECTION)}}{\text{(\% ORE MINERAL REJECTION)}}$$

The use of this variable allows the flotation performance at each stage to be analyzed with respect to the material which is removed at that stage.

The recoveries and separation efficiencies of minerals through the circuit can be used in conjunction to analyze the behaviour of individual flotation stages. Recovery vs. size data defines the flotability of minerals in each size class under the specified test conditions, while data on the separation efficiency helps to elucidate rejection mechanisms. A separation efficiency of 1.0 corresponds to random, non-selective gangue rejection and indicates that the ore and gangue minerals respond to flotation in an identical manner. High separation efficiencies indicate that the ore and gangue minerals respond differently to flotation, and that separation is taking place.

Mineral recoveries and separation efficiencies do not

necessarily have any direct correlation. It is quite possible, for instance, to reject only a minute amount of magnesium in a strongly floating size class, but to effect this rejection at only a mimimal zinc penalty (ie. low Mg rejection, but at a high efficiency). Likewise, it is possible during rapid flotation to reject almost all of the fine material, including both ore and gangue minerals (i.e. high Mg rejection, but at low efficiency).

The use of recoveries and separation efficiencies allows the performance of different size classes and different flotation stages to be analyzed on a relative basis. It is likely that the relative behaviour of particles in the experimental circuit is more correlatable with plant performance than laboratory-produced assay and distribution data.

3.10 Effects of the Acid Leach upon Calculations

The streams which were collected at the end of the locked cycle test were the final concentrate and tailings plus the four middling streams from the scavenger and three cleaners. The leach liquor was not collected in the test, since: a) soluble zinc was added during grinding, and soluble magnesium was present in considerable concentrations in the tap water used for flotation; b) the precise volume of leach liquor which was present could be estimated only by completely filtering the solids from the leachate, and this would require

much time and unwanted handling of the leached concentrate; c) the leach liquor was needed for third cleaner flotation.

The streams which were not directly sampled were calculated from the weighted sums of their component streams. For example, the rougher tailings were calculated as the weighted sum of the scavenger concentrate and the final tailings. The presence of the acid leach between the second and third cleaners causes problems since the amount of each mineral leached from the cleaner 2 concentrate is unknown. This affects the recalculated recoveries and separation efficiencies of the rougher and the first two cleaners. The problems presented by the leached material are not insurmountable since analysis of the leaching process can clarify the effects and, in part, the magnitudes of the errors which are introduced.

The concentrate entering the leach contains a large amount of zinc, a fair amount of iron (which is presumably, at the second cleaner, mostly locked into the sphalerite structure), and a relatively small amount of magnesium. While the leaching process removes a finite amount of zinc this amount is small compared to the total zinc present, and should not affect recalculated zinc recoveries to any significant extent. Likewise the iron, which is largely locked into the sphalerite structure, cannot be leached at an appreciably higher rate than the sphalerite. The principal minerals affected by the leach are calcite and dolomite. It is dolomite

which is of interest in this discussion.

When a homogenous material is ground and leached the rate of leaching is roughly proportional to the surface area which is exposed (ignoring the effects of fractures, lattice defects, surface irregularities and the like). Small particles are leached at a faster rate than large particles, usually, at a rate which is inversely proportional to particle size. In a series of size classes which follow a 1 : 2 progression the leaching rate of dolomite should ideally increase by 1.4 for every decrement in size class. During leaching there is both a removal of magnesium from all size classes of the concentrate and a selective removal of magnesium from the fine size classes. Consequently, the percentage rejection and the selection efficiencies of magnesium are elevated over their true values in all size fractions and are also elevated in the fine fractions relative to the coarse fractions.

Barring the possibility of dolomite flotation, magnesium recovery cannot exceed zinc recovery in any size class. In addition, larger size classes show slower leaching rates than fine size classes. A calculation is presented in Appendix 2 which uses these principles to formulate a rough estimate of the amount of magnesium which could be removed in the leach. The calculation suggests that the "real" amounts of magnesium which were present in the cleaner 2 feed may have been 0.2 to 2.0 times higher in the +400 mesh material and up to 12 times higher in the -10um material than the assays indicate.

The effects of the leach upon recalculated values are less as one moves back through the circuit towards the rougher. For example, further calculations in Appendix 2 show that the amount of +400 mesh magnesium in the cleaner 2 floats could be 0.7 to 0.9 times higher and the amount of -400 mesh magnesium could be up to 3.0 times higher than the recalculated assays indicate. In the rougher concentrate none of the size classes should have exhibited magnesium contamination more than 0.25 times over the recalculated assays.

It can be assumed that the leach has a major effect upon calculations involving both coarse (+400 mesh) and fine (-400 mesh) cleaner 2 material. The effects of the leach on calculations for the first cleaner are major for fine (-400 mesh) material and moderate for coarse (+400 mesh) material. The leach has small to moderate effects upon calculations for all size classes in the rougher.

Tabulated data in the sections which follow is presented as if the leach had no effect upon recalculated recoveries and distributions of magnesium. Arrows on the figures present a qualitative indication of the direction in which the "real" recovery, distribution and separation efficiency curves are displaced from the curves which are observed, and the relative effects of the leach upon the recalculated assays of the separate streams are discussed in the text.

3.11 Performance of the Rougher

Data for the rougher is presented in Tables 3.20 and 3.21 and in Figures 3.16 to 3.19. Figure 3.16 shows the recoveries of zinc, iron and magnesium, and reveals a zinc flotation profile which is typical of a strongly floating mineral (Trahar, 1978). The highest zinc recoveries (98-99%) are experienced in the -100/+400 mesh size range while slightly lower recoveries are experienced in the coarse (+100 mesh) and fine (-400 mesh) size fractions.

Magnesium shows "background" recoveries of three to four percent in all +400 mesh size fractions with higher recovery (over 11%) in the -400 mesh fines. The magnesium recovery profile is typical of recovery by entrainment. Iron shows an unusual recovery curve with recoveries of 40% to 50% in the intermediate size classes, higher recoveries in the fines, and lower recoveries in the coarse size classes. This profile is likely to be the combination of an entrainment profile for gangue iron and a flotation profile for iron in solid solution with zinc in sphalerite.

Figure 3.17 shows the separation efficiencies of magnesium and iron in the rougher. The most efficient magnesium rejection is experienced in the intermediate size classes (-150/+400 mesh), where magnesium is rejected up to 75 times more strongly than zinc. Efficiency of rejection is lower at the ends of the size spectrum. The low efficiency in the -400 mesh size range reflects a simultaneous drop in zinc

TABLE 3.20
ASSAY DATA FOR ROUGHER FLOTATION

ROUGHER FLOTATION: MASS RECOVERY 38.5%
DURATION: 7.0 MIN.

STREAM	SIZE	MASS%	ZINC%	IRON%	MG%
RECALC RGHR TAILS	+ 48	1.60	[illegible]	2.48	7.97
	+ 64	8.29	[illegible]	[illegible]	8.71
	+100	16.01	0.64	[illegible]	8.51
	+150	13.76	0.45	1.86	8.90
	+200	10.52	0.35	1.72	9.00
	+270	9.46	0.29	1.85	8.79
	+400	6.68	0.30	1.81	8.80
	-400	33.68	1.90	2.86	8.45
RECALC ROUGHER CON	+ 48	0.60	[illegible]	[illegible]	0.85
	+ 64	2.93	[illegible]	[illegible]	1.51
	+100	8.84	[illegible]	[illegible]	1.22
	+150	11.58	41.44	[illegible]	1.01
	+200	8.96	41.33	[illegible]	0.72
	+270	7.92	40.66	[illegible]	0.45
	+400	6.28	39.55	[illegible]	0.33
	-400	52.79	35.50	3.79	0.54

FIGURE 3.16

ROUGHER RECOVERIES

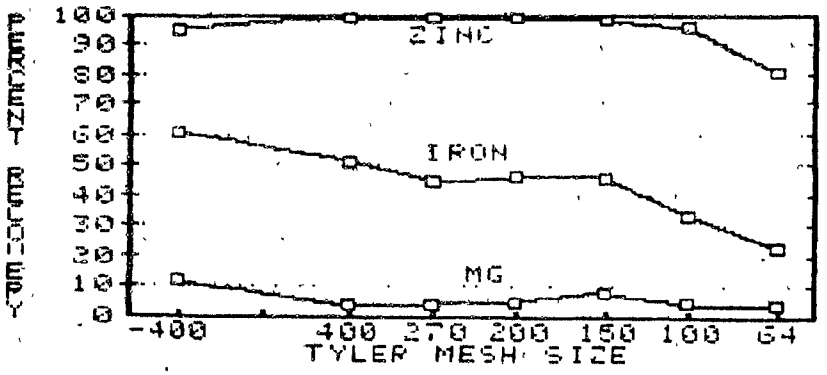

TABLE 3.21
CALCULATIONS FOR ROUGHER

ROUGHER RECOVERIES			
MESH	ZINC	IRON	MG
+ 48	80.74	[illegible]	[illegible]
+ 64	80.49	[illegible]	[illegible]
+100	95.89	[illegible]	[illegible]
+150	97.90	45.10	[illegible]
+200	98.43	46.05	4.08
+270	98.82	44.74	[illegible]
+400	98.72	51.10	[illegible]
-400	94.41	60.44	[illegible]

SEPARATION EFFICIENCY COMPARED TO ZINC			
MESH	ZINC	IRON	MG
+ 48	----	[illegible]	5.06
+ 64	----	[illegible]	[illegible]
+100	----	16.17	[illegible]
+150	----	26.14	[illegible]
+200	----	[illegible]	61.10
+270	----	40.04	[illegible]
+400	----	[illegible]	75.09
-400	----	7.08	15.88

DISTRIBUTIONS IN ROUGHER CONCENTRATE			
MESH	ZINC	IRON	MG
+ 48	0.72	0.51	0.51
+ 64	[illegible]	[illegible]	4.24
+100	10.52	7.67	[illegible]
+150	12.64	8.95	[illegible]
+200	10.08	6.59	6.16
+270	8.65	[illegible]	4.50
+400	6.67	[illegible]	[illegible]
-400	47.22	[illegible]	54.98

DISTRIBUTIONS IN ROUGHEF TAILINGS			
MESH	ZINC	IRON	MG
+ 48	[illegible]	1.87	1.48
+ 64	17.26	8.00	7.99
+100	9.20	[illegible]	15.83
+150	[illegible]	11.46	[illegible]
+200	[illegible]	8.34	10.99
+270	[illegible]	8.10	9.65
+400	1.76	[illegible]	[illegible]
-400	57.00	40.76	[illegible]

FIGURE 3.17

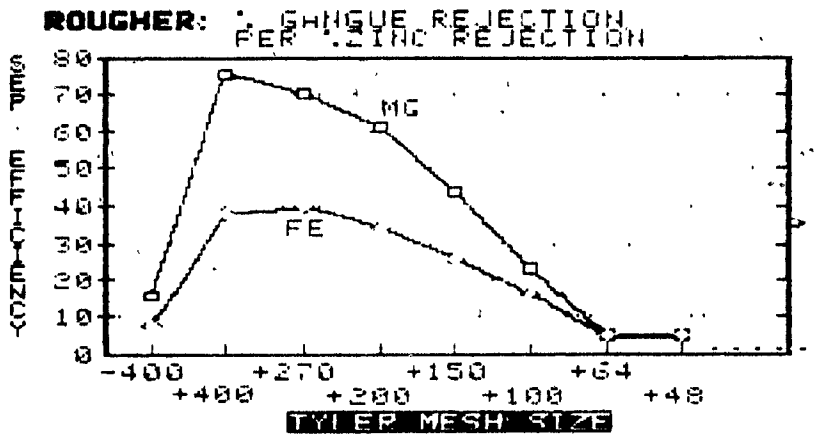

FIGURE 3.18

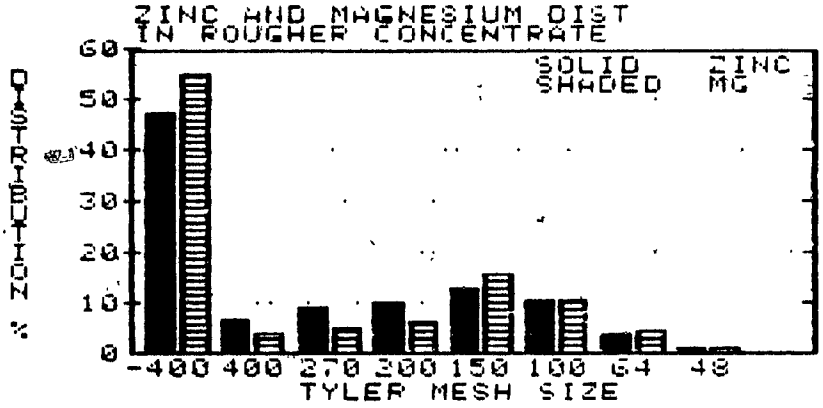

FIGURE 3.19

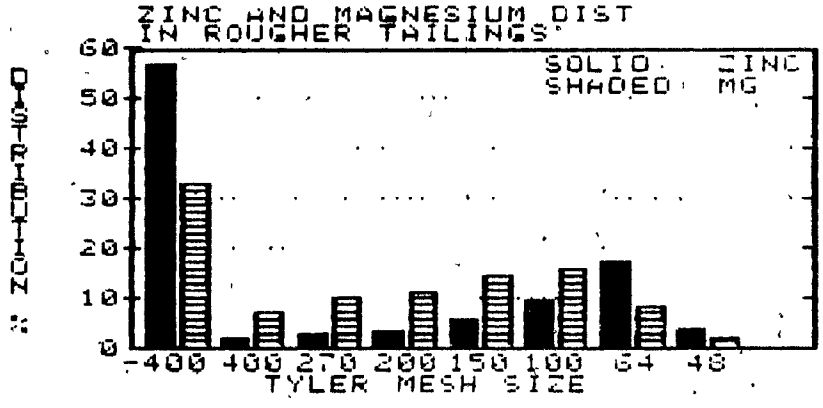

recovery and a rise in magnesium recovery. This is interpreted as the result of a low flotation rate for fine zinc and non-selective entrainment of fine magnesium. The low separation efficiencies in the coarse size classes are caused by a drop in zinc recovery, attributable in part to kinetic problems in the flotation of coarse particles.

The separation efficiency profile for iron is identical in form to that exhibited by magnesium but shows lower rejection rates relative to zinc. It appears that gangue iron is rejected, thereby giving the iron efficiency profile the same form as that of magnesium; however, iron recoveries are elevated over those of magnesium by the passage of iron-bearing sphalerite into the concentrate.

Figure 3.18 shows the distribution of zinc and magnesium in the rougher concentrate. Magnesium is distributed preferentially into the -400 mesh size range of the concentrate, and to a lesser extent into the +150 mesh size range. The best performance is seen in the -150/+400 mesh size classes.

Figure 3.19 illustrates the distribution of magnesium and zinc in the rougher tailings. Although the +64 mesh size fraction experiences the lowest overall recovery of zinc (Fig. 3.16) it is the more size-abundant -400 mesh size range which contributes most of the zinc in the rougher tailings. The -400 mesh size range contains 57% of the unrecovered zinc in association with only 33% of the tailings mass.

Summary of Rougher Performance:

Zinc in the rougher showed good recovery in all size fractions, with the best recoveries experienced in the -150/+400 mesh size fractions. The flotation profile of zinc was typical of a strongly floating mineral. Magnesium was effectively rejected in all but the -400 mesh size range, which showed indications of fine gangue entrainment. The behaviour of iron was intermediate between that of zinc and magnesium.

Zinc losses in the rougher were experienced mostly in the -400 mesh size fraction, although significant contributions were made by the +64 mesh material. This behaviour was typical of slow flotation in the fines and kinetic problems or locking with magnesium in the coarse size classes.

3.12 Performance of the Scavenger

Recoveries and distributions of elements in the scavenger are presented in Tables 3.21 and 3.22 and illustrated in Figures 3.20 to 3.23. Figure 3.20 shows recovery data for zinc, iron and magnesium in the scavenger. Zinc recovery is erratic with a tendency towards better recoveries at larger sizes. Magnesium recovery is negligible in all size classes and iron recoveries are very low, indicating that almost all of the iron in the scavenger is in the form of gangue sulphides. This conclusion is supported by the almost identical separation efficiency profiles exhibited by iron and magnesium (Figure 3.21).

Figures 3.22 and 3.23 show the distribution of zinc in the scavenger concentrate and tailings, respectively. It can be seen that most of the zinc loss occurs in the -400 mesh size range. The -400 mesh tailings contain only about 22% of the total mass; however, they contribute over 65% of the total zinc loss. The size classes coarser than 65 mesh contribute more zinc to the tailings than the intermediate particles but less than 20% of the total zinc loss. Fine (-400 mesh) zinc is therefore the major contributor to zinc loss in the circuit.

Summary of Scavenger Performance:

Zinc in the scavenger feed was found primarily in the -400 mesh and the +64 mesh size fractions. In the scavenger there was a slight trend towards higher recovery of zinc in

the coarse (+64 mesh) size fractions, thus producing a concentrate stream with zinc distributions similar to but slightly coarser than the zinc distribution in the scavenger feed, and a final tailings stream with zinc distributions similar to but finer than the feed distribution. Over 65% of the zinc lost in the circuit was -400 mesh, as compared with only 33% of the total tailings mass in that size range. Thus it can be concluded that fine zinc loss was a problem in this circuit.

TABLE 3.22
ASSAY DATA FOR SCAVENGER

SCAVENGER FLOTATION: MASS RECOVERY 3.8%
DURATION: 5.0 MIN.

STREAM	SIZE	MASS%	ZINC%	IRON%	MG%
SCAV. CONC	+ 64	15.94	25.18	7.11	4.66
	+100	16.27	11.19	5.26	4.79
	+150	9.04	11.67	5.87	4.77
	+200	5.27	15.51	4.58	4.89
	+270	4.31	15.40	4.43	4.87
	+400	2.28	13.90	4.49	5.78
	-400	50.93	15.15	5.24	6.54
SCAV. TAILS	+ 48	1.66	2.46	2.48	7.97
	+ 64	8.00	0.64	2.20	8.56
	+100	16.02	0.24	2.19	8.65
	+150	13.94	0.18	1.81	9.00
	+200	10.79	0.18	1.70	9.05
	+270	9.71	0.16	1.83	8.87
	+400	6.84	0.17	1.78	8.87
	-400	33.04	1.17	2.72	8.79

FIGURE 3.20

SCAVENGER RECOVERIES

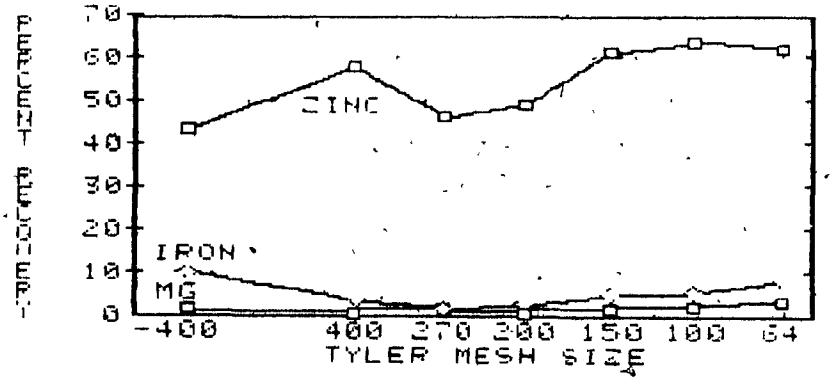

TABLE 3.23
CALCULATIONS FOR SCAVENGER

SCAVENGER RECOVERIES			
MESH	ZINC	IRON	MG
+ 64	62.05	7.85	9.27
+100	63.58	5.74	12.06
+150	61.24	4.92	1.27
+200	49.04	2.29	0.90
+270	46.31	1.62	0.47
+400	57.93	3.04	0.47
-400	43.47	9.98	1.64

SEPARATION EFFICIENCY COMPARED TO ZINC			
MESH	ZINC	IRON	MG
+ 64	----	2.43	2.55
+100	----	2.60	2.69
+150	----	2.45	2.55
+200	----	1.92	1.95
+270	----	1.87	1.86
+400	----	2.30	2.37
-400	----	1.59	1.74

DISTRIBUTIONS IN SCAVENGER CONCENTRATE			
MESH	ZINC	IRON	MG
+ 64	25.44	11.42	20.82
+100	11.54	12.27	51.87
+150	6.69	8.06	12.09
+200	3.17	2.66	4.43
+270	2.25	1.83	2.38
+400	2.01	2.36	2.16
-400	48.90	61.44	36.25

DISTRIBUTIONS IN SCAVENGER TAILINGS			
MESH	ZINC	IRON	MG
+ 64	15.98	9.87	9.30
+100	6.79	15.93	15.74
+150	4.35	11.46	14.25
+200	3.39	8.34	11.09
+270	2.68	8.10	9.76
+400	1.51	5.51	6.89
-400	65.30	40.76	32.97

FIGURE 3.21

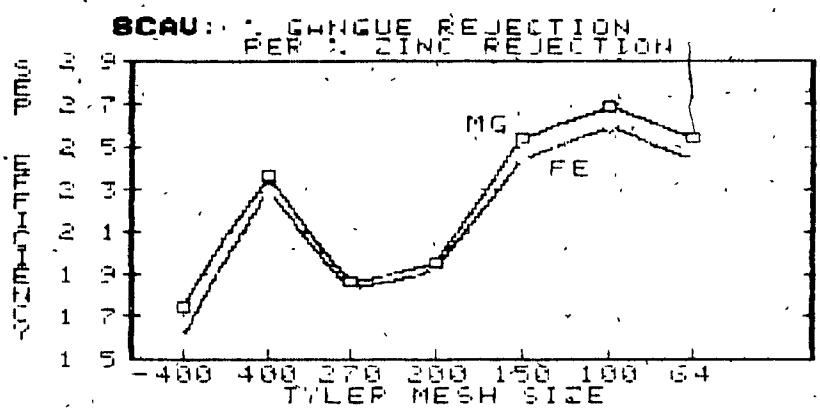

FIGURE 3.22

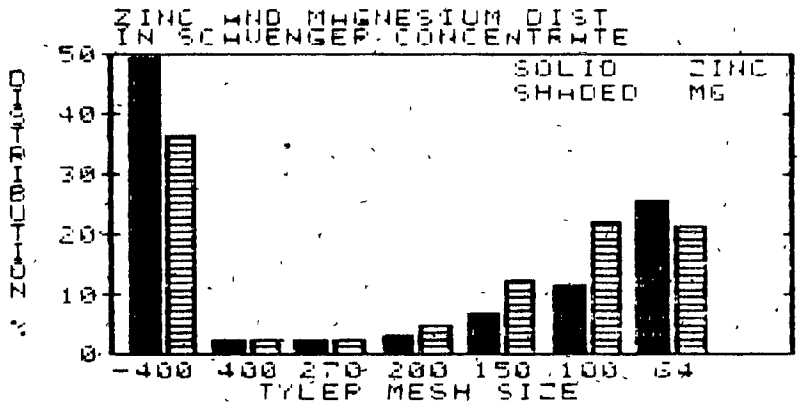

FIGURE 3.23

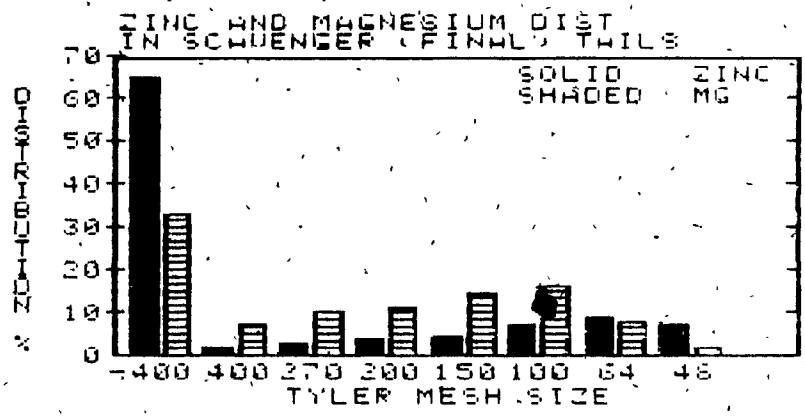

3.13 Performance of the First Cleaner

Recovery and distribution of elements in the first cleaner is shown in Tables 3.23 and 3.24 and illustrated in Figures 3.24 to 3.27. It can be seen in Figure 3.24 that the recovery of zinc is over 98% in all size fractions above 400 mesh but decreases steadily in the fines down to about 45% in the -10um size range. Iron recoveries are similar to but about 10 percentage points lower than zinc recoveries in all size fractions. The parallel recoveries of iron and zinc suggest that most of the iron entering the first cleaner is contained within sphalerite although residual amounts of gangue iron may be rejected at this point, thereby lowering the overall iron recovery. Magnesium recovery is only 11% in the -10μm size fraction but increases strongly with increasing size, reaching about 80% recovery in the +200 mesh size range. The recovery profile of magnesium suggests that entrainment in the first cleaner is minimal but that locking between dolomite and sphalerite is significant at sizes as low as 25μm.

Figure 3.25 shows the variation of separation efficiency with particle size in the first cleaner. Selectivity of flotation is highest for the -200/+270 mesh size range, in which zinc recovery is over 99% and magnesium recovery is just over 30%. In the fine sizes efficiency is low, primarily due to fine zinc rejection. Although about 70-90% of the -25μm magnesium is rejected this action is accompanied by zinc losses of up to 55%. In the coarser sizes separation

TABLE 3.24
ASSAY DATA FOR FIRST CLEANER

FIRST CLEANER FLOTATION: MASS RECOVERY 77.9%
DURATION: 2.5 MIN.

STREAM	SIZE	MASS%	ZINC%	IRON%	MG%
CLNR 1 TAILS	+150	3.78	13.46	3.51	6.54
	+200	0.98	10.94	3.00	6.22
	+270	1.35	8.67	4.74	6.87
	+400	1.71	9.10	4.36	5.41
	-400	92.18	25.79	4.75	2.10
	+25µm	2.57	13.46	5.58	4.50
	+15µm	6.20	20.06	5.36	3.98
	+10µm	15.09	28.28	5.00	1.92
	-10µm	68.00	25.98	4.52	1.76
RECALC CLNR1 CON	+ 48	0.82	43.49	1.16	0.89
	+ 64	3.96	43.36	1.99	1.51
	+100	11.97	43.20	3.24	1.22
	+150	14.35	42.05	3.91	0.89
	+200	11.77	41.54	4.45	0.69
	+270	10.24	41.00	4.82	0.78
	+400	8.02	40.06	5.01	0.73
	-400	38.88	37.46	5.61	0.43
	+25µm	6.54	39.24	5.28	0.16
	+15µm	9.74	38.45	5.70	0.18
	+10µm	8.06	36.60	5.71	0.27
	-10µm	14.95	35.09	5.78	0.24

FIGURE 3.24

CLEANER 1 RECOVERIES

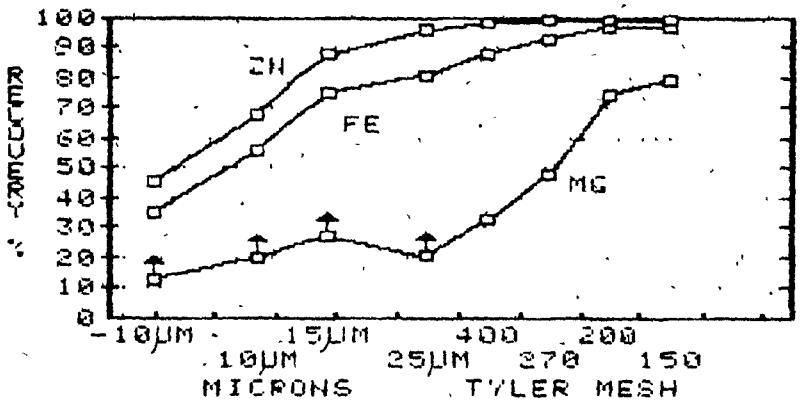

TABLE 3.25 CALCULATIONS FOR CLEANER #1

CLEANER 1 RECOVERIES

MESH	ZINC	IRON	MG
+150	98.59	96.40	78.64
+200	99.19	96.70	73.72
+270	98.97	92.15	47.58
+400	98.20	87.51	30.30
+25µm	95.58	80.67	20.09
+15µm	87.59	74.62	27.11
+10µm	67.78	55.20	18.72
-10µm	44.82	34.82	12.11

SEPARATION EFFICIENCY COMPARED TO ZINC

MESH	ZINC	IRON	MG
+150	----	2.55	15.15
+200	----	4.07	23.44
+270	----	7.62	50.89
+400	----	7.02	68.02
+25µm	----	4.34	17.96
+15µm	----	2.05	5.87
+10µm	----	1.39	2.49
-10µm	----	1.18	1.59

DISTRIBUTIONS IN CLEANER 1 CONCENTRATE

MESH	ZINC	IRON	MG
+150	33.03	28.40	59.67
+200	12.24	9.64	11.21
+270	10.47	8.40	5.28
+400	8.02	7.13	2.89
+25µm	6.41	6.70	1.91
+15µm	8.99	10.91	3.61
+10µm	7.47	10.44	4.66
-10µm	13.36	18.37	10.82

DISTRIBUTIONS IN CLEANER 1 TAILINGS

MESH	ZINC	IRON	MG
+150	2.12	2.07	11.03
+200	0.45	0.64	3.72
+270	0.49	1.40	3.96
+400	0.65	1.98	4.13
+25µm	1.33	3.13	5.17
+15µm	5.69	7.24	6.61
+10µm	15.84	16.51	12.91
-10µm	72.44	67.02	52.46

FIGURE 3.25

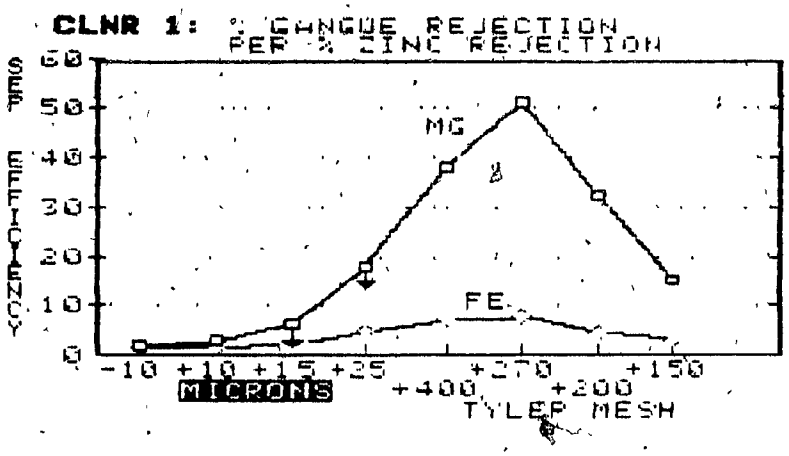

FIGURE 3.26

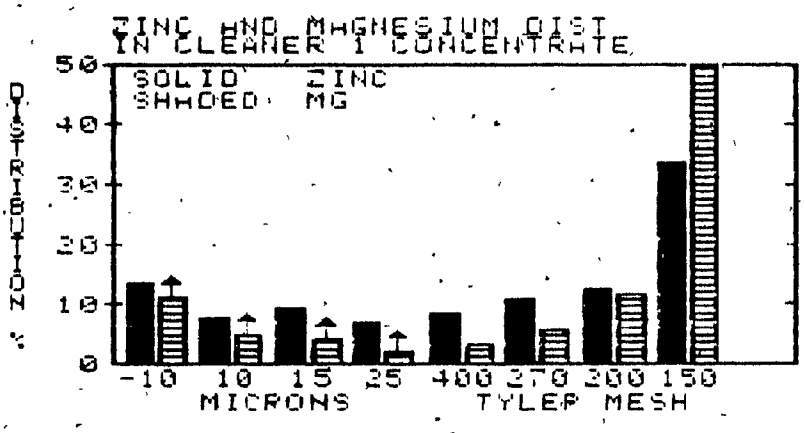

FIGURE 3.27

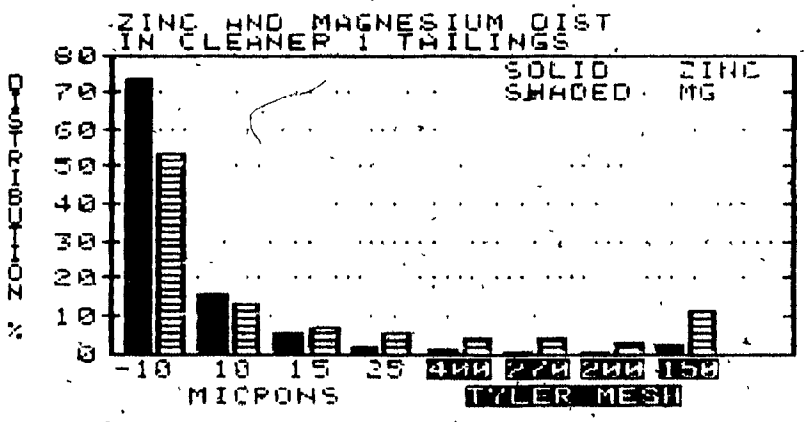

efficiency drops due to a strong increase in magnesium recovery, which reaches about 80% in the +150 mesh size range. It is probable that this increase is caused by the occurrence of locked particles, although the presence of such particles apparently exacts little or no toll upon zinc recovery. Recovery of zinc exceeds 98% at all particle sizes coarser than 400 mesh.

Figure 3.26 shows the distribution of zinc and magnesium in the first cleaner concentrate. It can be seen that the size classes coarser than 200 mesh contribute a disproportionately high amount of magnesium to the concentrate. The finer size classes (-270 mesh) contain 55% of the zinc but only 29% of the magnesium.

Figure 3.27 shows the distribution of zinc and magnesium in the first cleaner tails. It can be seen that the majority of both zinc and magnesium rejection is experienced in the -10μm size range. Over 70% of the zinc and 50% of the magnesium in the tailings have a size of less than 10μm. The buildup of recirculating fine zinc between the first cleaner and the rougher undoubtedly contributes to the fine zinc loss which is experienced in the circuit.

Summary of First Cleaner Performance:

Over half of the magnesium entering the first cleaner had a size of less than 400 mesh. This fine material was strongly rejected in the first cleaner but only at the expense of much

fine zinc rejection. Consequently, significant recirculating loads of fine dolomite and fine sphalerite developed between the rougher and the first cleaner. The recirculating loads of -10μm zinc and magnesium were approximately 125% and 500%, respectively.

There was no indication of significant entrainment of magnesium in the first cleaner; rather, magnesium recovery increased with size from about 12% in the -10μm size fraction to about 80% in the +150 mesh material. This suggested that locking was significant, and that locked particles may have exhibited high flotability. Such a conclusion is concordant with the high flotability exhibited by sphalerite in this circuit; overall zinc recovery in the +25μm size range was in excess of 98% in the first cleaner at a flotation time of only 2.5 minutes. The short flotation time appeared to cause a general rejection of fine particles rather than a selective rejection of coarse composites.

The recirculation of fine zinc back to the rougher undoubtedly contributed to high fine zinc losses in the circuit. The final tailings leaving the scavenger contained approximately 4% of the feed zinc, the majority of which occurred in the -400 mesh size range. The high rejection of fine zinc in the first cleaner is therefore a cause for concern.

3.14 Performance of the Second Cleaner

The recoveries and distributions of metals in the second cleaner are summarized in Tables 3.26 and 3.27, and are presented diagramatically in Figures 3.28 to 3.31. Results pertaining to the second cleaner can be presented only semi-quantitatively due to the effects of the acid leach upon the recalculated composition of the second cleaner concentrate.

The second cleaner tailings, which were not leached, provide the best indication of the rejection mechanisms which were operative in the second cleaner. Overall rejection was very low, since mass recovery was in excess of 92% at a flotation time of only one minute. Over 87% of the rejected mass was of a size less than 400 mesh. It appears, therefore, that the first and second cleaners behaved in a similar manner. Fines were rejected with low selectivity while the coarse particles (including coarse composites) were recovered at a high rate (Figure 3.28).

It is possible to examine the relative efficiencies of flotation performance in the first and second cleaners. Since the leach removed magnesium from the second cleaner concentrate and not from the tailings the separation efficiencies illustrated in Figure 3.29 for the second cleaner are all displaced upward from their "true" positions. It can be seen, therefore, that the second cleaner is much less efficient than the first. The separation efficiencies reported

TABLE 3.26
ASSAY DATA FOR SECOND CLEANER

SECOND CLEANER FLOTATION: MASS RECOVERY 92.3%
DURATION: 1 MINUTE

STREAM	SIZE	MASS%	ZINC%	IRON%	MG%
CLNR 2 TAILS	+200	8.76	[illegible]	[illegible]	[illegible]
	+270	2.01	[illegible]	[illegible]	[illegible]
	+400	1.67	[illegible]	[illegible]	[illegible]
	-400	87.56	[illegible]	[illegible]	[illegible]
	+25µM	[illegible]	[illegible]	[illegible]	[illegible]
	+15µm	8.45	[illegible]	[illegible]	[illegible]
	+10µm	[illegible]	[illegible]	[illegible]	[illegible]
	-10µm	[illegible]	28.01	4.95	0.99
RECALC CLNR2 CON	+ 48	0.88	[illegible]	[illegible]	0.89
	+ 64	4.29	[illegible]	[illegible]	1.51
	+100	12.97	[illegible]	[illegible]	[illegible]
	+150	16.52	[illegible]	[illegible]	0.89
	+200	12.02	[illegible]	[illegible]	0.58
	+270	10.93	41.15	[illegible]	[illegible]
	+400	8.55	40.14	[illegible]	[illegible]
	-400	34.82	[illegible]	[illegible]	0.05
	+25µm	6.82	[illegible]	[illegible]	0.11
	+15µm	9.41	[illegible]	[illegible]	0.10
	+10µm	6.89	[illegible]	[illegible]	0.07
	-10µm	11.70	37.81	[illegible]	0.10

FIGURE 3.28

CLEANER 2 RECOVERY

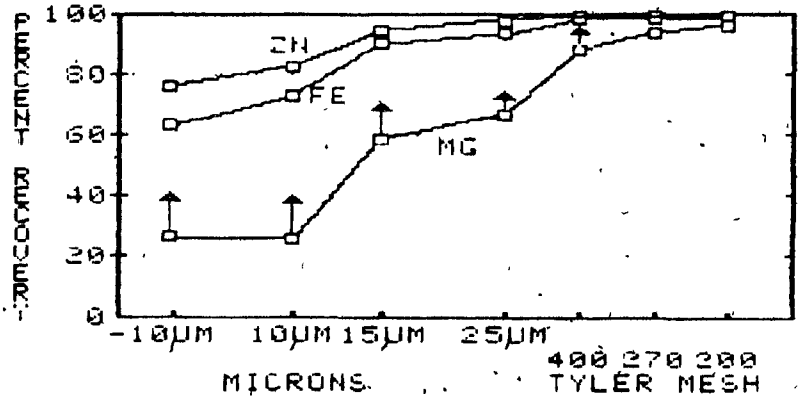

TABLE 3.27
CALCULATIONS FOR CLEANER #2

CLEANER 2 RECOVERIES

MESH	ZINC	IRON	MG
+200	98.60	98.39	95.27
+270	98.73	98.32	92.93
+400	98.75	97.85	87.60
+25µm	96.96	93.24	65.94
+15µm	94.30	88.88	57.84
+10µm	80.24	70.72	25.38
−10µm	75.94	62.84	26.04

SEPARATION EFFICIENCY COMPARED TO ZINC

MESH	ZINC	IRON	MG
+200	----	1.15	3.78
+270	----	1.32	5.57
+400	----	1.69	9.76
+25µm	----	2.22	11.20
+15µm	----	1.78	7.40
+10µm	----	1.54	4.20
−10µm	----	1.54	2.07

DISTRIBUTION IN CLEANER 2 CONCENTRATE

MESH	ZINC	IRON	MG
+200	47.55	42.60	82.02
+270	11.01	9.40	5.96
+400	8.42	7.94	3.08
+25µm	6.62	7.11	1.53
+15µm	9.00	11.16	2.54
+10µm	6.54	8.64	1.44
−10µm	10.81	12.14	3.42

DISTRIBUTIONS IN CLEANER 2 TAILINGS

MESH	ZINC	IRON	MG
+200	10.37	5.03	18.91
+270	2.17	1.17	2.11
+400	1.67	1.26	2.03
+25µm	2.19	2.74	3.67
+15µm	8.77	9.13	8.58
+10µm	21.68	23.44	19.59
−10µm	52.56	56.22	45.12

FIGURE 3.29

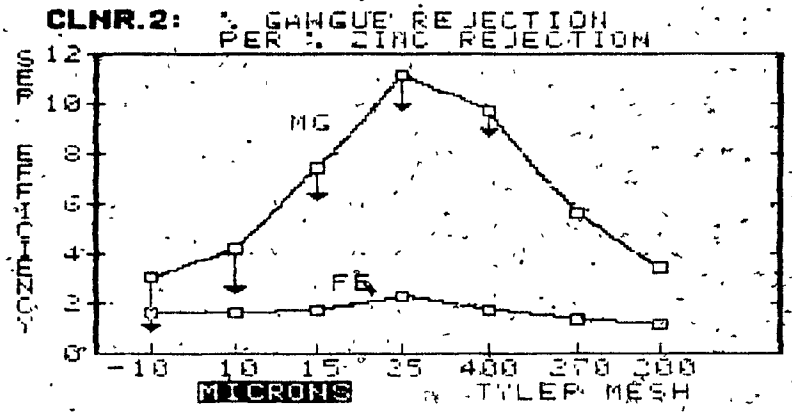

FIGURE 3.30

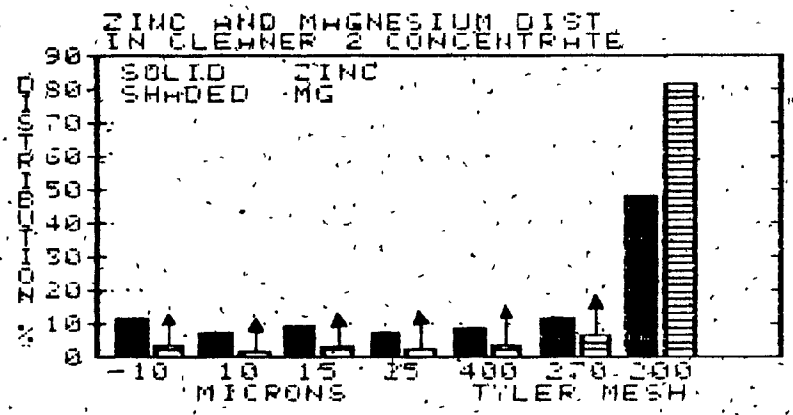

FIGURE 3.31

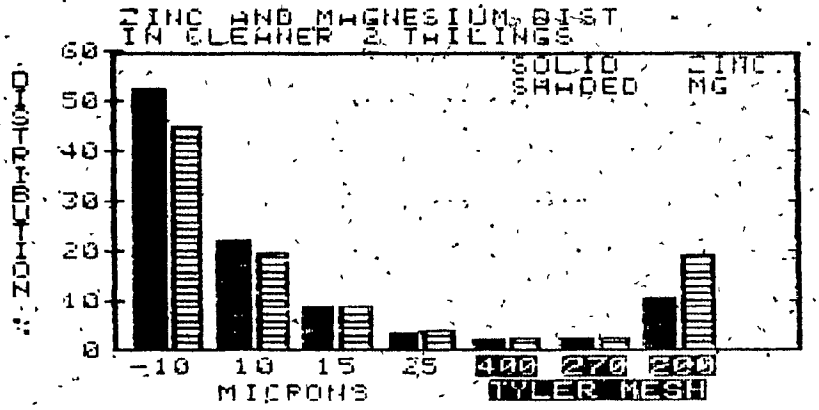

for the +270 mesh size classes range from 3-6 in the second cleaner, as compared to 15-50 in the first cleaner. Separation efficiencies for the -270/+25μm particles range from 6-11 in the second cleaner, as compared to 20-50 in the first. Efficiencies in the -25μm size range appear to be comparable between the two cleaners.

It appears from this comparison that the first cleaner removes most of the easily-rejected magnesium-bearing composites. The second cleaner removes almost no coarse magnesium, and removes fine magnesium only at high zinc penalties. Flotation in the second cleaner is so fast as to greatly reduce the selectivity of gangue removal. Over 70% of the magnesium in the second cleaner feed is coarser than 200 mesh; however, +200 mesh magnesium makes up only 19% of the second cleaner tailings. Recovery of +200 mesh magnesium is actually greater than recovery of -400 mesh zinc, thereby indicating that the rapidity of the float makes the flotation process more size-selective than composition-selective.

Iron recovery in the second cleaner is similar to zinc recovery in all size classes. This reaffirms that the principal source of iron in the second cleaner concentrate is sphalerite rather than gangue iron sulphides. The iron separation efficiency profile (Figure 3.29) shows that rejection of iron is a constant 1.5-2.0 times stronger than rejection of zinc in all size classes. This size-independent efficiency profile is what one would expect between elements

which are mineralogically associated; however, the expected separation efficiency between two elements in the same mineral is 1.0. The difference in rejection between zinc and iron opens the possibility that a certain proportion of "high-iron" sphalerite is rejected at a greater rate than sphalerite with little iron. This phenomenon is reported by Finkelstein and Allison (1976) and was observed repeatedly during the course of this research. The effects of iron content upon sphalerite recovery are measurable but small, and are judged to be metallurgically insignificant.

Summary of Second Cleaner Performance:

The second cleaner feed contained much coarse magnesium and smaller amounts of fine magnesium. The fine magnesium was strongly rejected; however, this rejection was not efficient and represented a general non-selective rejection of all fine material.

In the intermediate and coarse size classes (+400 mesh) 85-95% of the magnesium was recovered. Magnesium rejection and separation efficiencies of the second cleaner were both inferior to those calculated for the first cleaner. The low efficiency of separation was in part due to the extremely high flotation rate of the material. Over 92% of the mass was recovered during the one-minute float and most of the material which was left behind was finer than 400 mesh.

Iron showed similar recoveries to zinc in all size

classes and the separation efficiency was a constant 1.5 to 2.0. It is concluded that iron at this point in the circuit occurred primarily in the sphalerite structure and that high-iron sphalerite exhibited slightly lower flotability than sphalerite with low iron content.

3.15 Performance of the Third (Post-Leach) Cleaner

The recoveries and distributions of metals in the third (post-leach) cleaner are presented in Tables 3.28 and 3.29, and are illustrated in Figures 3.32 to 3.35.

The recoveries of elements in the post-leach cleaner are shown in Figure 3.32. The figure shows a general decrease in the recoveries of all elements compared to recoveries in the second cleaner. However, magnesium exhibits the greatest drop in recovery. Comparison between Figure 3.28 (second cleamer recoveries) and Figure 3.32 (third cleaner recoveries) shows that magnesium rejection increased by about 5% in the coarse size range (+200 mesh), by 20%-35% in the mid-sizes (down to +25μm) and by about 12% in the fine sizes (-25μm).

Comparison between the separation efficiencies for the second and third cleaners (Figs. 3.29 and 3.33) shows that magnesium rejection in the third cleaner is not only higher but also more efficient. The efficiency of coarse (+200 mesh) magnesium rejection rose from three Mg per Zn in the second cleaner to about seven in the third cleaner. Efficiency in the -200/+400 mesh material rose from 4-10 to 13-18. Efficiency of fine Mg rejection cannot be directly compared between the second and third cleaners; however, it can be noted that rejection of -15μm particles in the third cleaner is only 1.1 to 1.4 times stronger than zinc rejection and thus not very selective. The low selectivity of magnesium rejection in the third cleaner is probably attributable to the fact that fine

TABLE 3.28
ASSAY DATA FOR THIRD CLEANER

THIRD CLEANER FLOTATION: MASS RECOVERY 82.7%
DURATION 2.5 MIN.

STREAM	SIZE	MASS%	ZINC%	IRON%	MG%
CLNR 3 TAILS	+150	6.46	31.36	7.60	2.87
	+200	1.65	33.79	6.70	2.00
	+270	2.48	34.46	5.07	1.01
	+400	2.64	37.87	5.05	1.00
	-400	86.79	38.99	4.67	0.17
	+25µm	9.10	34.36	6.10	0.89
	+15µm	8.60	38.52	5.52	0.46
	+10µm	21.50	38.82	4.61	0.15
	-10µm	50.60	37.52	4.65	0.16
CLNR3 CON	+ 48	1.07	43.49	7.16	0.89
	+ 64	5.19	43.36	6.99	1.51
	+100	15.68	43.00	6.24	1.14
	+150	17.42	42.88	5.86	0.74
	+200	14.20	42.46	5.70	0.44
	+270	12.70	41.84	5.64	0.19
	+400	9.79	40.94	5.84	0.10
	-400	23.95	39.61	6.20	0.04
	+25µm	7.60	40.11	6.08	0.06
	+15µm	9.58	39.77	6.44	0.08
	+10µm	11.83	38.87	6.26	0.06
	-10µM	21.94	38.96	6.30	0.09

FIGURE 3.32

CLEANER 3 RECOVERIES

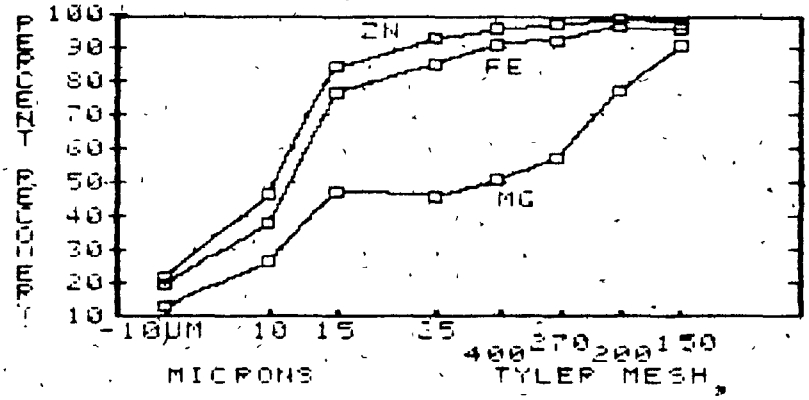

TABLE 3.29
CALCULATIONS FOR CLEANER #3

CLEANER 3 RECOVERIES			
MESH	ZINC	IRON	MG
+150	97.57	96.10	91.72
+200	98.74	96.84	77.42
+270	97.67	92.74	57.20
+400	96.21	90.93	50.65
+25µm	93.21	85.44	48.38
+15µm	84.50	76.88	46.97
+10µm	46.10	37.59	26.21
-10µm	21.42	19.20	12.57

SEPARATION EFFICIENCY COMPARED TO ZINC			
MESH	ZINC	IRON	MG
+150	----	1.60	3.57
+200	----	2.51	17.92
+270	----	3.12	18.37
+400	----	2.46	12.77
+25µm	----	2.14	8.04
+15µm	----	1.49	3.42
+10µm	----	1.16	1.37
-10µm	----	1.05	1.11

DISTRIBUTION IN CLEANER 3 CONCENTRATE			
MESH	ZINC	IRON	MG
+150	40.61	40.15	81.48
+200	14.44	12.86	9.10
+270	12.72	11.27	4.20
+400	9.69	9.34	1.92
+25µm	7.56	7.86	0.85
+15µm	9.02	11.08	1.47
+10µm	3.57	4.20	0.47
-10µm	2.74	3.60	0.53

DISTRIBUTIONS IN CLEANER 3 TAILINGS			
MESH	ZINC	IRON	MG
+150	5.54	5.58	13.54
+200	1.01	1.44	11.49
+270	1.66	2.02	13.61
+400	2.01	2.19	8.11
+25µm	3.91	4.58	4.46
+15µm	9.06	11.41	7.18
+10µm	22.82	23.85	5.64
-10µm	54.99	46.94	15.96

FIGURE 3.33

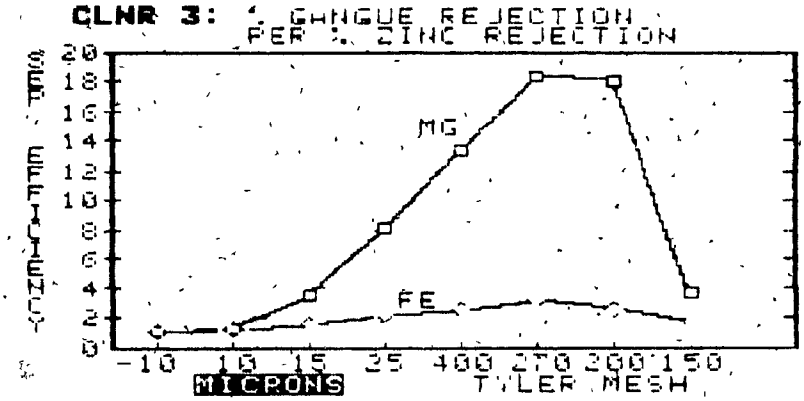

FIGURE 3.34

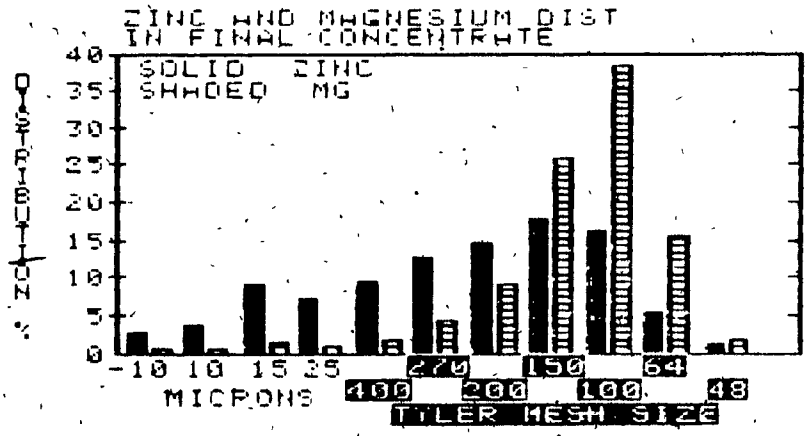

FIGURE 3.35

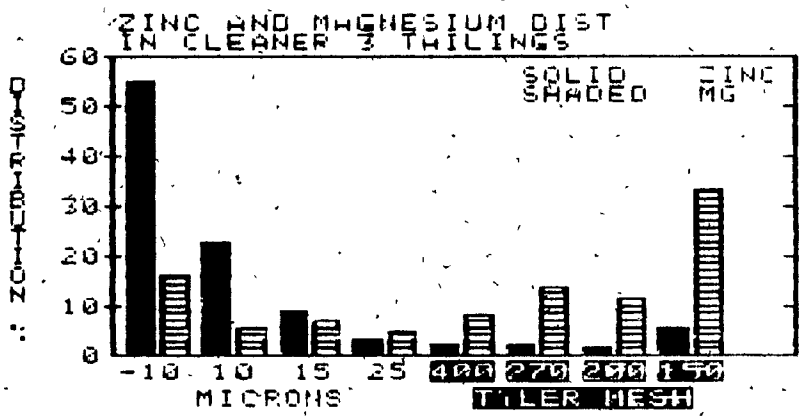

(-15μm) magnesium was little more than a trace constituent in the third cleaner feed.

The distribution of magnesium in the final concentrate is illustrated in Figure 3.34. There is strong evidence in the figure that magnesium contamination is caused by a locking problem. Over 90% of the magnesium in the concentrate is coarser than 200 mesh, as opposed to only 55% of the zinc of that size. There is no evidence that magnesium is recovered in this circuit by any mechanism other than locking.

The recovery of iron in the third cleaner parallels the trend which was observed in the second cleaner. Iron is recovered at a rate which is slightly lower than but parallel to zinc recovery. The separation efficiency of iron is essentially independent of particle size, thereby reaffirming that most of the iron is probably locked in the sphalerite structure.

Iron in the third cleaner is rejected 1-3 times more strongly than zinc. This rate is slightly (perhaps insignificantly) higher than the rejection rate experienced in the second cleaner. Since flotation in the third cleaner is conducted at a pH of 7 (as opposed to a pH of 10 in the second cleaner) gangue iron would be expected to float more favourably in the third cleaner than in the second. A simultaneous drop in iron and zinc recoveries from all size fractions is observed in the third cleaner, thereby suggesting that little if any of the iron at this point is in the form of gangue sulphides.

Summary of Third Cleaner Performance

Flotation in the third cleaner was more efficient than it was in the second cleaner. There was an overall drop in the recoveries of all elements at all sizes; however, the drop in magnesium recovery was the most substantial in all size classes above 25μm. The global decline in recoveries which was observed in this cleaner was not caused by a short flotation time, since the duration of flotation was 2.5 minutes, as compared to only one minute in the second cleaner. Rather, it appears that some physical or chemical changes were evoked by the leach which caused a general lowering of sphalerite flotability. This resulted in slower sphalerite recovery and increased rejection of composite particles.

Although recoveries of magnesium were substantially lower in the third cleaner than they were in the second, overall recoveries of coarse magnesium were still high. The major rejection mechanism in the third cleaner was the non-selective rejection of fine particles since the third cleaner tailings had a size of 87% -400 mesh and contained much fine zinc.

Examination of the final concentrate revealed that the vast majority of magnesium contamination was contributed by the coarse size fractions. There was no evidence that entrainment of fine magnesium was a problem. Thus, locking emerged as the major mechanism of dolomite contamination in the zinc concentrate. Magnesium levels in the concentrate were strongly related to size, and showed a strong upturn at sizes

coarser than 400 mesh (37μm). Mineralogical associations with approximately this grain size may have been responsible for high levels of magnesium contamination in the concentrate.

3.16 Summary of the Locked Cycle Test

The behaviour of material in the locked cycle test can best be summarized by flow diagrams, which are presented in Figures 3.36 to 3.41. The flow diagrams present a schematic view of the amount of material which passes through or which is rejected at each flotation stage in the circuit. Figures 3.36 to 3.38 present flow diagrams for coarse (+200 mesh) intermedite (-200mesh/+15μm) and fine (-15μm) zinc, respectively. The leach, which was located between the second and the third cleaners, is not shown on the diagrams. The width of the bars leaving any one flotation stage is proportional to the amount of zinc present at that stage. Thus in Figure 3.38, for example, the width of the zinc bar representing the fresh feed is equal to the sum of the widths of the zinc bars representing the concentrate and the tailings. Likewise, the width of the bar representing the feed to cleaner 3 is equal to the sum of the widths of the bars leaving the third cleaner as tails and as concentrate. The flow diagrams therefore provide a fast way of visualizing the circuit as a whole, and of evaluating circuit performance. The three zinc diagrams are drawn to the same scale, as are the three magnesium diagrams (Figures 3.39 to 3.41); however, due to the widely different masses of zinc and magnesium which are encountered in the cleaners it was not practical to draw the zinc and magnesium diagrams on the same scale. In cases where the mass flow is less than half a line width, a dotted line is

FIGURE 3.36
FLOW OF +200 MESH ZINC THROUGH CIRCUIT

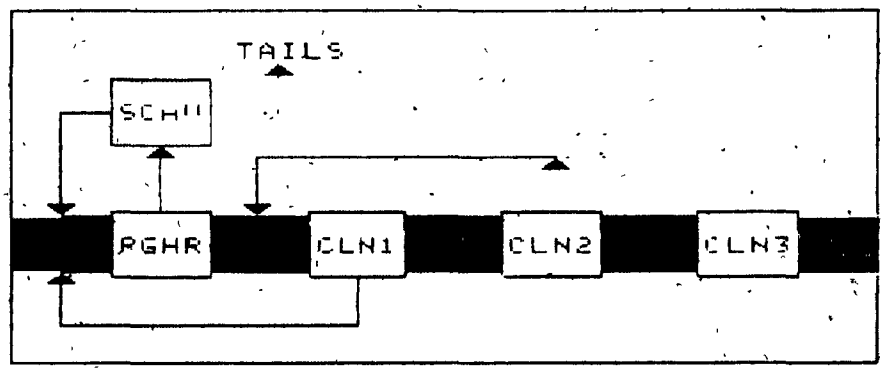

FIGURE 3.37
FLOW OF -200#/+15μM ZINC THROUGH CIRCUIT

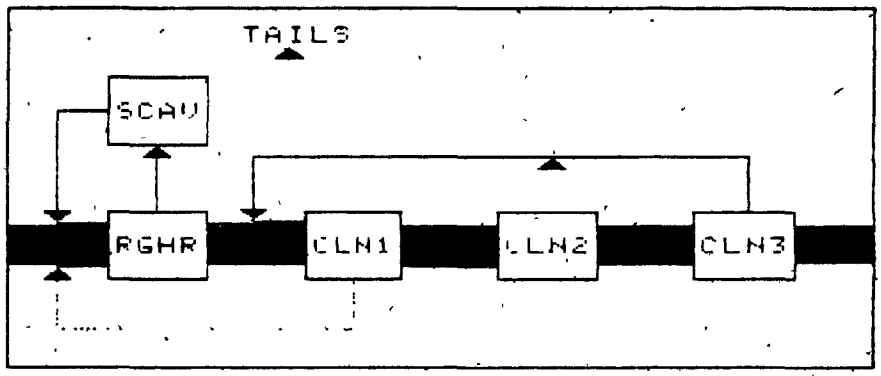

FIGURE 3.38
FLOW OF -15μM ZINC THROUGH CIRCUIT

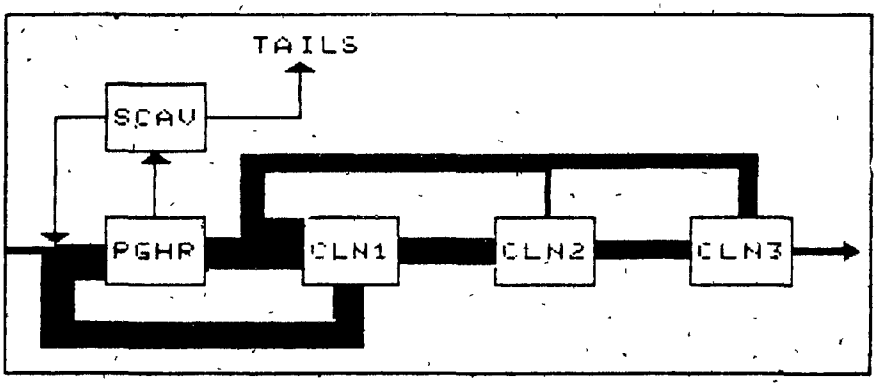

FIGURE 3.39
FLOW OF +200 MESH MG THROUGH CIRCUIT

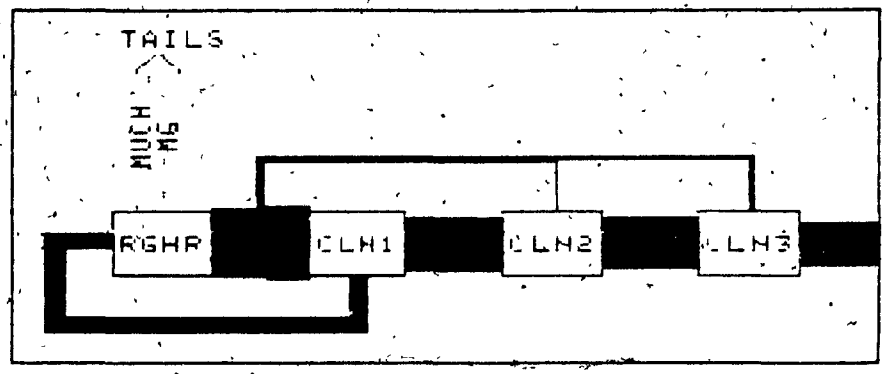

FIGURE 3.40
FLOW OF -200#/+15μM MG THROUGH CIRCUIT

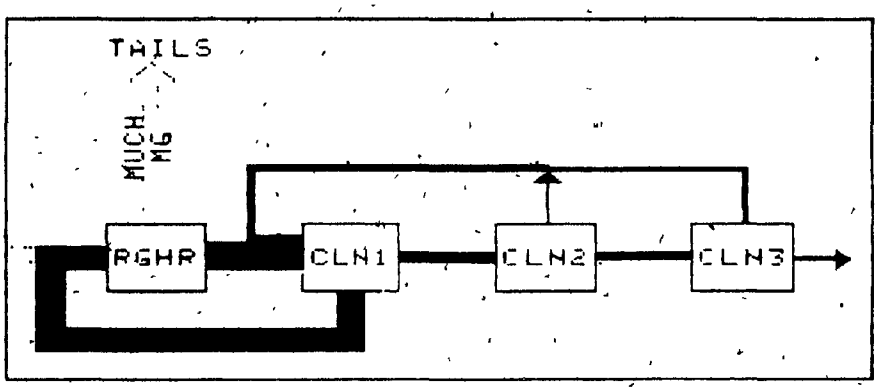

FIGURE 3.41
FLOW OF -15μM MG THROUGH CIRCUIT

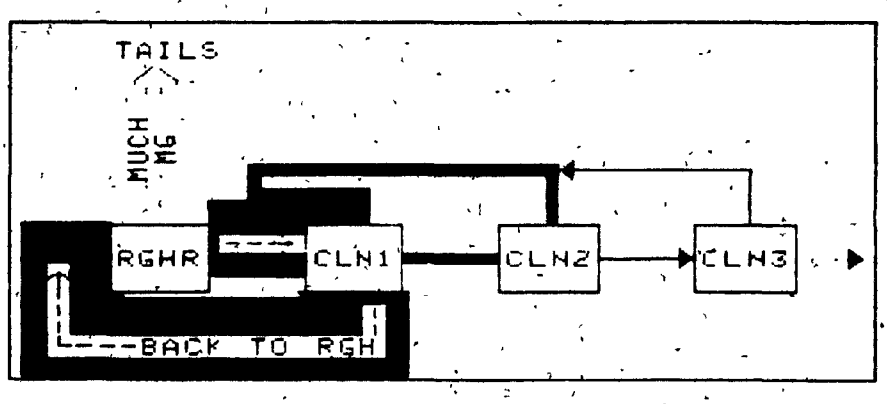

used.

Figures 3.36 and 3.37 illustrate the flow of coarse and mid-size zinc through the circuit. The behaviour of the two size ranges is essentially identical, and shows an almost unimpeded flow of zinc through the circuit. There are no significant recirculating loads at any point in the circuit. The situation is quite different, however, for fine (-15μm) zinc. Fine zinc passes the rougher with little problem, but is rejected at all cleaning stages. The net results of this are summarized as follows:

1) There is about a 200% recirculating load of fine zinc through the second and third cleaners, where the leach is situated. This means that there is about three times the fine zinc in the leach at any one time than one would expect by looking at the amount of fine zinc entering and leaving the circuit. Since these particles have very large specific surfaces it is possible that fine zinc particles are lost in the leach. For example, cubic 5μm zinc particles have specific surfaces over 300 times greater than the specific surfaces of a 100 mesh particles. Since they also have a recirculating load through the leach of 200%, 5μm particles could easily exhibit a rate of leaching 1000 times that of 100 mesh particles.

This potential problem is magnified when one considers the relative abundances of zinc and magnesium in the leach feed. There is about 15 times the volume of fine (-15μm) zinc

in the feed than there is coarse (+200 mesh) magnesium. This means that the surface area exposed to leaching by fine zinc is at least 15,000 times higher than the surface area exposed by coarse magnesium. Discussion of the principles and mechanisms of leaching is undertaken in the chapters which follow; however, it can be stated at this point that the creation of recirculating loads of fine zinc through the leach is a potential cause of high acid consumption, inefficient leaching of coarse magnesium and zinc loss.

2) The amount of fine zinc entering the first cleaner is eight times higher than the amount of fine zinc entering the rougher as fresh feed. This situation is the result of a major recirculation of fines from all cleaners, the latter two of which are in closed circuit with the first cleaner. Since the first cleaner is, in turn, in closed circuit with the rougher, much of the "fine zinc overload" which the cleaner receives is recirculated back through the rougher. This results in a 500% recirculating load of fine zinc between the rougher and the cleaner and inevitably results in fine zinc loss through the scavenger.

Figures 3.39 to 3.41 illustrate the flow of coarse, intermediate and fine-sized magnesium through the circuit. The flow of magnesium through the rougher is obviously very large and cannot be represented here. The diagrams are designed to illustrate the behaviour of magnesium in the cleaners.

The flow of coarse magnesium shown in Figure 3.39

presents a very disturbing picture from a processing point of view. Although there is a small recirculation of coarse magnesium between the rougher and the first cleaner the majority of coarse magnesium which is floated in the rougher ultimately ends up in the final concentrate. There is almost no rejection of +200 mesh magnesium in any of the cleaners.

Mid-size and fine magnesium behave in a different manner, as illustrated in Figures 3.40 and 3.41, respectively. A great deal of intermediate to fine magnesium is passed through the rougher; however, rejection in the cleaners is very good. Fine magnesium passing the first cleaner is negligible in comparison with the amount of coarse magnesium which is passed, and the small amount of fine magnesium which does pass is effectively removed in the second cleaner. Mid-sized magnesium shows the beginnings of the problems encountered in the coarser sizes, since rejection after the first cleaner is not as good as it is with the fine magnesium; however, rejection is reasonably good and mid-sized magnesium does not present a major problem.

The major points about magnesium flow in the circuit are as follows:

1) Coarse magnesium passing the rougher experiences a little rejection in the first cleaner, but almost no rejection in subsequent stages. Consequently there is a large flow of coarse magnesium straight through the circuit.

2) Mid-sized and especially fine magnesium-bearing particles are passed through the rougher in large quantities but are effectively rejected in the first cleaner. The second and third cleaners reject most of the mid-sized and fine magnesium-bearing particles which pass the first cleaner. Thus, relatively little mid-sized or fine magnesium enters the concentrate.

3) The flow of fine magnesium through the leach is very small. Almost all of the magnesium passing through the leach is contained within particles coarser than 200 mesh. Since there is a significant amount of fine zinc in the leach "competing" with the coarse magnesium there is a possibility that fine zinc affects the efficiency of magnesium leaching.

Assay data has previously been reported for the five separation stages in this test circuit (Tables 3.20, 3.22, 3.24, 3.26 and 3.28). Discussion of these assays has been avoided up to this point since no direct relationship between plant and test data can be established; however, the concentrate assays presented in Table 3.28 indicate that it is possible at least in theory to produce an acceptable concentrate from this "difficult" ore, provided that few particles of a size greater than 200 mesh enter the concentrate. This constraint could be met by installing a concentrate regrind somewhere in the cleaning circuit. The

assays of all -400 mesh size classes were all well below the acceptable limit of 0.25% Mg; however, the Mg assays rose rapidly in all size classes above 400 mesh, passing the acceptable limit at about 200 mesh. This suggests that there is a locking problem even at particle sizes as fine as 37μm (400 mesh). It is not known if this problem is typical of all Pine Point ores.

3.17 The Effects of Leaching upon Subsequent Flotation

An increase in the efficiency of flotation was realized between the second and third cleaners. The third cleaner rejected a greater proportion of coarse and mid-sized magnesium than the second cleaner, and at greater efficiency (ie. at less zinc penalty per %Mg rejected). The amount of fine magnesium rejection experienced in the fine size classes was higher in the third cleaner than in the second; however, rejection of fine material in the third cleaner was not very selective.

The third cleaner operated under the same external conditions (agitation, air-flow etc.) as the second cleaner. Since mass recovery in the second cleaner was in excess of 92% the pulp density in both cleaners can be considered to be identical. There was no reason, therefore, to expect that performance in the second and third cleaners should differ to any appreciable extent. It is generally considered that particles in any one cleaner are slightly "more flotable" on

average than particles in previous cleaners, by virtue of the fact that they passed the previous flotation stages while other "less flotable" material was rejected. It is generally expected, therefore, that rejection of magnesium in the third cleaner should be less efficient than rejection in the second cleaner, and that mass should be recovered more completely and at a faster rate in the third cleaner.

The behaviour of the third cleaner was clearly in opposition to the expected behaviour of this flotation stage. Overall mass recovery in the third cleaner was less than 8?% after 2.5 minutes as opposed to a ?2% mass recovery after one minute in the second cleaner. Moreover, the selectivity of flotation (as measured by the separation efficiency) was improved in the third cleaner over that which was observed in the second cleaner. Since the only difference between the operating conditions in the second and third cleaners were those caused by the acid leach it can be concluded that the leach had a beneficial effect upon metallurgical performance during subsequent flotation. This effect was not analyzed in detail, but may be the result of any one or a combination of hydrodynamic factors (water viscosity or specific gravity), electrochemical or physiochemical factors (ionic strength or surface tension), or destruction of the sphalerite surface.

3.18 Discussion

A variety of methods are traditionally used for the purification of "problem" concentrates. Among these are increased cleaning capacity (implemented by Pine Point in 1972), acid leaching (implemented by Pine Point in 1972, and used full-time as of 1980), and regrinding of the middlings streams or the concentrate. In view of the results of this test, it can be seen how some of these traditional solutions are inapplicable to the Pine Point situation.

It was seen in this experiment that rejection in the cleaners was mostly from the fine sizes. Overall recoveries of both coarse zinc and coarse magnesium in the cleaners were very high. Thus, when the Agar criterion was used to determine the optimum flotation times at each cleaning stage almost all of the coarse magnesium was collected in the time it took to collect acceptable amounts of fine zinc. Since the separation efficiency of coarse magnesium was greater than 1 in all cleaners it can be concluded that upgrading occurred during flotation of the coarse sizes; however, coarse magnesium-bearing "middlings" proved to be more flotable than pure fine sphalerite. The minimal amount of middlings which were rejected were accompanied by large amounts of relatively high-grade fines.

It can be predicted, therefore, what the effects of adding additional cleaning capacity would be. Since it is essential to recover the fine zinc, flotation times in the

cleaners are governed by the collection rates of these fine particles. This results in a consistent over-floating and high recovery of middling particles. Additional cleaners would be expected to remove only a very small fraction of the middlings at each stage, but a considerable fraction of the fines. This would result in even higher recirculating loads of fine zinc but only very modest gains in concentrate grade.

In cases where contamination is due primarily to locked particles one is faced with three alternatives. One can either accept the middlings and their contaminants, reject them and suffer losses in ore mineral recovery or regrind them and attempt to effect separation at a smaller size. At Pine Point magnesium contamination is unacceptable and only the two latter options can be considered.

A common concept in the flotation of middling particles is that particles with large amounts of gangue and small amounts of ore minerals float at a lower rate than particles with small amounts of gangue and a large proportion of ore minerals. These particles, in turn, are conceived as floating at a lower rate than pure ore particles with no gangue. Thus, flotation is conceived as being able to separate composite and pure particles, and the "cutoff" amount of gangue in any one particle is conceived as being controllable by adjusting the flotation time. In practice, however, these concepts appear to be of limited applicability in reference to Pine Point ore. The dominant factor affecting the recovery of any one

zinc-bearing particle is its size rather than its sphalerite content. Thus, it is nearly impossible to concentrate locked particles in the middling streams without generating huge recirculating loads of fines. It can be seen in Fig. 3.38 that in this circuit, where only about 5-10% of the locked magnesium was removed, there was a recirculating load of fine zinc equivalent to about 800% passing through the first cleaner (500% between the rougher and the first cleaner, and 300% between the first and subsequent cleaners). In order to reject significant amounts of locked middlings it would be necessary to build up huge recirculating loads of fine zinc.

It appears, therefore, that two of the common solutions to gangue contamination are of little or no applicability to this circuit. Since the majority of the magnesium contamination appears in the form of highly-flotable locked particles, additional flotation should not significantly improve the concentrate; nor can the locked particles be easily separated from the pure particles for size reduction. Of the conventional solutions to magnesium contamination only two remain: regrind of the bulk concentrate and leaching.

The potential problems associated with the leaching of coarse magnesium in the presence of fine zinc have already been discussed. A possible solution is the cycloning of concentrate prior to leaching. This is the practice employed at Pine Point. Experience has proven that leach efficiency is nevertheless very low. An evaluation of the possible benefits

of a bulk regrind is made at a later point, following the results of a detailed examination of the textural and liberation characteristics of the ore.

CHAPTER 4

RECOVERY OF CARBONATES BY FLOTATION AND BY ENTRAINMENT

CHAPTER 4: RECOVERY OF CARBONATES BY FLOTATION AND BY ENTRAINMENT

4.0 Introduction

The locked cycle test reported in Chapter 3 revealed locking as a dominant mechanism of magnesium recovery. Fine dolomite was recovered in only minimal amounts and it was concluded that Pine Point dolomite exhibited neither true flotation characteristics nor strong tendencies towards recovery by entrainment. This chapter reports the results of two flotation tests which were performed upon pure samples of Pine Point gangue. The goal of the tests was to further examine the possibility of true flotation of typical Pine Point gangue material under conditions similar to those in the Pine Point zinc circuit.

4.1 Recovery of Gangue Material in the Presence of Xanthate

A sample of Pine Point gangue was ground to 50% -200 mesh and floated in a Leeds flotation cell according to the procedure outlined in Appendix 1. The gangue had an assay of 0.07% zinc and was considered to be typical of the carbonates which host and which surround the Pine Point ore bodies. The results of the flotation test are presented in Table 4.1.

Figure 4.1 shows the recovery rates of water, coarse (+37μm) and fine (-37μm) gangue as a function of time, expressed as mass percent recovery per minute. An initial surge of froth over the top of the cell was experienced in the first two minutes; however, the froth quickly became unstable

TABLE 4.1

RECOVERIES OF SOLIDS AND WATER DURING FLOTATION

TIME MINUTES	PERCENTAGE RECOVERY WATER	SOLIDS -37 µM	SOLIDS +37 µM
0-1	13.0	1.9	.3
1-2	10.9	2.7	.1
2-4	7.2	1.9	.1
4-6	4.2	.5	NSS
6-8	4.1	.4	NSS
8-10	3.8	.3	NSS
RECOVERY RATES COMPARED TO WATER:		0.30	0.02
		0.25	0.01
		0.26	0.01
		0.12	0.00
		0.10	0.00
		0.08	0.00

NSS = INSUFFICIENT SAMPLE FOR MEASUREMENT

FIGURE 4.1

RECOVERY OF WATER AND SOLIDS VS. TIME

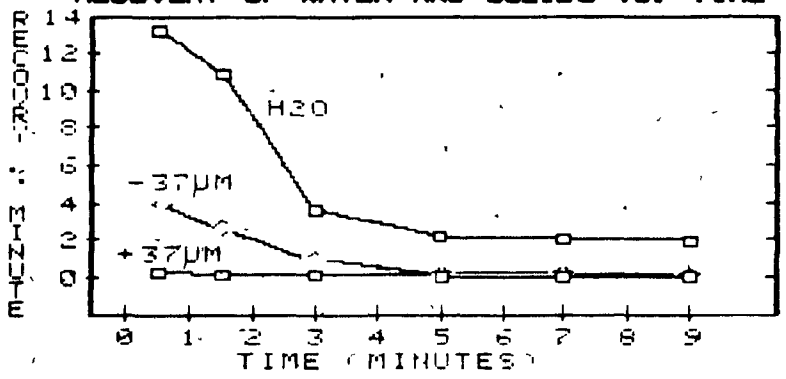

FIGURE 4.2

RECOVERY OF SOLIDS VS. WATER

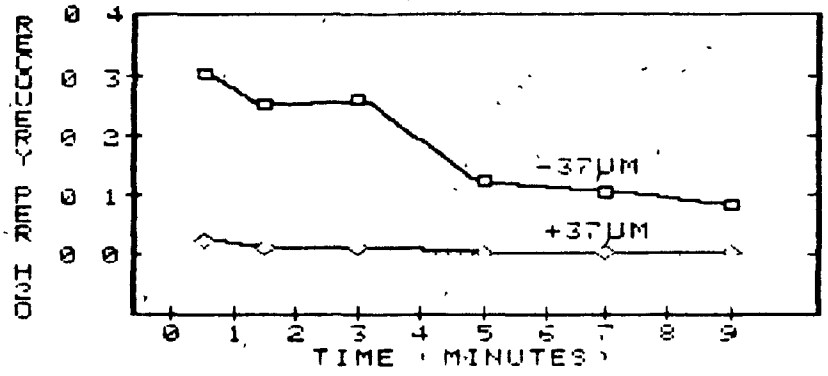

and water recovery after about 3 minutes was only about 2% per minute. Recovery of gangue in both the coarse and the fine size fractions was found to be lower than water recovery at all times.

Figure 4.2 shows the recovery rates of the coarse and fine gangue fractions relative to water. The fine fraction (-37μm) was recovered more quickly than the coarse (+37μm) material; however, the maximum recovery rate of fines (from 0-1 minute) was only 30% of the water recovery rate. The coarse material was recovered at only about 2% of the water recovery rate. There was therefore no indication that the gangue material floated under the experimental conditions. The mass recovered in the flotation test was found to assay 0.51% zinc, corresponding to a zinc recovery of 74%. It can be concluded that the sphalerite trace constituent floated but that the gangue was recovered entirely by entrainment.

A series of unpublished experiments was performed by Tony Little at McGill University in 1982. Two different types of Pine Point gangue were identified by their physical appearance and their different grindabilities, and the flotation responses of these two gangue types were compared to that of silica sand. The gangue types were <u>light</u> gangue, with a light colour and low grindability, and <u>dark</u> gangue, with a dark colour and high grindability. The samples were ground to 50% -200 mesh in the presence of sodium cyanide, zinc sulphate and copper sulphate, and were conditioned with sodium

isopropyl xanthate prior to flotation. Methyl isobutyl carbinol was used as a frother.

Results of the flotation tests are presented in Table 4.2 and Figure 4.3. Recovery of solids was a more or less constant 16% of water recovery for both gangue and silica, revealing no evidence of gangue flotation. The recoveries of silica and gangue as a function of water recovery were essentially the same, indicating that the gangue showed no unusual recovery characteristics under the conditions of the experiment.

FIGURE 4.3
RECOVERY OF GANGUE AND SILICA

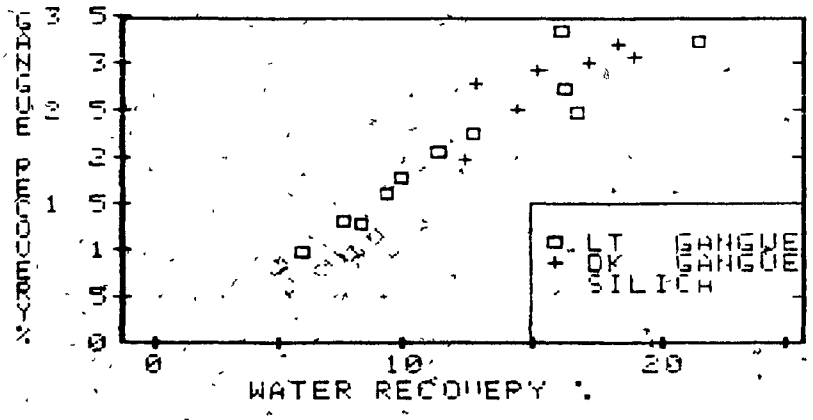

(from LITTLE, unpublished, 1982)

TABLE 4.2

RECOVERY OF WATER AND GANGUE DURING FLOTATION

	RECOVERY OF: WATER	SOLIDS	SOLIDS PER H2O	MEAN & S.D.
SILICA	5.39	0.78	0.14	
	5.51	0.68	0.12	
	8.97	1.27	0.14	
	6.74	0.79	0.12	
	10.81	1.82	0.17	
	8.34	1.01	0.12	
	9.84	1.12	0.11	
	6.46	0.80	0.12	
	5.47	0.49	0.09	
	7.73	0.95	0.12	.128
	6.83	0.93	0.14	+/- .020
LIGHT GANGUE	12.74	2.24	0.18	
	11.32	2.07	0.18	
	16.77	2.47	0.15	
	8.32	1.27	0.15	
	21.58	3.22	0.15	
	9.99	1.77	0.18	
	16.30	2.73	0.17	
	16.17	3.35	0.21	
	9.37	1.60	0.17	
	7.51	1.30	0.17	.169
	5.98	0.96	0.16	+/- .017
DARK GANGUE	11.70	2.80	0.24	
	14.49	2.95	0.20	
	14.80	2.35	0.16	
	12.37	1.96	0.16	
	19.17	3.18	0.17	
	17.66	3.11	0.18	.182
	18.79	3.32	0.18	+/- .029

(from LITTLE, unpublished, 1982)

4.2 Summary of Gangue Flotation

Flotation tests performed upon Pine Point gangue samples revealed that recovery of gangue was higher in the fine size fractions than in the coarse fractions. Both coarse and fine gangue were recovered at a rate less than that of water. Previous work at McGill University showed that Pine Point gangue exhibited no flotation characteristics under typical Pine Point flotation conditions. It was also found that the gangue material showed a similar flotation response to that of silica, which is considered to be strongly hydrophylic.

It is concluded that Pine Point gangue shows no flotation response under normal Pine Point flotation conditions and that recovery mechanisms of Pine Point gangue are typical of those exhibited by a strongly hydrophylic material. Consequently, the only gangue recovery mechanisms which are expected to be operative during the flotation of Pine Point sphalerite are entrainment and sliming in the fine size fractions and locking in the coarse size fractions.

CHAPTER 5

LIBERATION OF PINE POINT ORE DURING GRINDING

CHAPTER 5: LIBERATION OF FINE POINT ORE DURING GRINDING

5.0 Introduction; Goals of Comminution and Choice of Grind Sizes

The principal goal of comminution in ore processing is the liberation of valuable ore minerals from unwanted gangue and from each other so that physical separation may be achieved. Each mineral in an ore exhibits characteristic size and shape distributions (textures) which are governed by the petrogenesis of the ore deposit. The variety and distribution of mineral textures in the ore is the principal factor which determines the amount of size reduction which is needed to effect separation. Additional constraints are imposed by the size requirements of some separation processes. Flotation of sulphide minerals, for example, is generally not very efficient at grain sizes much above 64+100 mesh.

The grind size which is used for a particular ore is largely governed by economic considerations and is not necessarily the size which produces optimum metallurgical performance. The grind is generally kept as coarse as possible in order to minimize capital costs (cost of the mill) maintenance costs (liner replacement, etc.) and operating costs (energy consumption). Use of too coarse a grind, however, may result in low ore mineral recoveries and possible penalties due to the introduction of locked gangue into the concentrate. The optimum grind size can therefore be defined as the size at which the sum of (capital costs + maintenance costs + operating costs + value of lost recovery + penalties) is

minimized. Determination of the optimum grind size is a complex process which requires prediction of anticipated costs and performance prior to purchase of the mill and adjustments to operating procedures following mill startup. Periodic adjustments must also be made when ore from a mine exhibits variable grindability.

Ore at Pine Point is ground to approximately 50% passing 200 mesh (74μm). The discussion which follows focuses upon textural features in Pine Point ore which show mineral associations at a size finer than 50-70μm. It is assumed that such associations could cause significant locking at the current grind size. A liberation study is carried out upon a sample of Pine Point zinc concentrate in order to relate the observed textural features to the amount of magnesium which enters the concentrate. Due to possible discrepancies between metallurgically and economically optimum grind sizes it is not possible to evaluate the feasibilty of changing the grind in order to effect greater liberation of the sphalerite from the gangue; however, an estimate is made regarding the amounts of magnesium which are contributed by the introduction of locked particles into the concentrate under the current operating conditions.

5.1: Textural Characteristics of Pine Point Ore and Ore Mineral Distribution in the Rod Mill Feed

In this section the textures of the "difficult" ore used in the locked cycle test are examined in order to identify mineral associations which could give rise to processing problems. Hand samples were obtained by screening the original batch of rod mill feed at four centimeters and collecting the oversize. A total of 137 hand samples were obtained, only 45 of which contained visible mineralization. The mineralized specimens contained an estimated 25-95% ore minerals by volume with only 3 specimens appearing to contain less than 25% sulphides. This observation is concordant with the geology of the area since mineralization tends to terminate abruptly without any disseminated fringes. The feed to the mill can be characterized as a mixture of high-grade material (approximately 30% of the feed) and apparently barren gangue (approximately 70% of the feed). Approximately one third of the specimens contained abundant calcite.

Twenty-three specimens were made into polished sections. Of these twelve were chosen at random from the sulphide-rich specimens, ten were chosen at random from the carbonates and one was chosen from the three sulphide-poor specimens.

Examination of the mineralized polished sections under a reflected-light ore microscope revealed the presence of distinct textural types in the ore. Six of the thirteen

mineralized specimens were composed almost entirely of sulphides (colloform ore). Four were composed of finely associated dolomite and sphalerite (disseminated ore) and three were composed of blocky sphalerite in dolomite (blocky ore).

The ten gangue samples were classified into three categories. Two were composed of very fine dolomite with some primary textures and high porosity (micritic dolomite). Seven were composed of coarse dolomite intergrowths with no primary textures and high intercrystalline porosity (sucrosic dolomite) and one was composed of coarse dolomite spar with vuggy porosity (sparry dolomite). None of the gangue samples were found to contain visible galena or sphalerite in polished section.

The following discussion elaborates upon the textural features of the various ore and gangue types which were identified in the mill feed. By relating the textures to episodes of ore deposition and alteration it is possible to create a petrogenetic definition of ore which could present potential processing problems. Such a definition has potential mill-site applications since foreknowledge of the occurrence of difficult ores could allow both the blending and stockpiling of ore according to texture and the implementation of compensating changes to mill procedures before problems arose.

The illustrations which follow were created by one of three techniques:

a) Conventional colour photography, used for 2:1 magnification of polished sections.

b) Microphotography under plane-polarized reflected light, used for illustration of surface features at high resolution.

c) Microphotography under cross-polarized reflected light, used for illustration of sphalerite banding at low resolution.

Plane-polarized light reveals the relative reflectivities of the mineral surfaces. Galena is more reflective than sphalerite, which in turn is more reflective than carbonate or the mounting medium. Thus, galena appears to be white, sphalerite appears to be gray, and both carbonate and the mounting medium appear to be dark gray or black. This photographic technique is used to illustrate detailed textural features.

Since both galena and sphalerite are optically isotropic insertion of an analyzing polarizer (cross-polarized light) eliminates surface reflections. The only light which is seen under such conditions is that which is multiply reflected from sub-surface crystal interfaces. Since the amount of internally reflected light is related to the translucency of the specimen colour banding in sphalerite is revealed; however, since the

image is created by subsurface reflections resolution is low and the image is slightly diffuse. Galena, under such conditions, appears to be black.

Colloform Ore:

The term "colloform" is generally used to describe laminated botryoidal masses of a mineral, especially sphalerite from Mississippi Valley-type ore deposits. The term may be misleading since there is some dispute as to whether or not these textures were formed by true colloidal deposition (Roedder, 1968). For the purpose of this disscussion the term "colloform" is used exclusively as a texturally descriptive term with no genetic implications.

A polished section of colloform ore is illustrated in Figure 5.1. The sample consists almost entirely of sphalerite in a wide variety of colours which range from an almost porcelanous light tan to a more vitreous dark brown. Some small steel-gray grains of galena (gn) can be observed. No carbonate is visible in this polished section.

Figure 5.2 presents a good example of colloform textures in sphalerite viewed under cross-polarized reflected light. A large sphalerite (sph) botryoid in the centre of the diagram has nucleated around a blocky grain of galena (gn).

Pine Point galena can also occur in colloform ore as dendritic crystals (Figure 5.3). This texture is indicative of rapid crystal growth. Galena has a cubic structure and

FIGURE 5.1
POLISHED SECTION OF COLLOFORM ORE

FIGURE 5.2
SPHALERITE BOTRYOID NUCLEATING AROUND GALENA

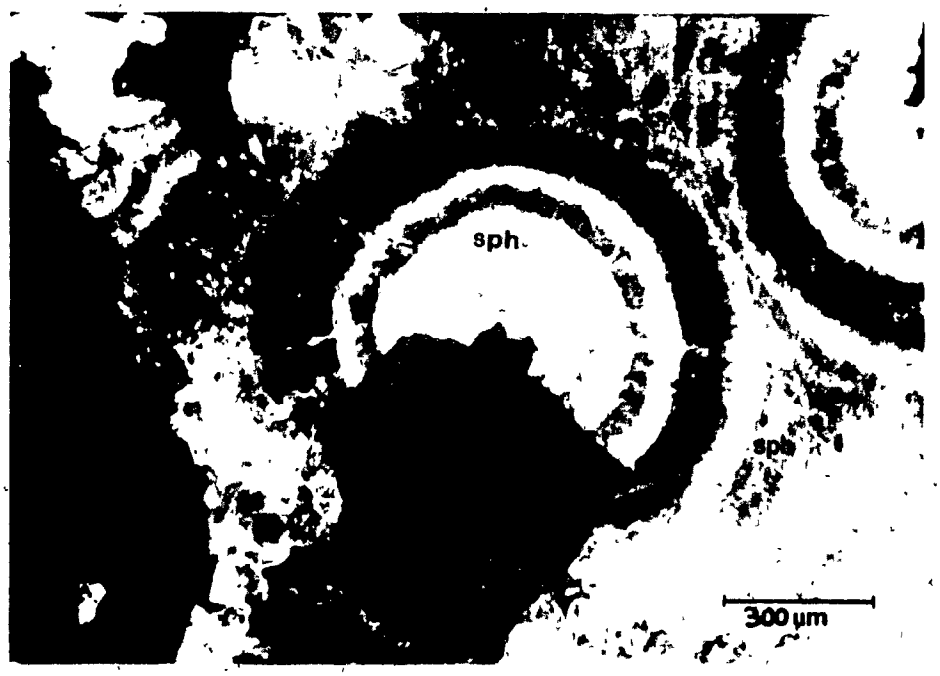

(cross-polarized light)

FIGURE 5.3
DENDRITIC GALENA IN SPHALERITE (COLLOFORM ORE)

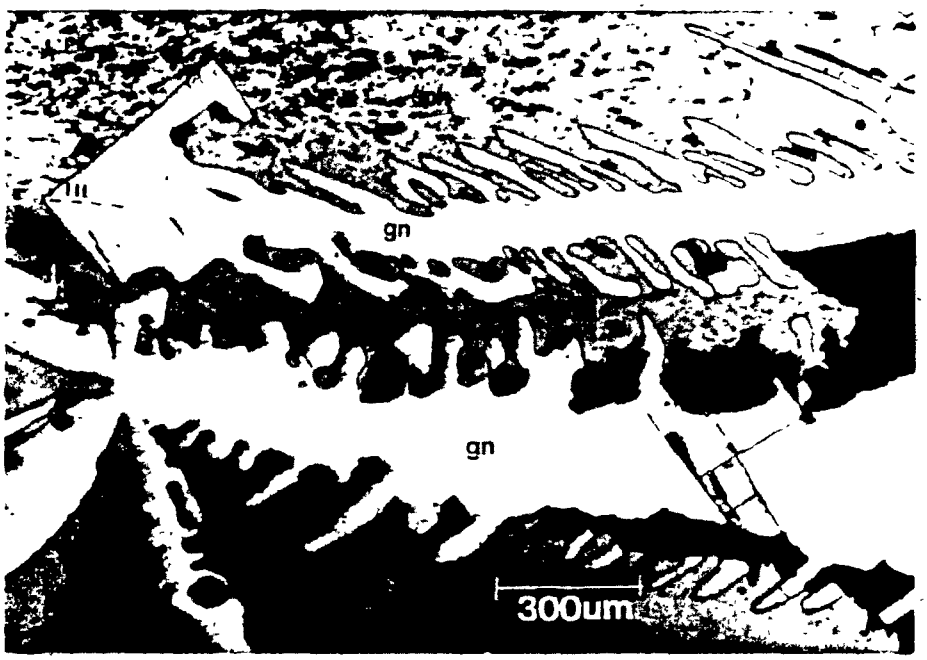

(plane-polarized light)

therefore grows most rapidly in the (111) direction, as seen in the illustration. The sphalerite in this sample was banded perpendicular to the growth axis of the galena. The textures seen in Figure 5.3 reveal a potential locking problem since individual galena dendrites vary from 10μm to 30μm in thickness and would not be expected to liberate completely at the current Pine Point grind size. Dendritic galena could therefore cause zinc flotation in the lead circuit.

The depositional episodes recorded in the previous two figures are simple and exhibit no visible post-depositional alteration. Figure 5.2 records deposition of botryoidal sphalerite upon pre-existing galena while Figure 5.3 records concurrent and rapid growth of sphalerite and galena. Textural relationships seen in colloform ore often exhibit a much greater degree of complexity. The Pine Point deposits were formed during several episodes of deposition and dissolution of both the ore minerals and the country rock. Single hand specimens of ore may therefore show a variety of complex textures caused by this repeated deposition and remobilization of the constituent minerals.

Figure 5.4 shows a different area of the sample in Figure 5.2, photographed under plane-polarized light. The figure shows basic colloform textures; however, some alteration can be seen. The clear white area marked "gn" in the top left of the figure is primary galena. This galena is separated from a large primary sphalerite botryoid below it by a wedge of

FIGURE 5.4
SECONDARY ALTERATION IN COLLOFORM ORE

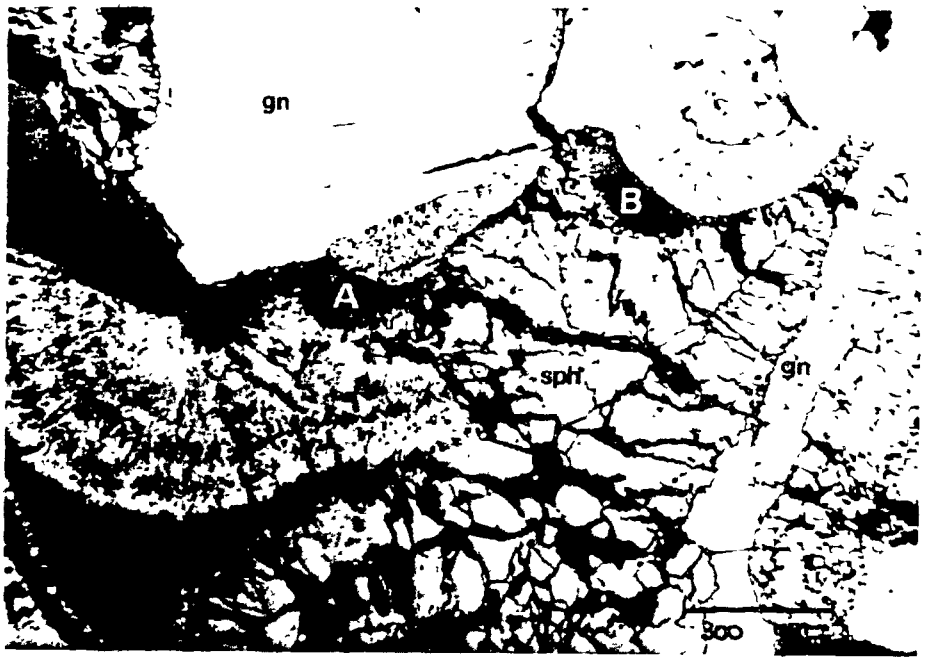

(plane-polarized light)

FIGURE 5.5
SECONDARY ALTERATION IN COLLOFORM ORE

(cross-polarized light)

carbonate (cb). The sphalerite botryoid can be more clearly seen in Figure 5.5 which is a view of the same field under cross-polarized light.

The two figures record a secondary episode of replacement during which "grainy" galena replaced sphalerite. This secondary galena replaced sphalerite along the bands of botryoids (the curved galena just above the label "B" on the sample) and along botryoid interfaces (the vein of secondary galena marked "gn").

After deposition of secondary galena the sample underwent tensional fracturing which preferentially separated the sphalerite botryoids either perfectly parallel to the banding (area "B" in Figure 5.4) or perfectly perpendicular to it (just below the label "cb" on the same figure). Preferential parting occurred at sphalerite/galena interfaces (eg. between sphalerite and the primary and secondary galena at "A", and between sphalerite and the secondary galena at "B"). The fractures were filled with carbonate, possibly at the same time as they were developing. There is no evidence that the carbonate-bearing solutions dissolved major amounts of sulphides.

Figure 5.6 shows a third area of the sample shown in Figure 5.2. In addition to the features generated by primary textures, secondary galena and fracturing this figure shows features caused by the replacement of sphalerite with carbonates. The following features can be noted on the figure:

FIGURE 5.6
CARBONATE REPLACEMENT TEXTURES IN COLLOFORM ORE

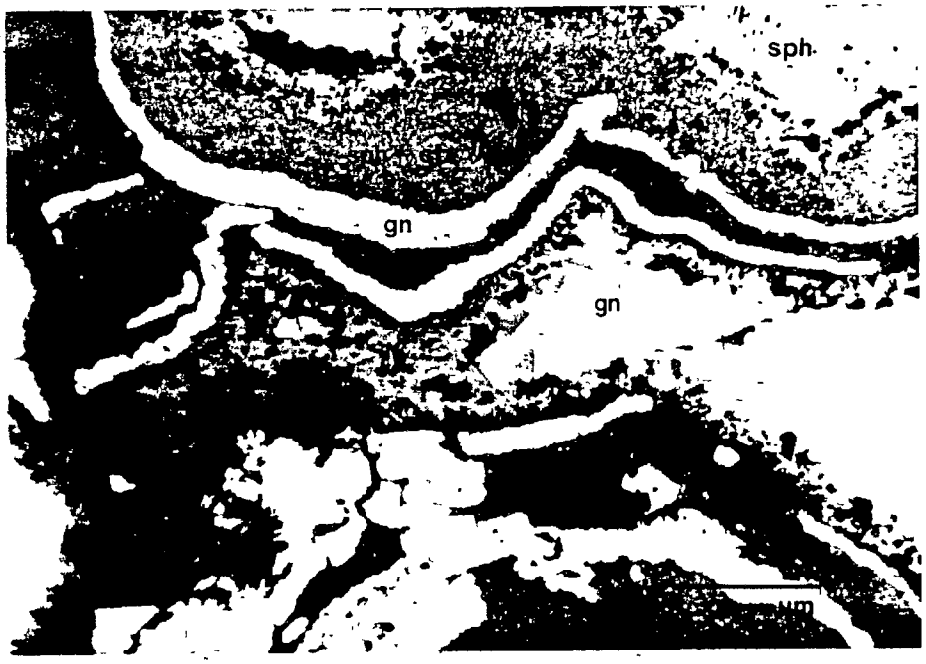

(plane-polarized light)

- Galena (gn) is found in two principal forms. The first is a replacement form which follows the outlines of former sphalerite botryoids (the elongated galena running the length of the figure, and the slightly more blocky galena at the bottom-centre). The second form is a late void-filling galena (the bright, massive galena at centre-right).

- Sphalerite is found in three principal forms. The first is primary sphalerite, as seen in the upper right-hand corner of the figure. The second is corroded sphalerite, seen at the rims of primary sphalerite in association with carbonate (cb), and the third type is void-filling sphalerite, seen lining the rim of the void-filling galena.

- Carbonate is seen in one form, replacing sphalerite and filling voids.

On the basis of the above information and the petrogenetic interpretations of Figures 5.2 and 5.4 the following history of the sample can be constructed:

1) Sphalerite was deposited in colloform textures. Galena was probably not present in major amounts.

2) Galena selectively replaced some bands in the sphalerite botryoids. This replacement predated the void-filling galena.

3) A second episode of sphalerite precipitation resulted in the deposition of euhedral void-filling grains. This deposition was terminated by a third episode of galena deposition which completely occluded the void space.

4) Tensional fracturing opened up new void spaces in the sample. Concurrent sphalerite dissolution and carbonate deposition altered much of the primary colloform sphalerite. The grainy nature of the "sph+cb" area suggests that dissolution occurred along grain boundaries, leaving tiny islands of undissolved sphalerite at the former sites of complete botryoids. The void-filling sphalerite shows only minor corrosion around the edges and may have been protected from replacement by its larger grain size.

The observed textures reveal a variety of ways in which the constituent minerals of colloform ore associate. Blocky and replacement galena generally have grain sizes over 50μm; however, the dendritic variety of galena exhibits elongated dendrites which often have thicknesses as low as 10-20μm. Sphalerite is generally massive and botryoidal; however, fractured sphalerite may contain fillings of carbonate with thicknesses of as little as 10μm and replacement textures with grain sizes in the sub-micron range.

Further examination of sphalerite/carbonate replacement textures was conducted under an electron beam microprobe. Figure 5.7 is a secondary electron image (SEI) of a sample of corroded sphalerite while Figures 5.8 and 5.9 show the zinc and calcium K-alpha emissions, repectively. Magnesium emissions were low, thereby revealing calcite as the replacement mineral in this sample. Dissolution of the sphalerite botryoids was evidently band-selective since

FIGURE 5.7
SECONDARY ELECTRON IMAGE OF REPLACEMENT TEXTURE

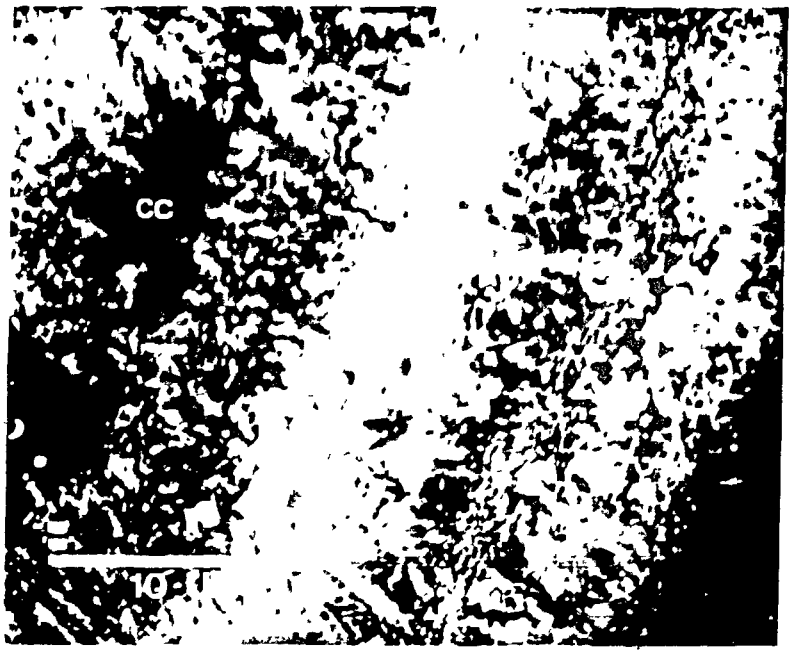

(WHITE BAR = 10μM)

FIGURE 5.8
ZINC K-ALPHA EMISSIONS FROM AREA OF FIG. 5.7

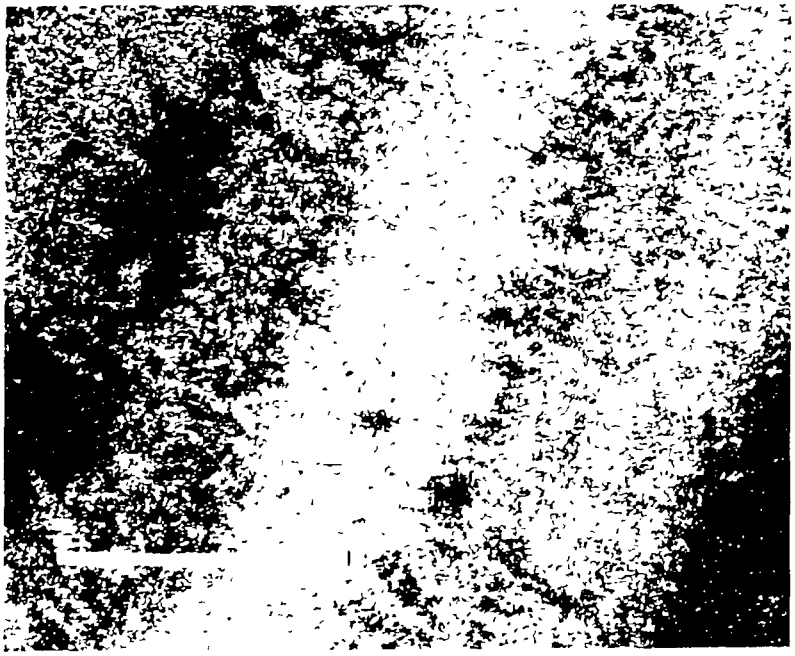

(WHITE BAR = 10μM)

FIGURE 5.9
CALCIUM K-ALPHA EMISSIONS FROM AREA OF FIG. 5.7

(white bar = 10um)

Figure 5.9 shows three banded areas which exhibit no calcium emissions.

The high-calcium areas are composed of sub-micron associations of calcite and sphalerite. There is evidence that sphalerite particles may have sizes as low as 0.1μm in diameter; however, such ultrafine surface features are obscured by surface irregularities left during sample preparation.

Disseminated Ore:

A polished section of disseminated ore is illustrated in Figure 5.10. In hand sample the ore appears to consist of sphalerite flakes which "float" in carbonate. Galena is generally not visible to the naked eye.

Microscopic examination of disseminated ore reveals textures which are fundamentally different from those exhibited by colloform ore. Two common disseminated textures are illustrated in Figures 5.11 and 5.12 and are referred to as void-filling and co-precipitated subgroups, respectively, of the disseminated ore type.

The void-filling texture seen in Figure 5.11 was formed by the introduction of sphalerite into void spaces in the dolomitic host rock. Pyrite and galena are generally no more than trace constituents in this type of ore. The host consists of euhedral dolomite crystals which exhibit planar intercrystalline boundaries (equivalent to "sucrosic

FIG. 5.10

POLISHED SECTION OF DISSEMINATED ORE

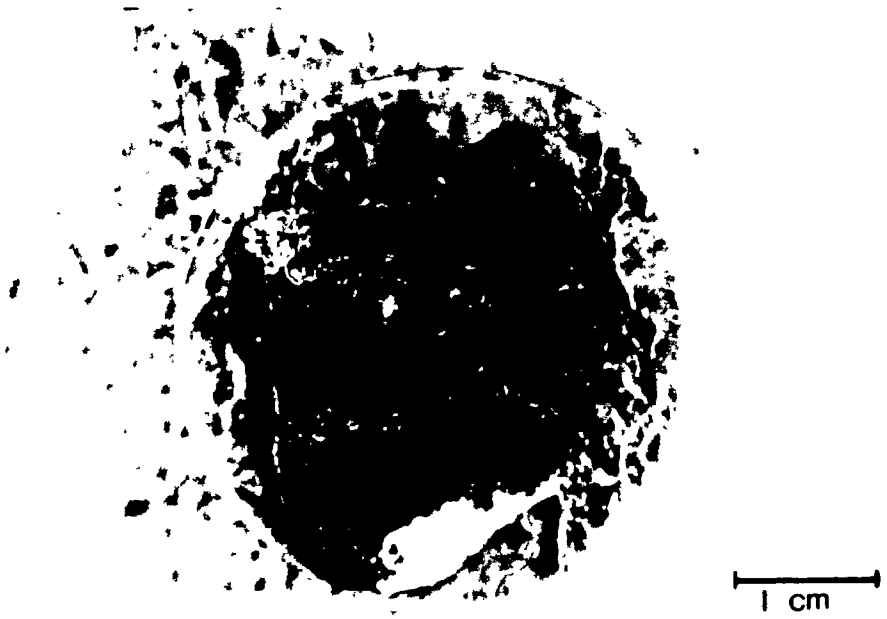

dolomite"). The void-filling sphalerite seen in the illustration appears to be euhedral since its deposition was controlled by the configuration of pores in the host rock. Sphalerite completely occluded the porosity, at which point mineralization ceased. There is no evidence that the mineralizing solutions caused carbonate dissolution; nor is there any evidence of secondary alteration.

The co-precipitated texture illustrated in Figure 5.12 shows textural associations which are more intricate than

FIGURE 5.11
VOID-FILLING VARIETY OF DISSEMINATED TEXTURE

(plane-polarized light)

FIGURE 5.12
CO-PRECIPITATED VARIETY OF DISSEMINATED TEXTURE

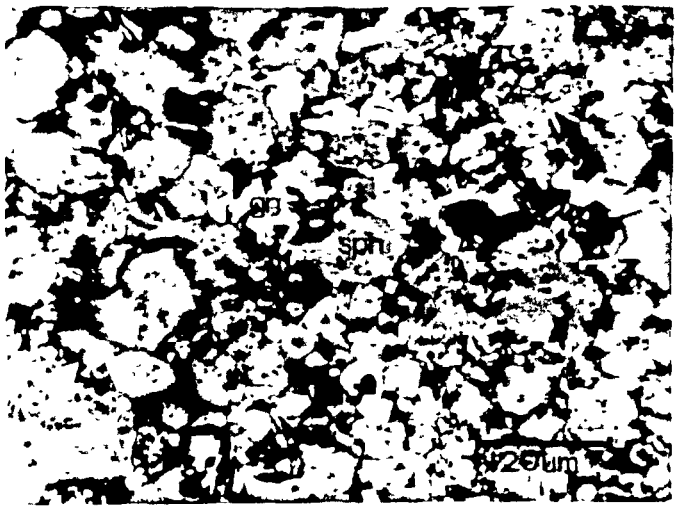

(plane-polarized light)

those exhibited by the void-filling texture. Galena, pyrite and dolomite occur as secondary minerals filling interstices between well-developed sphalerite blebs. In some samples areas exhibiting void-filling textures can be seen; however, the dolomite exhibits corroded boundaries and shows evidence of dissolution. It is interpreted that an episode of concurrent carbonate dissolution and sulphide precipitation resulted in the liberation of euhedral grains of sphalerite such as those seen in Figure 5.11. Secondary sphalerite accreted upon these grains, thereby forming the spheroidal sphalerite grains observed in Figure 5.12. Galena and pyrite had few pre-existing nucleation sites and therefore formed small, dispersed crystals in between the sphalerite grains. The deposition of interstitial dolomite probably reflects a change in solution chemistry following alteration and secondary ore deposition. It is unlikely that the secondary dolomite was deposited at the same time that the primary (host) dolomite was dissolved.

The grain sizes seen in Figures 5.11 and 5.12 are much smaller than those which were observed for the colloform ore. The mean size of sphalerite grains in Figure 5.11 is approximately 50um; thus, particles of void-filling ore with grain sizes above approximately 50μm are expected to be substantially locked. The co-precipitated sphalerite of Figure 5.12 has a mean grain size of approximately 70μm; however, these grains are separated by only about 20μm and the

interstitial material is composed largely of dolomite. Thus, many particles of co-precipitated ore with a grain size much above 20μm are expected to be locked. It can be appreciated, therefore, that in a flotation feed with a size of 80 % passing 200 mesh disseminated ore could introduce substantial amounts of locked magnesium into the concentrate.

Blocky Ore:

A polished section of blocky ore is illustrated in Figure 5.17. The ore consists of coarse sphalerite spar hosted in sparry dolomite or sparry calcite. The grain size of the sphalerite often approaches 1.0-1.5 cm. The interfaces between the sphalerite and the carbonates are generally planar and free of alteration.

Examination of blocky ore in polished section reveals that the sphalerite is free of intricate textures and contains no inclusions of other minerals. The only feature which can be observed under the microscope is a uniform field of apparently pure sphalerite. This type of ore is expected to show excellent liberation characteristics due to its lack of intricate textures and large grain size.

FIGURE 5.13
POLISHED SECTION OF BLOCKY ORE

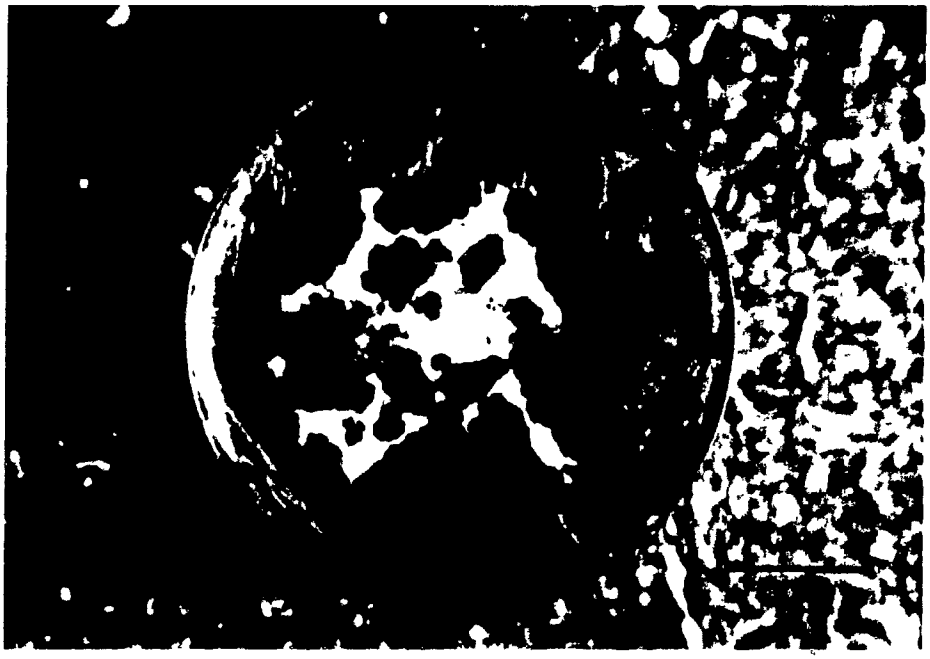

Varieties of Gangue:

The gangue material found in the rod mill feed was classified into micritic, sucrosic and block types. The most common form of gangue was the sucrosic type which constituted about 85% of the non-mineralized gangue samples. About 10% of the samples were composed of sparry gangue and about 5% of the gangue samples were of the micritic type. Only a small proportion of the gangue-bearing samples were mineralized. Ninety-two of the 137 hand samples in the study, (67%) contained no mineralization, while 34 samples (25%) contained mixed sulphides and gangue and 11 samples (8%) were composed of essentially pure sulphides.

A polished section of micritic dolomite is shown in Figure 5.14. The grain size of this type of dolomite was very fine (although not fine enough to classify as true micrite according to the geological definition of the word) and primary structures, in this case bedding laminations, could be seen. The dark laminations in this sample contain sub-micron sized pyrite which is interpreted as being diagenetic. Micritic dolomite was found to be very porous; dark areas can be seen around the border of the sample in Figure 5.14 where mounting resin soaked into the pores of the rock. No mineralized samples of micritic dolomite were found.

Sucrosic dolomite is illustrated in Figure 5.15. This type of dolomite showed no primary textures, and had a relatively coarse grain size (up to 1mm). Porosity was highly

FIGURE 5.14
MICRITIC VARIETY OF DOLOMITE GANGUE

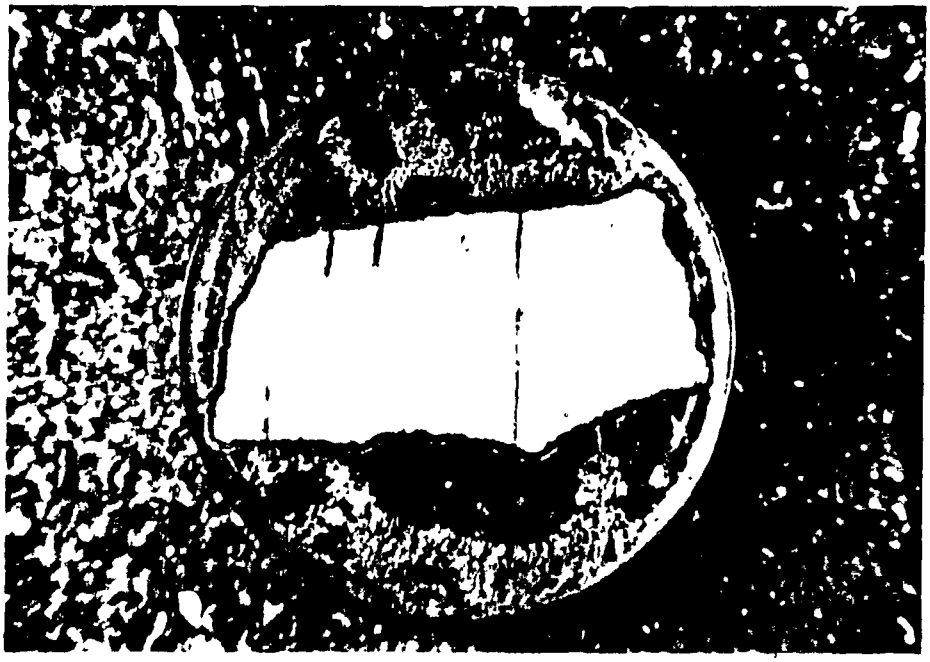

FIGURE 5.15
SUCROSIC VARIETY OF DOLOMITE GANGUE

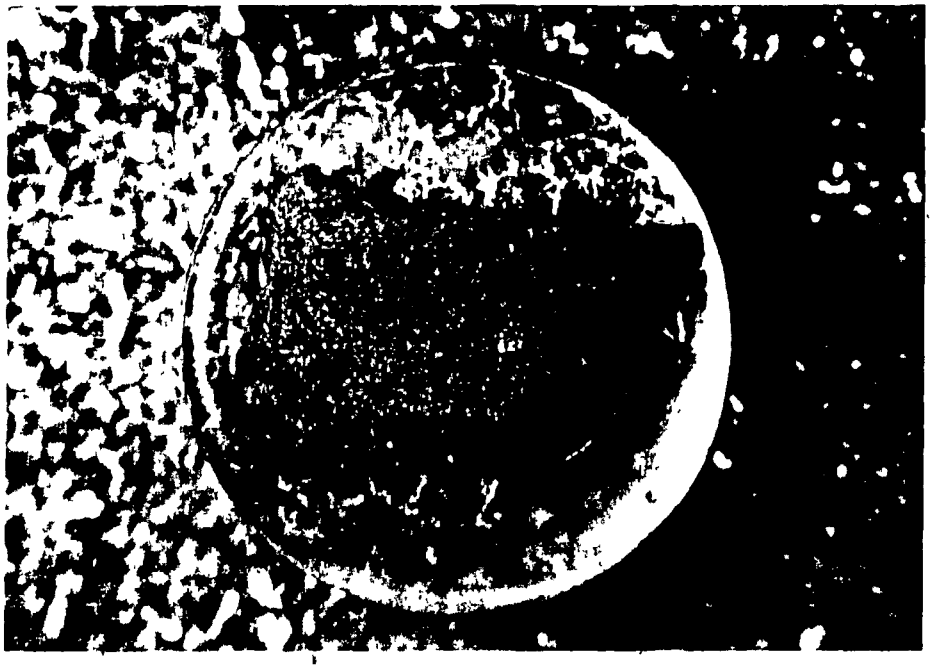

FIGURE 5.16
SPARRY VARIETY OF DOLOMITE GANGUE

variable. It appeared that all samples had a certain amount of original porosity which showed variable infilling by late calcite. In cases where the porosity contained infillings of sphalerite this type of gangue hosted the void-filling variety of disseminated ore.

Sparry gangue is illustrated in Figure 5.16. This type of gangue consisted of large crystals (up to 3 cm) of either calcite or dolomite with high amounts of vuggy porosity. Sparry gangue containing sphalerite crystals was previously referred to as blocky ore.

Discussion:

The principal characteristics of the +4cm rod mill feed have been discussed. Quantitative extrapolation from the +4 cm size fraction to smaller size fractions must be carried out with great reservations since the sulphides and gangue may have different crushabilities. The principal observations made in this section are summarized below:

1) Approximately 70% of the hand samples obtained from the rod mill feed were barren. The other 30% of the samples contained from 25% to almost 100% sulphides by volume. There were almost no samples which showed sparse mineralization.

2) The mineralized samples could be divided into three textural types. These were <u>colloform</u> ore, <u>disseminated</u> ore and <u>blocky</u> ore.

3) Colloform ore was characterized by banded sphalerite

and dendritic galena. No primary carbonates were observed in the samples.

4) Secondary carbonates were introduced into colloform ores along fractures. In the majority of cases it was not determined whether these carbonates were dolomite or calcite, although the samples which were tested revealed the presence of both carbonates. The carbonates often replaced sphalerite and led to the development of complex associations of carbonate and sphalerite with grain sizes down to 1μm.

5) Secondary carbonates were not seen in all areas of all colloform samples, but appeared to be local phenomena.

6) Disseminated ores consisted of fine-grained associations of sphalerite and sucrosic dolomite with variable amounts of galena and pyrite. Two varieties of disseminated ore were identified. The void-filling variety was formed by the introduction of sphalerite into pores in the dolomite. The co-precipitated variety was interpreted as an altered form of void-filling disseminated ore which was formed by concurrent dissolution of the dolomite host and precipitation of sphalerite, galena and pyrite during a secondary episode of mineralization.

7) Three types of gangue were identified. Micritic gangue was composed of fine grained dolomite which showed primary textures and exhibited high porosity. Sucrosic gangue was composed of coarser grained dolomite which showed no primary textures and exhibited intercrystalline porosity. Sparry

gangue was composed of coarse, void-filling dolomite and calcite with vuggy porosity. Only a small proportion of the gangue samples were mineralized and classified as ore.

It is evident from the previous discussion that Pine Point ore does not consist of a uniform assemblage of minerals. Hand samples taken from the rod mill feed show great variability in texture and in composition. Even single polished sections may exhibit different textures in different areas of the sample. This has great impact upon the application of liberation models to the ore. It can be roughly estimated that over 90% of the carbonate is barren, and is therefore liberated at any grind size. The remaining carbonate is liberated only at a fine grind size and some carbonate (that in the corroded colloform samples) cannot really be liberated at all.

Ore which is processed at Pine Point is blended from various stockpiles. It is not known, therefore, whether the various textures seen in the ore represent ore from different pits or whether single pits produce ore with a variety of textures. It is evident, however, that some textures are more amenable to liberation than others. A mill feed containing a high amount of blocky ore or a high proportion of unaltered colloform ore would produce a mill feed which was easily liberated, while a pit which contained a highly altered colloform ore or a high proportion of disseminated ore would produce a mill feed which was much more difficult to process.

Variability in ore texture is clearly a factor which could have major effects upon mill performance.

During the course of this research no opportunity arose for the author to collect ore samples from working pits at Pine Point. Consequently, no direct evaluation can be made in this thesis regarding the importance of textural variations as a processing variable. The only other available samples of Pine Point ore were polished sections made for the geology department of McGill University some time in the mid to late 60's. These sections were composed almost entirely of colloform ore and showed a remarkable lack of alteration. No conclusions can be made, however, since the samples were likely to have been chosen with bias in order to show clean textures. Analysis of the spatial distribution of textural ore types in the Pine Point area is an area for further research which could potentially be used to explain and to predict the occurrence of difficult ores.

5.2 Liberation in a Sample of Pine Point Leach Plant Feed

A sample of leach plant feed (second cleaner concentrate) was collected from the Pine Point concentrator on the same day during which the rod mill feed was collected for use in the locked cycle test and the textural study. The concentrate was screened and assayed (Table 5.1) and the separate size classes were prepared for assessment of their liberation. Due to low contrast between carbonate and the mounting medium it was difficult to accurately count carbonate particles in the size classes smaller than 270 mesh (74μm); therefore, it was decided to conduct the liberation study upon the four size classes between -64 and +270 mesh. One thousand magnesium-bearing particles were counted from each of the size classes and classified according to their magnesium content, which was visually estimated, and their textural type, as outlined below.

TABLE 5.1

ASSAY OF SECOND CLEANER CONCENTRATE

MG ASSAY AS A FUNCTION OF SIZE		
SIZE	MASS%	MG%
+64	7.20	1.62
+100	15.21	1.23
+150	17.59	0.76
+200	14.31	0.32
+270	12.03	0.18
+400	9.51	0.13
-400	23.15	0.18

The feed contained two distinct types of locked particle. The first type was what one would consider a "conventional" locked particle containing sphalerite and carbonate joined by a single boundary, as illustrated in Figure 5.17. These particles are referred to in the discussion as simple locked particles. The second type of locked particle consisted of intimate associations of sphalerite and carbonate, usually in the form of carbonate inclusions in a sphalerite matrix. The inclusion size ranged from about 3μm to 50μm with an average size of 10μm. This type of locked particle is illustrated in Figure 5.18 and is referred to as complex. Little gradation was observed between the simple and complex particle types. It is interpreted that simple locked particles were formed by the comminution of blocky and colloform ore while complex locked particles were formed by the comminution of disseminated ore.

The expected liberation characteristics of the two locked particle types are widely different. Reduction of the simple locked particle of Figure 5.17 by two or more size classes would clearly result in the production of at least one liberated particle; however, in order to produce significant liberation in the complex particle of Figure 5.18 one would have to reduce its size by approximately five or six size classes. The particle shown in the figure is from the -64/+100 mesh size fraction and would not expected to show significant liberation at particle sizes above approximately 20-25μm.

The results of the particle counting study are presented

FIGURE 5.17

SIMPLE LOCKED PARTICLE

(plane polarized light)

FIGURE 5.18

COMPLEX LOCKED PARTICLE

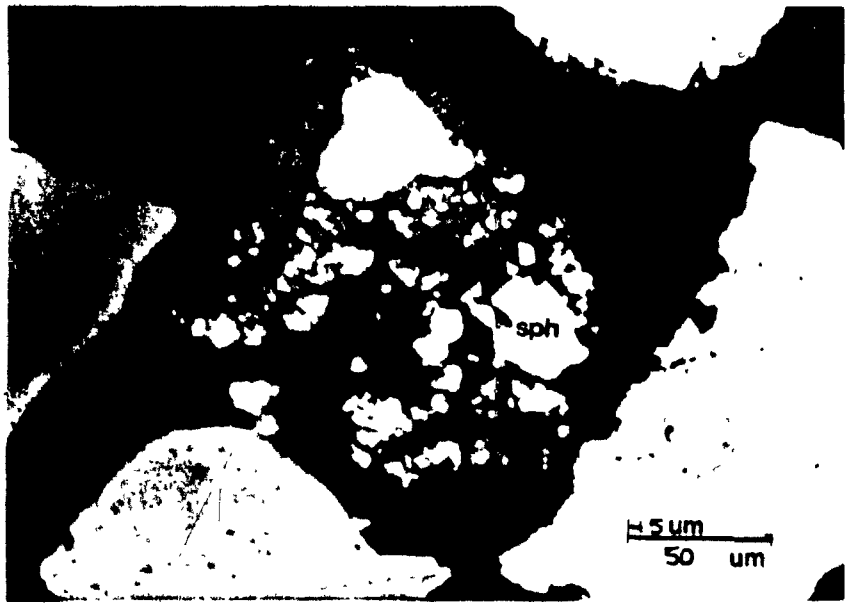

(plane-polarized light)

in Tables 5.2 to 5.5 and in Figures 5.19 and 5.20. The figures show the relative abundances of locked particles with various compositions. It can be seen in Figure 5.19 that the simple locked particles were more or less evenly distributed throughout the entire range of possible particle compositions. In contrast, most of the complex particles had low gangue content (Figure 5.20).

The even distribution of particle compositions seen in Figure 5.19 is not what one would normally expect in a flotation product. Particles with high amounts of gangue are usually considered to be less flotable than particles with little gangue and should therefore be less abundant in the concentrate; however, the distribution of particle compositions observed in the figure is concordant with the locked-cycle observation that coarse magnesium rejection in the cleaners was negligible. It appears that composite particles containing only small amounts of sphalerite were highly flotable.

The simple particle profile for +270 mesh particles seen in Figure 5.19 is different from the profiles which are observed for the three coarser size classes. The +270 mesh size fraction shows an increased frequency of particles with low amounts of gangue. It is probable that the coarsest carbonate inclusions in the complex particles, with a size of about 50um, began to exhibit simple locking at -200/+270 mesh (-74/+50um). This phenomenon would explain the increased

TABLE 5.2
LIBERATION OF +100 MESH PARTICLES

+100 MESH:	AMOUNT OF PARTICLES CONTAINING A GIVEN PERCENT OF MAGNESIUM						
% MG:	1-20	20-40	40-60	60-80	80-99	100.00	TOTAL
SIMPLE:	121	115	137	120	117	185	795
COMPLEX:	112	32	28	17	16		205
	ABOVE NUMBERS AS A PERCENT OF TOTAL PARTICLES IN ANY ONE TYPE						
SIMPLE:	15.2	14.5	17.2	15.1	14.7	23.3	100
COMPLEX:	54.6	15.6	13.7	8.3	7.8		100
	MG CONTRIBUTION AS A % OF TOTAL MAGNESIUM IN SAMPLE						
SIMPLE:	2.2	6.3	12.4	15.3	19.1	33.6	88.9
COMPLEX:	2.0	1.7	2.5	2.2	2.6		11.1

TABLE 5.3
LIBERATION OF +150 MESH PARTICLES

+150 MESH:	AMOUNT OF PARTICLES CONTAINING A GIVEN PERCENT OF MAGNESIUM						
% MG:	1-20	20-40	40-60	60-80	80-99	100.00	TOTAL
SIMPLE:	108	101	125	104	87	163	688
COMPLEX:	183	59	35	20	15		312
	ABOVE NUMBERS AS A PERCENT OF TOTAL PARTICLES IN ANY ONE TYPE						
SIMPLE:	15.7	14.7	18.2	15.1	12.7	23.7	100
COMPLEX:	58.7	18.9	11.2	6.4	4.8		100
	MG CONTRIBUTION AS A % OF TOTAL MAGNESIUM IN SAMPLE						
SIMPLE:	2.2	6.1	12.5	14.6	15.7	32.7	83.8
COMPLEX:	3.7	3.6	3.5	2.8	2.7		16.2

TABLE 5.4
LIBERATION OF +200 MESH PARTICLES

+200 MESH:	AMOUNT OF PARTICLES CONTAINING A GIVEN PERCENT OF MAGNESIUM						
% MG:	1-20	20-40	40-60	60-80	80-99	100.00	TOTAL
SIMPLE:	75	95	71	79	109	97	526
COMPLEX:	331	43	46	28	26		474
	ABOVE NUMBERS AS A PERCENT OF TOTAL PARTICLES IN ANY ONE TYPE						
SIMPLE:	14.3	18.1	13.5	15.0	20.7	18.4	100
COMPLEX:	69.8	9.1	9.7	5.9	5.5		100
	MG CONTRIBUTION AS A % OF TOTAL MAGNESIUM IN SAMPLE						
SIMPLE:	1.7	6.6	8.2	12.7	22.6	22.4	74.2
COMPLEX:	7.6	3.0	5.3	4.5	5.4		25.8

TABLE 5.5
LIBERATION OF +270 MESH PARTICLES

+270 MESH:	AMOUNT OF PARTICLES CONTAINING A GIVEN PERCENT OF MAGNESIUM						
% MG:	1-20	20-40	40-60	60-80	80-99	100.00	TOTAL
SIMPLE:	151	75	45	38	38	39	386
COMPLEX:	391	110	60	26	27		614
	ABOVE NUMBERS AS A PERCENT OF TOTAL PARTICLES IN ANY ONE TYPE						
SIMPLE:	39.1	19.4	11.7	9.8	9.8	10.1	100
COMPLEX:	63.7	17.9	9.8	4.2	4.4		100
	MG CONTRIBUTION AS A % OF TOTAL MAGNESIUM IN SAMPLE						
SIMPLE:	5.0	7.4	7.4	8.7	11.2	12.8	52.5
COMPLEX:	12.8	10.8	9.9	6.0	8.0		47.5

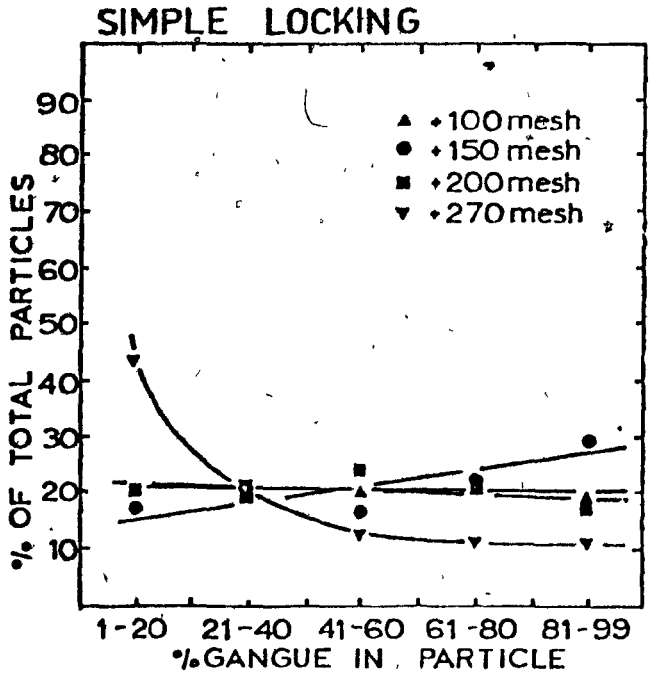

FIG. 5.19

ABUNDANCE OF SIMPLE LOCKED PARTICLES OF VARIOUS COMPOSITIONS

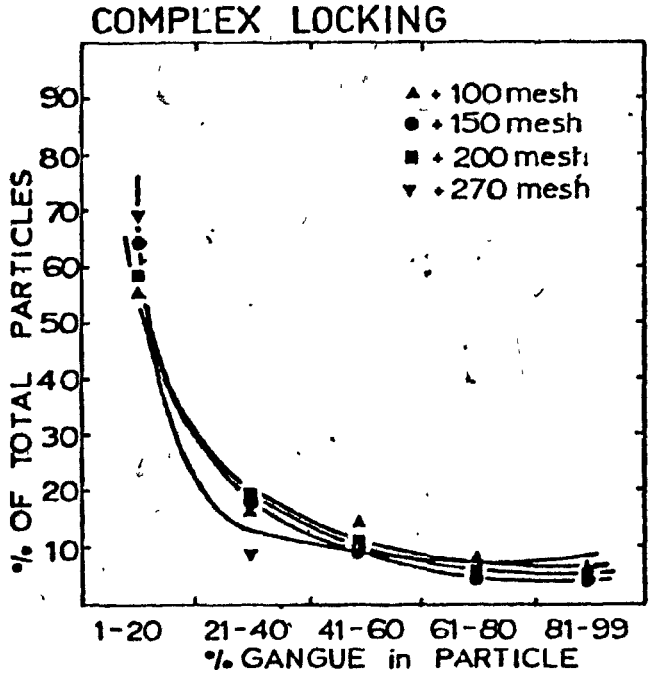

FIG. 5.20

ABUNDANCE OF COMPLEX LOCKED PARTICLES OF VARIOUS COMPOSITIONS

amount of gangue-poor simple particles which were observed.

The profile which is shown in Figure 5.20 for complex particles indicates that the majority of these particles contained less than 20% carbonates. It was seen in the locked cycle test and it was suggested in Figure 5.19 that rejection of coarse composite particles in Fine Point zinc flotation is low, regardless of particle composition. Moreover, the particle sizes used in the liberation study were higher than the size at which significant liberation of the complex particles would be expected to occur. It is therefore concluded that the distribution of particle compositions seen in Figure 5.20 was caused by the original ore textures. It appears that the majority of the disseminated ore contained less than 20% carbonates.

Disseminated ore was previously found to consist of void-filling and co-precipitated varieties. The void-filling variety contained sphalerite inclusions with a mean grain size of approximately 50μm hosted in a dolomitic matrix. The co-precipitated variety of disseminated ore consisted of interstitial dolomite grains with a size of approximately 20μm within a sphalerite matrix. Since the majority of the complex locked particles consisted of dolomite in a sphalerite matrix it is interpreted that the co-precipitated variety of disseminated ore was more abundant in the mill feed than the void-filling variety.

It is possible that the concentrate contained a certain

amount of unlocked carbonate-bearing particles, since a number of apparently free carbonate sections were counted in all size fractions. These sections could represent either pure gangue particles or simple locked particles oriented in such a way as to make them appear to be free. The apparently free sections are examined in more detail in the discussion which follows.

An estimate was made regarding the contributions of simple, complex and "free" carbonate-bearing particles to total magnesium contamination in each of the four size fractions of the concentrate. The magnesium assay contributed by simple particles is expected to decrease as size decreases due to increased liberation of the particles. On the other hand, the complex particles are not expected to show increased liberation over the range of particle sizes which was studied and their magnesium contribution is expected to be constant. The magnesium contribution of "free" sections would be expected to decrease at finer sizes if the sections were produced from locked particles, or to increase at finer sizes if the particles represent free entrained carbonates.

The method used to evaluate magnesium contributions from the three particle types (simple, complex and "free") is summarized below:

A(X) = Magnesium assay of size fraction "X"

T = Particle type

F(T) = Fraction of particles of type "T"

F(T(I)) = Fraction of type "T" with I% gangue

Mg assay in size class "X" from type "T" equals:

$$\frac{\sum_{F} \{ N(T(I)) * I \}}{\sum_{T}\sum_{F} \{ N(T(I)) * I \}} * A(X)$$

The results of these calculations are presented in Table 5.6 and in Figure 5.21.

It can be seen in Figure 5.21 that the amount of contamination introduced by simple locked particles decreased with decreasing size, presumably due to increased liberation of the particles. The magnesium contribution from apparently free sections decreased in a similar manner, thereby suggesting that most of these sections were produced from locked particles. In contrast, the amount of contamination introduced by complex particles was a more or less constant 0.1% Mg over the size range studied. This level of contamination would be expected to persist down to particle sizes of about 20-25µm, at which point the particles would begin to liberate.

The magnesium contribution of complex locked particles is high enough to have significant effects upon zinc metallurgy. It is estimated that the complex particles contribute approximately 0.1% Mg to all size fractions coarser than 20-25µm and somewhat less than 0.1% Mg to the finer size fractions. This represents a large proportion of the 0.25% Mg which is acceptable in the concentrate. Variations in the amount of disseminated ore in the mill feed could be

TABLE 5.6

CONTRIBUTION OF SIMPLE AND COMPLEX LOCKED PARTICLES TO MG CONTAMINATION

SIZE (MESH)	SIMPLE LOCKING	COMPLEX LOCKING	FREE PARTICLES	MG ASSAY	MG% FROM SIMPLE	MG% FROM COMPLEX	MG% FROM FREE
-64/+100	55.3	11.1	33.6	0.99	0.55	0.11	0.33
-100/+150	51.1	16.2	32.7	0.50	0.26	0.08	0.16
-150/+200	51.8	25.8	22.4	0.43	0.22	0.11	0.10
-200/+270	39.7	47.5	12.8	0.33	0.13	0.16	0.04

FIG. 5.21

TYPE OF LOCKING VS. ESTIMATED MAGNESIUM CONTRIBUTION

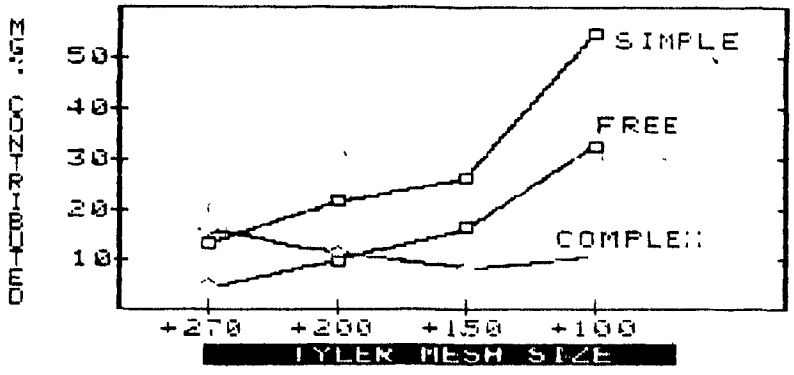

responsible for variations of about 0.1% Mg in zinc concentrates produced from different Pine Point ores.

5.3 A Model for the Sectioning of Locked Particles

The covariance in Figure 5.21 between the magnesium contributions of simple locked particles and apparently free particles suggests that most of the apparently free sections were produced by locked particles; however, it was decided to examine in greater detail the effects of sectioning upon observed particle distributions.

In order to simulate the sections which can be produced from any given locked particle it is necessary to simulate the following:

1) All possible volumetric proportions of gangue.
2) All possible sections through the sample.
3) All possible orientations of the sample relative to the section.

A simple model can be developed if it is assumed that:

1) The particles are spherical.
2) The boundaries between ore and gangue are planar.

These assumptions are reasonable for many sulphide concentrates. Most sulphide minerals break during comminution into particles with low aspect ratios. While these particles are often fairly angular there is a compensating factor

introduced by the nature of sectioning and particle counting. Odd corners which are intersected by the plane of the section produce only very small mineral sections which are generally disregarded during particle counting; thus, angular particles are essentially "rounded out" by the compensating bias in the counting method.

The assumption that locked minerals have planar boundaries is valid at or below a certain grain size which is specific to the material being studied. At particle sizes well below the grain size the mineral boundaries are expected to be essentially planar; however, as the particle size approaches the grain size one may find mineral aggregates which exhibit irregular or angular boundaries. At very large particle sizes one may find gangue enclosed by sulphides, or vice versa.

It is evident that the complex locked particles seen in this study did not exhibit planar boundaries over the size range which was examined. In fact, the grain sizes observed in the complex particles were so much smaller than the particle sizes that the carbonate contents which were observed in the particles should have been insensitive to orientation and sectioning. The simple locked particles, however, exhibited mineral boundaries which were very close to planar in most of the particles. Examination of Figure 5.17 reveals that the simple locked particles could exhibit a variety of section compositions depending upon their orientations relative to the plane of the section.

The unique intersections between locked particles and sections through them can be examined by taking a fixed orientation of the sample and rotating the section through all possible unique orientations. The unique orientations of the section are limited by the symmetry of the particle.

A spherical particle composed of two minerals separated by a planar boundary has an axis of symmetry passing from the centre of the particle through the center of the boundary. Figure 5.22 shows a locked particle with the mineral boundary oriented horizontally and the axis of symmetry passing vertically through the center of the particle. A horizontal section is shown on the sample, located a distance "X" away from the center. In this orientation the observed section would be a free ore particle with gangue below the surface. If the section is rotated (Fig. 5.23) it intersects the gangue and a locked particle is seen. If rotation continues the section will eventually leave the gangue and a free ore particle will be seen once again. Due to the symmetry of the particle there are no unique intersections produced by "spinning" the particle out of the plane of the paper; thus, the total possible intersections between the mineral and the section can be simulated by keeping the orientation of the sample constant and by rotating the section through π radians in the plane of the paper. The total possible combinations of sample and section orientation can therefore be simulated by performing the following operations:

FIG. 5.22
VERTICAL SECTION THROUGH LOCKED PARTICLE

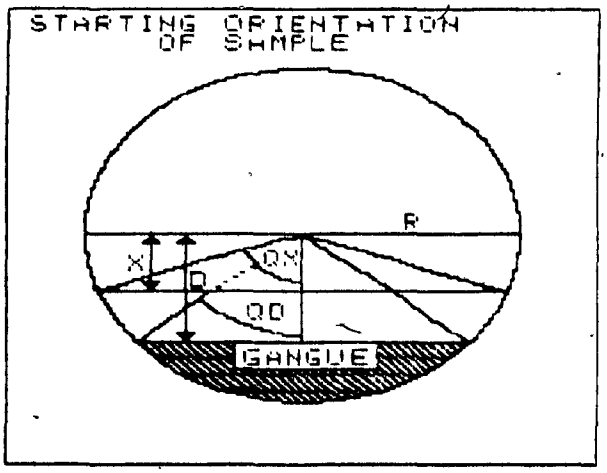

FIG. 5.23
VERTICAL SECTION SHOWING ROTATED PLANE OF INTERSECTION

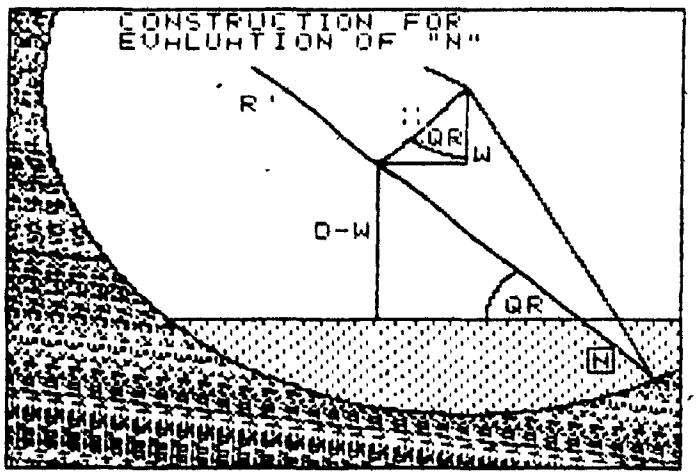

1) The distance "X" is simulated between (X=0) and (X=R), where R = the radius of the particle.

2) Since the volumetric proportion of gangue is related to the distance "D" of the mineral interface from the center of the particle (Fig. 5.22), "D" is simulated from (D=R) to (D= -R).

3) At any given "X" and "D", the section is rotated from (QR=0) through (QR=π).

Figures 5.22 and 5.23 illustrated a combination of "D" and "X" which could not produce any free gangue sections. Sections of apparently free gangue are produced from locked particles only when (X D).

Figure 5.24 illustrates a possible section through a locked particle at some arbitrary "X", "D" and "QR". The observed mineral boundary is always planar since it represents the intersection of two planes, ie. the true mineral boundary and the section. The section exhibits a radius of "R'", which is a function of "X", and an area percentage of gangue which is a function of "X", "D" and "QR".

FIG. 5.24
SIMULATED SURFACE OF SECTIONED PARTICLE

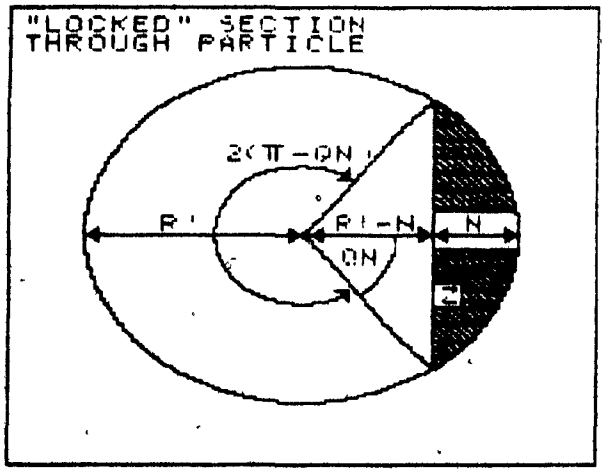

Mathematical Development of the Model

The volumetric proportion "V" of gangue in a locked particle is related to the distance "D" in Fig. 5.22 by the equation:

$$(3*D)/R - (D/R)^3 = 2 - 4*V$$

In Figure 5.22 it can be seen that for any distance "D" the gangue occupies (QD/π) of the total circumferance of the particle, where:

$$QD = \text{ARCCOS } (D/R)$$

The angular separation of the section from the gangue is equal to:

$$QX - QD$$

where:

$$QX = \text{ARCCOS } (X/R)$$

The three possible types of mineral section are a) free gangue; b) locked particles; c) free ore. These three particle types are produced in three ranges of QR, as summarized below:

a) $\{ \quad 0 \quad < QR < |(QX - QD)| \}$ (FREE GANGUE)

b) $\{ |(QX - QD)| < QR < (QX + QD) \}$ (LOCKED)

c) $\{ (QX + QD) < QR < \pi \}$ (FREE ORE)

If (QX > QD) it is not possible to produce free gangue sections. In this case, free ore is seen in both (a) and (c).

By calculating the three ranges it is possible to evaluate the amount of "free gangue" and "free ore" sections which will be produced by a given "X" and "D". If X is stepped through the range (0 X R) then one can obtain an estimate of the total amount of free sections produced by a particle of known "D" (ie. known composition) in random orientation.

Sections which lie in the second range (as described above) are locked. The area of a locked section which is occupied by gangue is a function of X, D, QX, QD and QR. If these parameters are all specified it can be seen from the construction in Fig. 5.24 that:

$$W = X * COS(QR)$$

and

$$N = R' - (D-W)/SIN(QR)$$

where $R' = X * SIN(QX)$

Given the value of N, one can calculate the area percent of gangue in the sample. In reference to Fig. 5.24:

$$\text{TOTAL AREA OF SECTION} = \pi * (R'^2)$$

$$QN = ARCCOS((R'-N)/R')$$

$$Z = R' * SIN(QN)$$

and the percentage of gangue is equal to:

$$1 - (QN)/\pi - Z(R'-N)/(\pi(R'^2))$$

TABLE 5.7

MATRIX PRODUCED BY SIMULATION PROGRAM

			COMPOSITION OF PARTICLES (% GANGUE)									
			00-10	10-20	20-30	30-40	40-50	50-60	60-70	70-80	80-90	90-100
C		FREE ORE	56.15	39.90	31.51	25.37	20.39	16.12	12.34	8.85	5.55	2.15
O	S	00-10	22.79	11.26	7.71	5.72	4.35	3.61	2.64	1.85	1.12	0.42
M	E	10-20	11.06	16.61	8.64	5.92	4.34	3.21	2.35	1.61	0.96	0.36
P	C	20-30	3.02	12.58	15.19	8.14	5.45	4.00	2.81	1.89	1.12	0.40
O	O	30-40	1.50	4.87	11.69	15.14	8.17	5.47	3.67	2.41	1.39	0.51
S	F	40-50	0.99	2.75	5.27	10.47	15.65	9.24	5.44	3.38	1.89	0.66
I	O	50-60	0.66	1.89	3.38	5.44	9.24	15.65	10.47	5.27	2.75	0.99
T	N	60-70	0.51	1.39	2.41	3.67	5.47	8.17	15.14	11.69	4.87	1.50
I	S	70-80	0.40	1.12	1.89	2.81	4.00	5.45	8.14	15.19	12.58	3.02
O		80-90	0.36	0.96	1.61	2.35	3.21	4.34	5.92	8.64	16.61	11.06
N		90-100	0.42	1.12	1.85	2.64	3.61	4.35	5.72	7.71	11.26	22.79
		FREE GANGUE	2.15	5.55	8.85	12.34	16.12	20.39	25.37	31.51	39.90	56.15

The distribution of observed gangue percentages from particles of a given volume percent gangue can be simulated by evaluating the above expression through the range (|QX-QD| OR (QX+QD)) for all values of X in the range (0 X R).

The simulation need only be applied to particle compositions between 0 and 50 volume percent gangue. In order to obtain data for higher gangue compostions one need only consider the following:

- The amount of sections showing (Y)% gangue from a particle of (Z)% gangue is equal to the amount of sections showing (Y)% ore from a particle of (Z)% ore.
- Since gangue plus ore must total 100%, this is equal to the amount of sections showing (100-Y)% gangue from a particle of (100-Z)% gangue.

Thus, for example, the calculated amount of sections containing 35% gangue from a particle of 45% gangue must equal the calculated amount of sections containing 65% gangue from a particle of 55% gangue.

A program was written to generate simulated sections at various orientations through particles of various compositions (Appendix 3). The input variables for the program are:

1) The stepping rate for particle compositions (ΔV).
2) The stepping rate for sections (ΔX).
3) The stepping rate for rotation angles (ΔQR).

4) The dimension (M) of the output matrix.

The output of the program is a square (I * J) matrix where (I,J) is the fraction of particles of composition "I" which are produced during the sectioning of particles with composition "J".

Table 5.7 is an output matrix which was produced using (V = 0.02), (X = 0.02), (DR = 0.0057) and (M = 10). A total of 500,000 sections were simulated during generation of the matrix. The output can be used to examine the distribution of sections which are expected from single particle compositions and to recalculate the original particle assemblages which are represented by a given assemblage of section compositions.

Figure 5.25 shows the model prediction for the amount of free sections produced by particles of any given volumetric composition of ore and gangue. As one may expect, particles with small volumetric proportions of gangue produce many free ore sections and few free gangue sections while particles with large amounts of gangue produce few free ore sections and many free gangue sections.

It is a common practice in liberation studies to count only the minor constituent minerals of the sample. In Fine Point zinc concentrates, for example, carbonate accounts for only about 0.5% of the concentrate volume. If free ore particles were counted it would be necessary to evaluate many thousands of particles in order to count sufficient carbonate

FIG. 5.25
AMOUNT OF FREE SECTIONS PRODUCED BY PARTICLES OF VARIOUS COMPOSITIONS

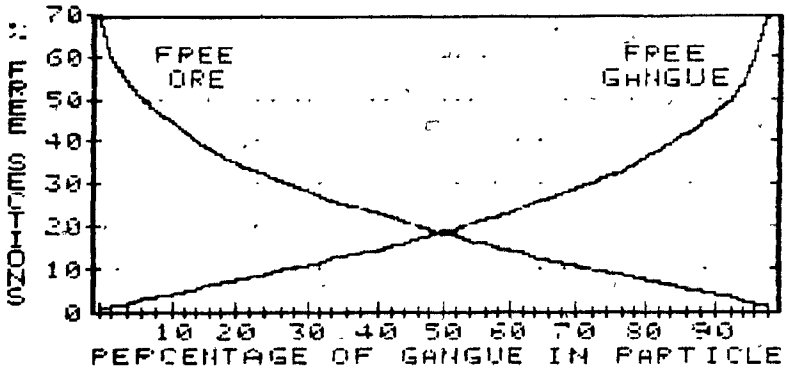

FIG. 5.26
AMOUNT OF FREE GANGUE OBSERVED WHEN FREE ORE IS NOT COUNTED

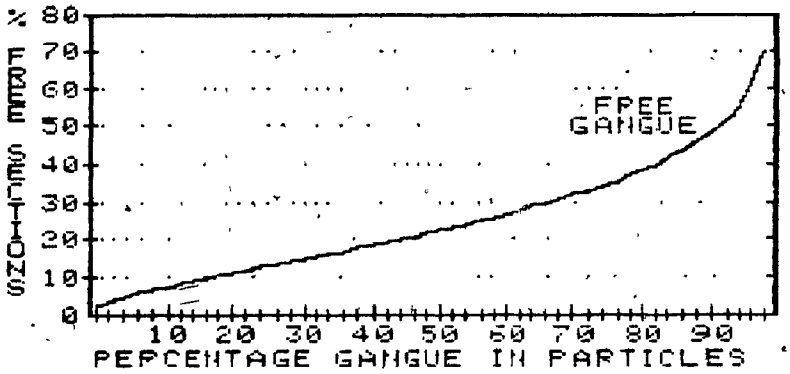

particles to perform a meaningful statistical analysis. Thus, in order to count as many carbonate-bearing particles as possible free ore is often omitted. The results shown in Figure 5.25 must therefore be adjusted. It can be seen from the figure that a particle containing 30% gangue will produce about 11% free gangue sections and 28% free ore sections, with the remaining 61% composed of locked sections. However, when free ore is not considered the observed amount of free gangue will be 11/(1-0.28)% and the observed amount of locked sections will be 61/(1-0.28)%. The adjusted amount of expected free gangue sections is presented in Figure 5.26.

It can be seen in Figure 5.26 that locked particles may produce significant amounts of apparently free gangue sections. Twenty-two percent of the sections produced from a particle with 50% gangue should be free gangue sections while 50% of the sections produced from a particle with 90% gangue should appear to be free gangue. This reveals a fundamental weakness in liberation models which use the direct observation of free gangue particles as a criterion for assessing liberation. Samples which contain absolutely no free particles may exhibit significant amounts of apparently free sections. Is therefore advantageous to find a method by which a distribution of section compositions can be manipulated to produce an estimate of the parent particle assemblage.

Recalculating the Compositions of Assemblages

The observed distribution of sections from a particular assemblage of particles is equal to the weighted sum of the sections generated by the individual component particles. Table 5.7 was produced by simulating particle compositions in two percent intervals (from 1% gangue to 99% gangue) then combining the profiles into groups of five to produce ten evenly-spaced composition intervals. The distributions of sections reported in the table are, by themselves, assemblages since each represents the sum of sections produced by five individual particle compositions. Figure 5.27 shows the distributions of sections which are produced by three of the composition intervals of Table 5.7. The section compositions describe an approximately normal distribution around the mean particle compositions of the intervals. These profiles can be combined to simulate assemblages with a wider range of compositions.

Figures 5.28 and 5.29 show two simple types of locked particle assemblages and their expected profiles. In Figure 5.28 the simulated assemblage has an equal amount of locked particles of all compositions. The particle compositions are divided into five intervals of 20% which each contain 20% of the total particles. None of the particles in the parent assemblage are considered to be free. The distribution of expected particle sections is similar in form to the assemblage of true particle compositions, except that the five

FIG. 5.27
DISTRIBUTION OF SECTIONS PRODUCED BY PARTICLES OF VARIOUS COMPOSITIONS

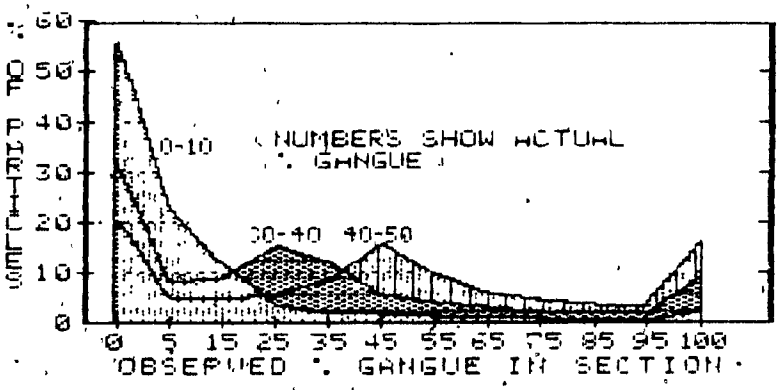

FIG. 5.28
DISTRIBUTION OF SECTIONS PRODUCED BY
EVEN DIST. OF PARTICLE COMPOSITIONS

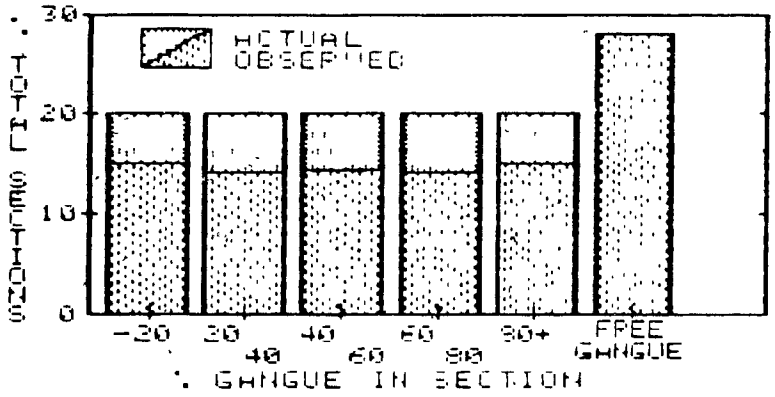

FIG. 5.29
DISTRIBUTION OF SECTIONS PRODUCED BY
SKEWED DIST. OF PARTICLE COMPOSITIONS

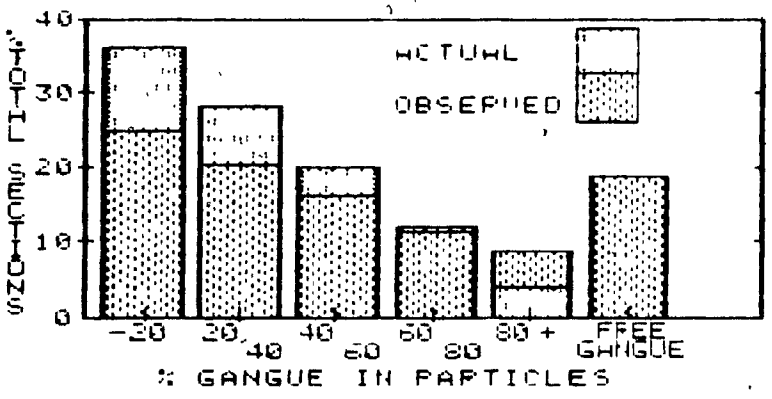

composition intervals each contain only about 14% of the particles; the balance is made up by free gangue sections, which make up over 30% of the expected observations.

Figure 5.29 shows an assemblage of particles whose abundance is inversely proportional to gangue content. This could be typical of many flotation products. It can be seen that the model assemblage is once again similar in form to the real assemblage, except that the abundance of sections with large amounts of gangue is exaggerated and approximately 20% of the observations are expected to be free gangue sections.

It is possible to use an observed distribution of section compositions to interpret the true composition of a particle assemblage. Table 5.7 is a square (J * I) matrix, where (J , I) is the amount of composition (J) produced by the sectioning of particles of composition (I). The observed distribution of sections from particle counting is an (I X 1) vector, and the original particle assemblage can be simulated by multiplying the (I X 1) vector with the inverse of the (I X J) matrix.

Table 5.7 was condensed into five 20 percent intervals plus one class for apparently free gangue, and the model was applied to the particle counts of Tables 5.2 to 5.5. The condensed matrix and its inverse are presented in Tables 5.8 and 5.9, and the recalculated distributions of particle types in the four size classes of the liberation study are presented in Table 5.10.

TABLE 5.8 ABRIDGED MATRIX FROM SIMULATION

		CONDENSED VERSION OF MODEL MATRIX					
ACTUAL % GANGUE		00-20%	20-40%	40-60%	60-80%	80-100%	FREE GANGUE
OBSERVED %	00-20%	61.78	19.74	9.52	4.74	1.50	0.00
	20-40%	19.67	35.23	14.20	6.05	1.79	0.00
	40-60%	5.74	16.97	30.46	13.82	3.30	0.00
	60-80%	3.12	7.47	14.07	28.03	11.54	0.00
	80-100	2.61	5.86	9.46	15.61	32.05	0.00
FREE GANGUE		7.08	14.72	22.28	31.75	49.81	100.00

TABLE 5.9 INVERSE OF ABRIDGED MATRIX

		INVERSE OF CONDENSED MATRIX					
ACTUAL % GANGUE		00-20%	20-40%	40-60%	60-80%	80-100%	FREE GANGUE
OBSERVED %	00-20%	1.961 E+00	-1.037 E+00	-0.103 E+00	-0.551 E-01	-0.341 E-02	0.000 E+00
	20-40%	-1.221 E+00	4.309 E+00	-1.670 E+00	0.133 E+00	-0.594 E-02	0.000 E+00
	40-60%	0.339 E+00	-2.259 E+00	5.191 E+00	-2.368 E+00	0.428 E+00	0.000 E+00
	60-80%	-0.599 E-01	-0.145 E+00	-2.061 E+00	5.563 E+00	-1.796 E+00	0.000 E+00
	80-100	-0.725 E-03	-0.107 E+00	-0.215 E+00	-2.030 E+00	3.880 E+00	0.000 E+00
FREE GANGUE		-0.121 E+04	-0.497 E-03	-0.148 E-02	-0.226 E-02	-0.145 E-01	0.100 E-02

TABLE 5.10 RECALCULATED ASSEMBLAGE

PARTICLE SIZE:		+100	+150	+200	+270
NUMBER COUNTED:		795	688	526	386
OBSERVED:	00-20	15	16	14	39
	20-40	15	15	18	19
	40-60	17	18	14	12
	60-80	15	15	15	10
	80-100	15	13	21	10
	FREE GANGUE	23	24	18	10
RECALC.:	00-20	12	13	7	57
	20-40	16	15	39	17
	40-60	32	36	7	11
	60-80	23	25	20	13
	80-100	21	13	45	13
	FREE GANGUE	-5	-2	-18	-10

It can be seen in Table 5.10 that the reconstituted particle assemblages are similar to the observed section distributions except that the reconstituted assemblages contain no free gangue particles. The model contains no constraints to prevent the generation of negative results. The negative amounts of free gangue which are reported in the reconstituted assemblages indicate that, in fact, fewer free gangue particles were observed than were expected, given the distributions of section compositions which were observed in the study. It is therefore apparent that the free sections which were observed during particle counting can all be considered to be locked particles. In the two size classes with the highest simple locked particle counts the reconstituted assemblages balanced almost perfectly without having to add large negative amounts of free gangue. This suggests that the fundamental assumptions of the model are fairly accurate for the zinc concentrate which was studied.

5.4 Summary of the Liberation and Textural Study

A liberation study was performed upon a sample of Pine Point leach feed in order to examine the amount and types of locked particles in the zinc concentrate. Two distinct types of locking were observed, and these types reflected two distinct types of textural association in the ore. It was interpreted that the colloform and blocky textures produced simple locked particles, which consisted of sphalerite and

dolomite separated by planar boundaries. The disseminated ore produced complex locked particles, which contained small inclusions of dolomite in sphalerite, or vice versa. The simple locked particles showed evidence of increased liberation between the size classes +100 to +270 mesh; however, the complex particles appeared to contribute a more or less constant 0.10% Mg in this range of size classes. The contribution of complex particles to magnesium contamination was not expected to decrease until about 25μm, since the size of the magnesium inclusions was typically 3-50 μm. Magnesium contributions from complex locked particles could remain high at particle sizes down to about 5-10μm.

Many free sections were observed during particle counting, and it was not known whether these sections represented free particles or whether they were actually locked. A model was developed to reconstruct the original particle assemblages based upon particle counting data, and it was found that the free sections which were observed were likely to have all been locked.

It was therefore concluded that locking was the principal source of magnesium contamination in the zinc concentrate, and that variation in ore textures is a probable cause of variable metallurgical performance exhibited by Pine Point ores. Intricate textural associations between sphalerite and carbonates could be responsible for variations of about 0.10% in the Mg content of various Pine Point zinc concentrates.

CHAPTER 6

LEACHING OF PINE POINT CONCENTRATES

CHAPTER 6: LEACHING OF PINE POINT CONCENTRATES

6.0 Introduction

The Pine Point leach plant was previously described in Chapter 1. The operating parameters which are under direct control at the Pine Point mill include acid addition, pulp density and residence time of the pulp in the digestors. A series of controlled tests were performed upon a sample of Pine Point leach feed in order to examine which if any of these operating parameters affect the efficiency of leaching. Two series of leach tests were performed in order to evaluate the effects of varying pulp density and residence time in the leach tank. An acid addition corresponding to 391g/tonne (94lbs/ton) was used in all tests. The feed was ultrasonically dispersed in distilled water and leached in plastic vessels. Magnetic stirring rods were used to keep the pulp in suspension during leaching. At the completion of the tests the pulp was filtered through a Buchner funnel and rinsed three times with distilled water. The leachate was analyzed for zinc, iron, calcium and magnesium.

6.1 Leaching Tests at Various Pulp Densities

The concentrate used in the tests assayed 62.46% zinc, 0.494% iron, 0.524% magnesium and 0.725% calcium prior to leaching. The concentrate was leached for 90 minutes at pulp densities from 10% to 70% solids and the amounts of each metal removed during the leach were calculated from the assays of

the leachates. Table 6.1 and Figure 6.1 show the masses of soluble metals which were found at the conclusion of the tests.

It was found that pulp density had little effect upon the efficiency of the leach. There was no statistically significant variation in the amounts of zinc, iron and magnesium which were removed over the range of pulp densities used in the tests. There was a decrease significant at the 90% level in the amount of calcium removed with increasing pulp density. It is interpreted that this decrease was caused by the limited solubility of calcium sulphate (about 2g/litre) which may have been precipitated at high pulp densities. The scatter in the amount of calcium detected in solution is most likely to have been caused by variable amounts of calcium sulphate precipitate which were dissolved during rinsing of the leached concentrate.

The results of this series of experiments are in agreement with prior work involving the sulphuric acid leaching of carbonates. Frenay (1977) found that the leaching rate of manganese carbonate (a chemically and crystallographically similar species) was independent of pulp density.

A control experiment was performed in order to examine the amounts of soluble material present in the unleached feed. The amount of soluble metals found in the control leachate was about two orders of magnitude lower than the amount found in

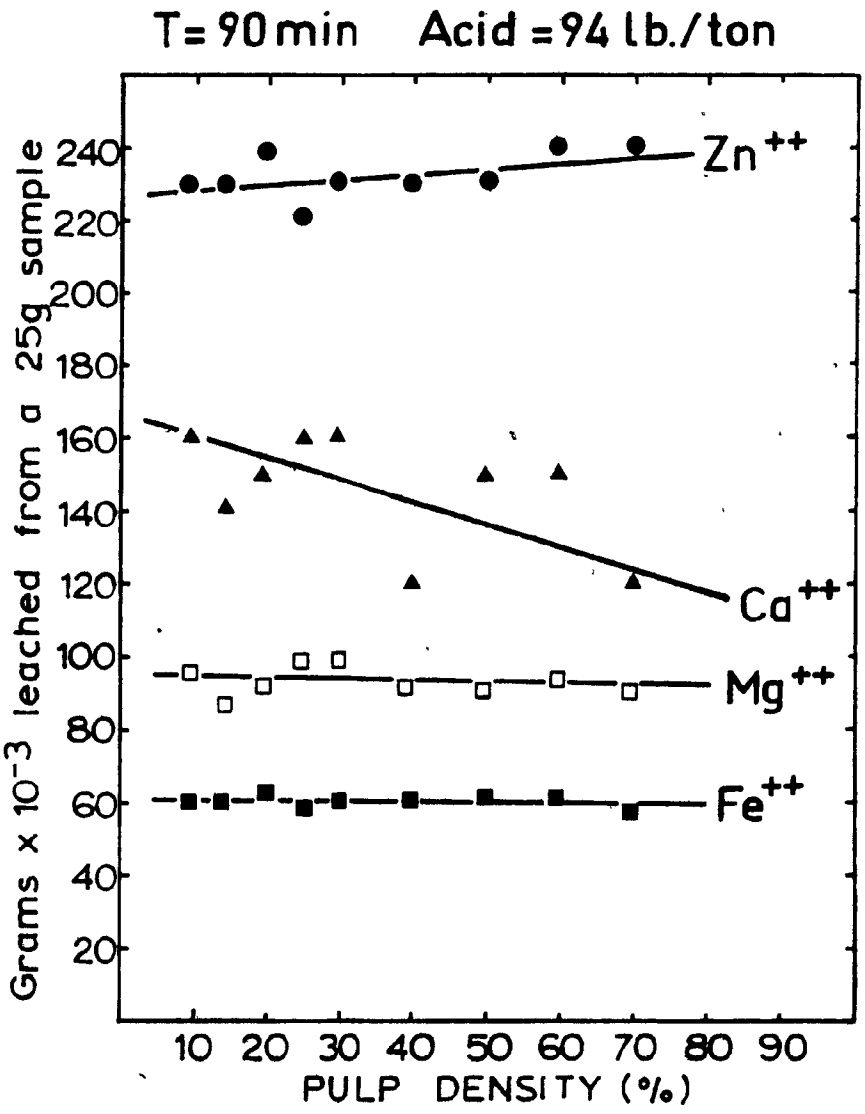

FIGURE 6.1

LEACHING OF PINE POINT ZINC CONCENTRATE AT VARIOUS PULP DENSITIES

EFFECT OF PULP DENSITY UPON LEACH EFFICIENCY

PULP DENSITY	MASS LOST	LOST ZINC	LOST IRON	LOST CA	LOST MG
	(GRAMS LOST FROM A 25 GRAM SAMPLE)				
70	1.30	0.24	.057	0.12	.088
60	1.44	0.24	.060	0.15	.092
50	1.44	0.23	.061	0.15	.090
40	1.44	0.23	.060	0.12	.090
30	1.43	0.23	.060	0.16	.097
25	1.46	0.22	.059	0.16	.097
20	1.45	0.24	.062	0.15	.090
15	1.46	0.23	.060	0.14	.085
10	1.52	0.23	.060	0.16	.093
CONTROL (NO ACID) (P.D.20%)		.0013	.001	.005	.001

TABLE 6.1 ACID LEACHING AT VARIOUS PULP DENSITIES

the leachates from experiments using acid (Table 6.1). It was therefore concluded that virtually all of the metals found in solution were solubilized by the leach.

Since the leaching rates of zinc, iron and magnesium were insensitive to pulp density it is possible to determine an approximate efficiency of the leach. It can be readily calculated from the feed assay and from the data of Table 6.1 that approximately 70% of the magnesium was dissolved during the tests, along with 1.5% of the zinc and 60% of the iron. The dissolution rate of zinc which was observed in these tests is similar to a 1% zinc loss which was experienced during test leaching of Missouri zinc concentrates (Schweitzer, 1987).

The rate of zinc leaching is only about 2% that of magnesium; however, since zinc is much more abundant than magnesium in the concentrate the amount of acid used to dissolve zinc is comparable to the amount used to dissolve magnesium. It can be calculated that for every mole of acid which dissolves dolomite there are approximately 0.6 moles of acid which dissolve iron and zinc. Thus, no more than 60-65% of the acid is consumed by the dissolution of dolomite. Moreover, a certain amount of calcite, galena and trace minerals are dissolved in the leach and there is always some acid which passes unused through the leach circuit due to plug flow through the leach tanks; thus, the amount of acid which is available for the dissolution of dolomite is probably somewhat less than 60% of the acid which is added to the

digestors. Acid addition must therefore be approximately twice the amount which is required to stoichiometrically dissolve the dolomite. In order to reduce the magnesium level in a concentrate from 0.35% Mg to 0.05% one must add approximately 48-60 kg of acid.

6.2 Leaching Tests of Variable Duration

Table 6.2 and Figure 6.2 show the concentration of zinc, iron and magnesium in the leachate as a function of time. In Figure 6.1 it was seen that leach efficiency at 90 minutes was independent of pulp density. Two different pulp densities (20% and 50%) were used in this series of tests in an attempt to examine the possible effects of pulp density upon leaching kinetics at short leaching times.

The leaching times used in this series of tests ranged from 30 minutes to 50 hours. It was difficult to perform experiments with leaching times of less than 30 minutes, since no neutralizing agents were used to arrest the dissolution process and the time required to filter and wash the concentrate at the end of the leach was about 10 minutes.

The results shown in Figure 6.2 indicate that the leach is essentially complete at 30 minutes. No significant changes in the masses of soluble metals were observed at times greater than half an hour. Gorman et. al. (1976) found that the reaction between zinc concentrates and sulphuric acid at the Bauget refinery was essentially complete after 90 minutes.

TABLE 6.2 EFFECT OF TIME UPON ACID LEACHING

PULP DENSITY	TIME	GRAMS OF METAL DISSOLVED ZINC	IRON	MG	CA
20%	30 MIN	0.22	0.05	0.09	0.15
	60 MIN	0.25	0.06	0.07	0.15
	120 MIN	0.24	0.06	0.09	0.16
	240 MIN	0.24	0.06	0.09	0.16
	3000 MIN	0.22	0.06	0.10	0.15
50%	30 MIN	0.22	0.06	0.09	0.15
	60 MIN	0.22	0.06	0.07	0.15
	120 MIN	0.23	0.06	0.09	0.16
	240 MIN	0.21	0.05	0.10	0.16
	3000 MIN	0.22	0.06	0.10	0.15

FIG. 6.2
LEACHING OF PINE POINT ZINC CONCENTRATES FOR VARIOUS TIMES

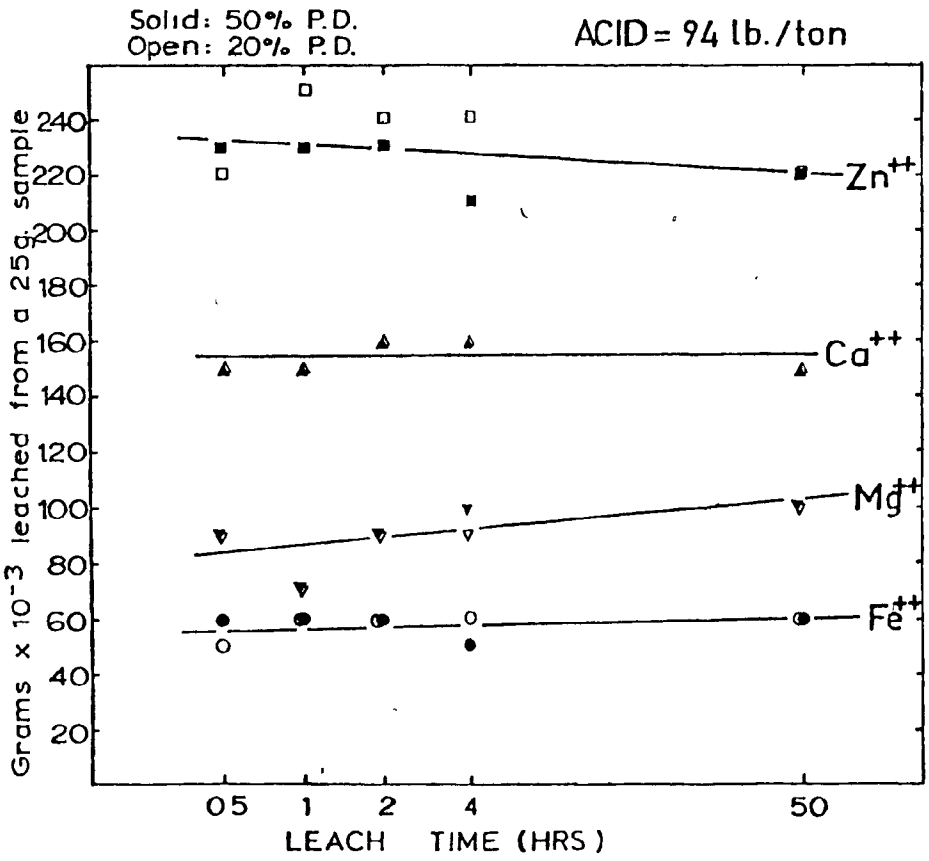

Tests at the Sauget refiner, were performed on a pilot plant scale, and may have required longer leach times than the experiments presented here due to less intense agitation of the pulp or due to a component of plug flow in the leach tanks.

6.7 Production of Calcium Sulphate During Leaching

The dissolution of dolomite and calcite results in the production of calcium sulphate. This species has a solubility of only 2 grams per liter, and may form a precipitate if leaching is conducted at high pulp density. Calcium sulphate precipitation during leaching is a problem at Ama's Sauget refinery, where fine needles of calcium sulphate reduce the efficiency of post-leach filtration (Gorman et. al., 1978).

A sample of Pine Point ore was floated and the tailings were retained for leach tests. X-ray diffractometry revealed that the sample was composed primarily of dolomite, with traces of calcite. A test was set up to simulate a feed of 0.4% dolomite, leached at 50% pulp density with an acid addition of 45 kg/tonne. Leach residue was collected at times ranging from 10 minutes to 10 hours, and the residues were analyzed by diffractometry. Three distinct polymorphs of calcium sulphate were detected at various leach times.

Figure 6.7 presents a semi-quantitative approximation of the amounts of each species which were present at different times during the test, based upon relative diffraction peak

FIG. 6.3
COMPOSITION OF LEACH PRECIPITATE AS
A FUNCTION OF TIME

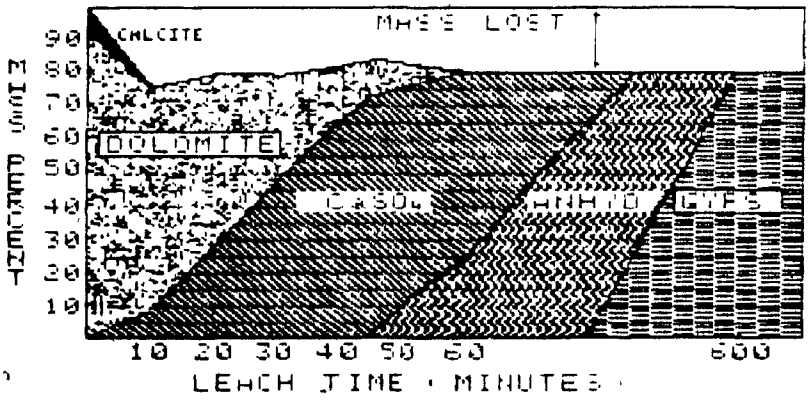

heights. It can be seen that calcite was dissolved within 10 minutes, and dolomite dissolved completely within 45 minutes. An anhydrous monoclinic calcium sulphate polymorph was precipitated as dolomite dissolved ($\lambda CaSO_4$; however, this form was found to be unstable in solution and spontaneously converted to anhydrite ($CaSO_4$). The anhydrite converted to gypsum ($CaSO_4.2H_2O$) within 10 hours. Mass loss in the sample was small since each mole of dolomite (M.W. 184g/mol) produced one mole of calcium sulphate (M.W. 136g mol, or 156g mol when hydrated). The calcium sulphate precipitated out of solution as fine acicular needles.

Tests were performed at three different pulp densities in order to examine the mechanisms and the kinetics of calcium sulphate precipitation (Figure 6.4). Varying the pulp density is equivalent to varying the concentration of acid in solution, since pulp density and acid concentration (at constant acid addition per tonne of solids) are proportional. At 10.5% pulp density there was no precipitation of calcium sulphate and mass loss reached almost 100% by 60 minutes. At 25% pulp density, mass loss reached 80% after 30 minutes, at which time calcium sulphate precipitated rapidly out of solution. It is interpreted that calcium sulphate supersaturated in solution prior to precipitation. The results of leaching at 50% pulp density have already been discussed. It was shown that dolomite dissolution was essentially complete after 45 minutes. The minimal volume of water at 50%

FIG. 6.4

MASS LOSS IN LEACH AS A FUNCTION OF TIME

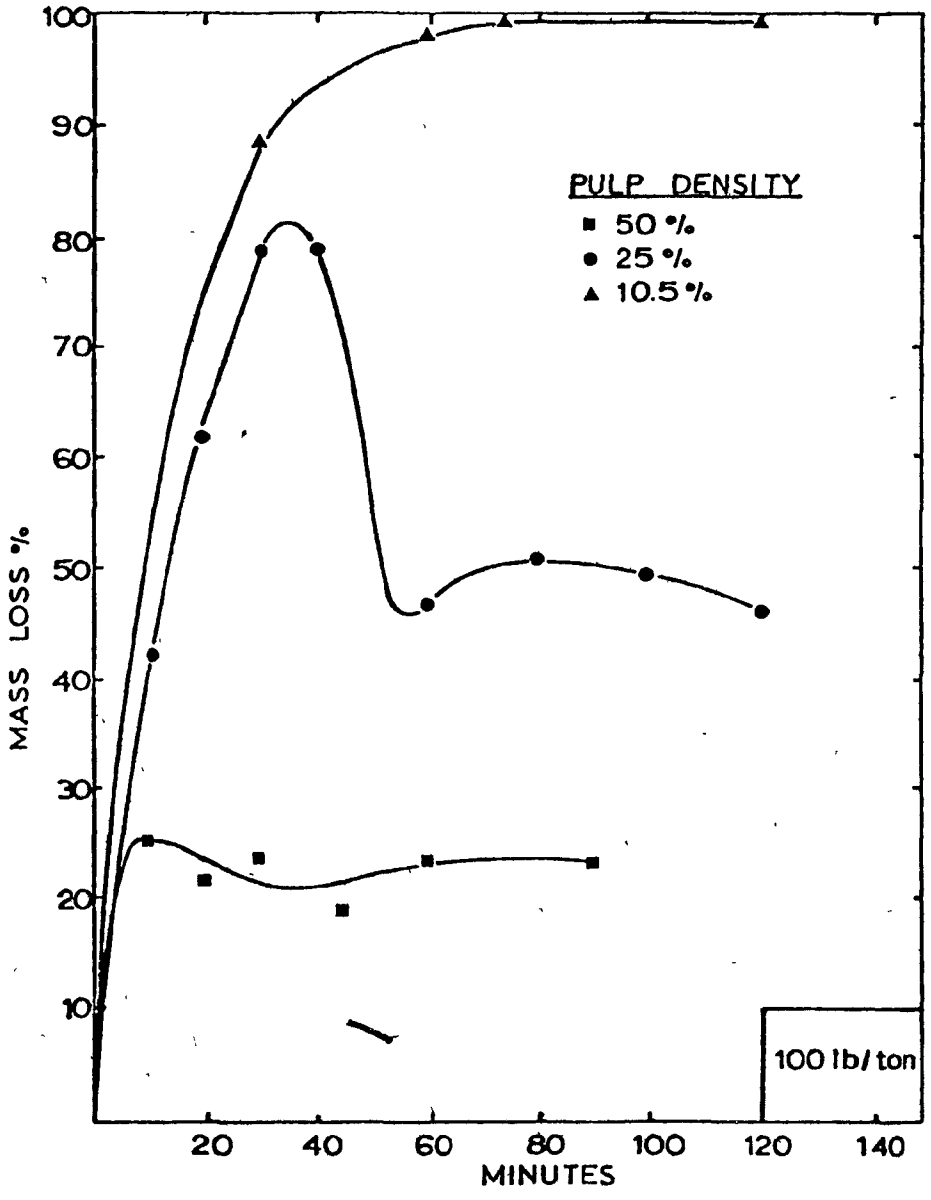

pulp density caused fast supersaturation of the solution, so that little mass change was observed when the supersaturated material precipitated.

The results indicate that there is little or no kinetic advantage to increasing the concentration of acid in solution. Dissolution of dolomite was essentially complete after 45-60 minutes, regardless of acid concentration. Repeat tests were performed at acid addition rates from 20 to 150 kg/tonne, and it was found that the curves reported in Figure 6.4 were duplicated at acid addition rates over 75 kg/tonne. The amount of acid needed for stoichiometric dissolution of a feed with 0.4% Mg is 77 kg/tonne, so that it appears that in the absence of sulphides little excess acid is needed to complete the dissolution reaction.

6.4 The Path of Dissolved Magnesium through the Processing Circuit

Magnesium which is removed during the leach is not expected to precipitate as a sulphate since the solubility of magnesium sulphate is about 300 g/liter at room temperature.

It is expected that most of the magnesium ions which go into solution should be lost during thickening and filtration. There exists, however, a possibility that magnesium which is removed in the leach may be reprecipitated as magnesium hydroxide in the neutralizer at the end of the leach. Theoretical calculations made for a hypothetical circuit can

predict the likelihood and the approximate magnitude of the problem.

If a magnesium reduction of 0.3 weight percent is effected in a leach feed at 65 percent pulp density the final concentration of magnesium ions in solution should be .003 tonnes per 0.5 tonnes of water. This is equal to about 0.25 moles per litre. The solubility product of $Mg(OH)_2$ is 1.2 x 10E-11 (CRC Handbook, 63rd ed.). When the solution is neutralized to a pH of 7 the solubility of magnesium is equal to:

(1.2 x 10E-11 / 1.0 * 10E-7) , or 0.00012 mol/litre

It is expected, therefore, that neutralizing the leachate should result in the reprecipitation of over 99.95% of the magnesium ions as a hydroxide. This calculation is an oversimplification since the solubility of magnesium in the neutralizer may be affected by factors such as the ionic strength of the solution, possible supersaturation etc.; however, there exists a distinct possibility that the magnesium is solubilized in the leach, only to be reprecipitated in the neutralizer. Such a phenomenon would explain the fact that leaching never seems to remove all of the magnesium from leach feeds, even though dolomite should be readily soluble in sulphuric acid.

A sample of post-leach (final) zinc concentrate from the Pine Point concentrator was tested for soluble magnesium. The concentrate was dry and agglomerated upon receipt, and assayed

0.34% Mg, 0.78% Ca. The material exhibited strong hydrophobicity and could not be wetted in water at room temperature. Two 100 gram subsamples were boiled for 30 minutes in distilled water, then filtered and dried. The dried concentrate was powdery and showed none of the agglomerates which were present in the original sample. The assays of the two subsamples after boiling were (0.23% Mg, 0.45% Ca) and (0.19% Mg, 0.36% Ca). Thus, it appears that up to 45% of the magnesium and up to 55% of the calcium in the concentrate was in the form of soluble salts. No soluble salts were detected in the control experiment which was performed upon the Pine Point pre-leach zinc concentrate (Table 6.1). Thus, it can be concluded that the soluble magnesium extracted from the post-leach concentrate was produced during the leach.

The possibility of $Mg(OH)_2$ precipitation in the neutralizer merits further examination. It is found at Pine Point that the neutralizer reduces soluble zinc to metallurgically insignificant levels (Jones, 1980). It is not known whether the zinc precipitates as a hydroxide or as an ammonia complex; however, it is possible that zinc is not the only metal to precipitate out of solution. The problem could be compounded if $Mg(OH)_2$ nucleates upon sphalerite since this would, in effect, create "locked" sphalerite / $Mg(OH)_2$ composites and result in low magnesium rejection during post-leach flotation.

6.4 Summary of Acid Leaching

The major points concerning the leaching of Pine Point zinc concentrates can be summarized as follows:

1) Leaching efficiency was found to be independent of pulp density.
2) The dissolution reaction was essentially complete after 30 minutes, but could take longer in a tank with less agitation. The mean residence time of concentrate in the Pine Point leach plant is approximately two hours (Figure 1.4); therefore, it is probable that the dissolution reaction reaches completion.
3) Dissolution of zinc sulphide was approximately 1.5% under conditions similar to those at Pine Point; however, soluble zinc is generally reclaimed in the neutralizer (Jones, 1980).
4) Selectivity of leaching was found to be high, with magnesium leaching rates reaching approximately 50 times the leaching rate of zinc; however the amount of zinc in the concentrate was approximately 50 times higher than the amount of magnesium. The amount of acid consumed by the dissolution of sphalerite was therefore comparable to the amount of acid consumed by the dissolution of dolomite.
5) It was approximated that the amount of acid needed to reduce the magnesium assay in the zinc concentrate

by 0.3% is between 48 and 60 kg/tonne. This is approximately twice the amount of acid which is needed for stoichiometric dissolution of the dolomite. The excess acid is needed due to the dissolution of sphalerite. When pure dolomite was leached it was found that the stoichiometric amount of acid was sufficient to complete the dissolution reaction.

6) Calcium sulphate was found to precipitate from solution at high pulp densities. The amount of sulphate precipitated depends upon both the pulp density and the amount of dolomite dissolved. A feed assaying 0.4% Mg precipitates significant amounts of sulphate at pulp densities over 20%.

7) There exists a possibility that magnesium which is dissolved in the leach may be reprecipitated as $Mg(OH)_2$ in the neutralizer. It was found that soluble magnesium comprised approximately 35-45% of the total magnesium in a sample of zinc concentrate shipped from the Pine Point concentrator. Soluble magnesium was not found in a sample of Pine Point pre-leach zinc concentrate.

CHAPTER 7

DISCUSSION, CONCLUSIONS AND RECOMMENDATIONS

CHAPTER 7: Discussion, Conclusions and Recommendations

7.1 Discussion

The test work reported in this thesis indicates that locking is a major source of contamination in Pine Point zinc concentrates. Locked particles were subdivided into a "simple" type, which would be unlocked by a modest reduction in grind size, and a "complex" type, which would not be expected to liberate at grind sizes over approximately 25µm.

The batch grinding process used in laboratory work typically yields a wider particle size distribution than that which is experienced in plant-scale closed cycle grinding. A laboratory-produced assemblage with a grind size of 50% -200 mesh contains more coarse and more fine particles than its plant-scale counterpart. For this reason it is expected that the simple locking problem experienced in the laboratory should be of a lesser magnitude in the plant. The contamination introduced by complex locking, however, should be of a similar magnitude in the laboratory and in the plant. It is therefore possible that complex locking could cause a background level of about 0.1% Mg during plant processing of the "difficult" ore used in this study.

The two different types of locked particle were related to two distinct petrographic textures which were not found together in single hand samples of ore. It is probable that different Pine Point ore bodies could contain variable proportions of the two textural ore types.

The presence of fine textures in Pine Point mill feeds poses a problem which is difficult to solve. It was found that dolomite-bearing sphalerite particles were strongly flotable, and could not be easily separated into middling streams. Thus the only conventional ways to remove the magnesium are by leaching, as per the current mill procedure, or by installing a zinc regrind, as was done at the Magmont concentrator in Missouri (Schweitzer, 1983).

Zinc concentrates produced from Pine Point ore contained little fine magnesium. It was observed that rejection of fine gangue was not very selective since large recirculating loads of fine zinc were built up between the cleaners and the rougher during locked cycle testing. This resulted in high losses of fine zinc into the tailings, and a lowering of overall zinc recovery from over 98% in open cycle testing to about 95% in the locked cycle test. The low selectivity of flotation in the fine sizes could give rise to an entrainment problem if flotation times were increased to boost zinc recovery.

Magnesium contamination in the fine sizes is often but not always a problem at the Pine Point concentrator. In an internal Cominco report (Aug.8, 1974) it was stated that:

> "Occasionally, cleaning results in the MgO grade being lowest in the -325# fraction. However, this is not consistent and the grade is not less than 0.4%"

Tests were performed upon samples of Pine Point gangue in order to verify that the gangue exhibited no flotation response. It was found that gangue was recovered at a significantly lower rate than water under typical Pine Point flotation conditions, and that the recovery of gangue was similar to the recovery of pure silica sand under the same flotation conditions. Fine gangue was recovered at a faster rate than coarse gangue, but at a lower rate than water. It was concluded that the behaviour of Pine Point gangue was typical of a strongly hydrophylic material. This conclusion was supported by a liberation study which was performed upon a sample of Pine Point zinc concentrate. It was found that carbonates in the concentrate occurred only as locked particles.

The test work performed at McGill revealed no hydrophobicity of the carbonate particles; nor were there indications of major sliming or entrainment of carbonates during locked cycle flotation of Pine Point ore. It appears to be possible, at least in theory, that circuit or operational changes could be effected which would result in more reliable fine-particle performance.

One of the most striking phenomena observed in the flotation of Pine Point sphalerite was the size selectivity of flotation. The recovery of composite particles in the coarse size fractions was at one point observed to be higher than the recovery of presumably liberated fine sphalerite. Under such

conditions it is impossible to generate significant locked-particle-bearing middling streams without rejecting unacceptable amounts of fine zinc. It could possibly be worthwhile to cyclone the rougher concentrate and to treat the fines in a flotation column. Not only would this reduce the recirculating loads of fine zinc (and hence fine zinc losses), but it would also be possible to reduce the flotation times of coarse particles in the cleaners, with the goal of generating locked middling streams for a selective regrind.

Leaching tests performed upon samples of Pine Point leach feed (second cleaner concentrate) revealed that the leaching process is insensitive to pulp density and time over approximately 45 minutes. However, test work at Pine Point indicated that increased pulp density was beneficial to leach efficiency (Cominco report TL402, Nov.9, 1977). It is possible that temperature affects leach efficiency, since addition of 40 kg/tonne of 96% sulphuric acid to a feed at 65% pulp density could result in a temperature rise 10°C over that which would be experienced at a pulp density of 20%. The effect of temperature upon leach efficiency was not experimentally examined.

When pure gangue was leached and filtered it was found that the dolomite dissolved completely, leaving a residue of calcium sulphate; however, when zinc concentrate samples were leached and the pulp was neutralized prior to reflotation magnesium was found in the final concentrate. It was suggested

that neutralization may cause the precipitation of magnesium ions as a hydroxide. Tests on a sample of zinc concentrate from the Pine Point mill indicated that up to 45% of the magnesium in the concentrate could be in the form of sparingly soluble salts. It is also possible that complex locked particles may contain dolomite inclusions which are protected from acid attack by the surrounding sphalerite.

The flotation response of zinc concentrate was found to change after leaching. Recoveries of all elements were lower in post-leach flotation; however, it was found that the efficiency of separation was elevated. The precise reasons for changes in the flotation behaviour were not examined.

It is possible that the leach could be used in a modified form to alter the flotation characteristics of the zinc concentrate early in the flotation circuit. If the rougher concentrate was exposed to a low-acid, short-duration leach it is possible that flotation selectivity could be higher throughout the zinc cleaning circuit.

7.2 Conclusions

The major conclusions which were made pertaining to Pine Point zinc flotation and leaching are summarized as follows:

- Sphalerite was found to float extremely rapidly. Zinc recoveries during batch flotation were typically over 90% within one minute, and the factors which limited the zinc

recovery rate appeared to be air flow rate in the flotation cell and carrying capacity of the froth.

- Composites containing dolomite and sphalerite floated at a rate which was comparable to the flotation rate of pure sphalerite. It was therefore necessary to use very short flotation times in order to effect a separation.

- The use of very short flotation times resulted in high recirculating loads of fine zinc. This is presumably caused by the low probability of fine-particle/bubble collisions.

- The middling streams which were collected in locked cycle flotation contained a small amount of composite particles and a much larger amount of fine particles, including both sphalerite and gangue. The middling streams were typically found to contain over 80% -400 mesh material. Very little fine gangue entered the concentrate; however, the large recirculating loads of fine particles resulted in fine zinc loss.

- The magnesium assays found in laboratory-produced zinc concentrates were proportional to particle size. The fine size classes produced a relatively pure concentrate, while the coarse size classes contained considerable magnesium. Locking therefore emerged as the dominant mechanism of gangue contamination. The lack of fine contamination in the concentrate ruled out entrainment and sliming as major gangue recovery mechanisms in the test circuit.

- Textural study of a sample of Fine Point mill feed

revealed the presence of several distinct ore textures. The most important of these were colloform and disseminated textures. The two textures were not found together in single hand samples of ore, and it was interpreted that the, reflected two different modes of ore deposition. The two textural types could originate from different Pine Point mines.

- The two dominant ore textures had different grain sizes. Colloform ore showed few intricate associations between sphalerite and carbonates; however, disseminated ore had a fine grain size and displayed intricate associations between sphalerite and carbonates.

- Particle-counting analysis of a sample of Pine Point second cleaner concentrate revealed the presence of two distinct types of locked particle which reflected the two predominant ore textures. Colloform ore produced simple locked particles, which consisted of sphalerite and carbonate joined by a single planar boundary. Disseminated ore produced complex locked particles, which contained fine inclusions of carbonate in sphalerite.

- It was found that the magnesium assay contributed to the concentrate by simple locked particles decreased with decreasing size between 64 and 270 mesh; however, due to the fine grain size of inclusions in complex particles no appreciable liberation was experienced in this size range. It was estimated that complex particles contributed 0.1%

magnesium to the zinc concentrate in all size classes between 64 and 200 mesh, and this level of contamination was expected to persist down to sizes of about 15-25μm. It was concluded that simple locking would respond to small changes in grind size, but that the "background" levels of magnesium contamination introduced by complex locking would remain constant over the range of grind sizes which would normally be employed at Pine Point. Variable amounts of disseminated textures in Pine Point mill feeds could cause variable background levels of Mg contamination and variable metallurgical performance.

- Many apparently free sections of gangue were seen during particle counting. A model was constructed to interpret the particle counting results. It was determined that the free gangue sections could all be explained by the random sectioning of simple locked particles. Thus it appeared that the only major mechanism of gangue contamination above 270 mesh was locking.

- This conclusion was supported by work involving the flotation of pure gangue samples under typical Pine Point conditions. It was found that recovery of material over 37μm (400 mesh) was only about 2% of the recovery rate of water. Recovery of -37μm particles was higher, but still only a fraction of water recovery. The recovery of Pine Point gangue was similar to the recovery of silica sand under identical flotation conditions. It was therefore concluded that Pine

Fine gangue behaved as a hydrophylic species. In the absence of sphalerite the only distinguishable gangue recovery mechanism was entrainment, which recovered gangue preferentially from the fine size classes. Entrained dolomite was successfully rejected in locked cycle testing by successive cleaning flotation stages.

- Leaching tests were performed upon samples of Fine Point leach plant feed. It was discovered that leach efficiency was independent of pulp density, and that the dissolution reaction was completed within about 45 minutes.

- When pure gangue samples were leached the dolomite was completely dissolved, leaving a residue of calcium sulphate; however, when concentrates were leached the magnesium was not completely removed. It was suggested that carbonate inclusions in sphalerite could be shielded from the acid, or that $Mg(OH)_2$ could precipitate during neutralization of the pulp. In theory, 99.95% of the dissolved magnesium could be reprecipitated as $Mg(OH)_2$ during neutralization.

- In leach tests involving pure gangue it was found that the dissolution reaction could be completed without adding any acid over the amount needed for stoichiometric dissolution of the dolomite. However, in tests involving zinc concentrates it was found that up to 1.5% of the sphalerite could dissolve. The required acid addition was approximately twice that which would be needed for stoichiometric dissolution of the dolomite.

- The recovery rates of all elements dropped during post-leach flotation. The greatest decrease in flotation rate was experienced by magnesium. It was interpreted that the flotability of sphalerite decreased during leaching, thereby causing a general slowing of recovery rates and an increased rejection of locked particles. There exists a possibility that this phenomenon could be exploited by installing a short, low-acid leach near to the head of the cleaning circuit in order to allow better rejection of composites in the cleaners.

7.3 Recommendations for Further Work

The conclusions made in this thesis could be greatly enhanced by correlation with plant results. The following studies are suggested:

1) A textural study should be carried out in order to determine differences in the textures of "easy" and "difficult" ores. The spatial occurrences of colloform and disseminated ore in the Pine Point area should be examined.

2) Magnesium levels in Pine Point concentrates should be correlated with the proportion of disseminated ore which occurs in the mill feed.

3) Textural studies of "difficult" zinc ores from other Mississippi Valley-type deposits should be conducted in order to evaluate possible textural reasons for variable metallurgical performance.

4) Since sliming, entrainment and gangue flotation were

all found to be unimportant as gangue recovery mechanisms in laboratory test circuits, a study should be conducted in order to identify any aspects of plant layout or operations which could give rise to fine entrainment problems.

5) The possibility of separate treatment of fine and coarse size fractions should be examined. Removal of the fine size fractions could allow the use of shorter flotation times in the cleaners, and a possible increase in locked particle rejection. The fine-sized particles may be amenable to column flotation.

6) The effect of temperature as a factor in leach efficiency should be examined.

7) Fine Point zinc concentrates should be examined for the possible occurence of $Mg(OH)_2$ or other sparingly soluble magnesium precipitates.

8) The behaviour of zinc concentrates in post-leach flotation needs to be examined, with the goal of determining whether changes in recovery rates are caused by physical characteristics such as the specific gravity or viscosity of the water, or whether they are caused by chemical changes at the mineral surfaces. Acid leaching should be examined as a possible method of increasing flotation selectivity.

APPENDICES

APPENDIX 1

EXPERIMENTAL AND ANALYTICAL PROCEDURES

A1.1 Flotation Procedure

The following standard reagent addition rates and operating procedures were used for the locked cycle flotation test (LCFT) of Chapter 3 and for the entrainment test of Chapter 4:

Reagents:

The following reagents were added prior to grinding:

NaCN	10ml @ 2% per kg.	(0.2 kg/tonne)
$ZnSO_4$	20ml @ 10% per kg.	(2.0 kg/tonne)
Na_2CO_3	20ml @ 10% per kg.	(2.0 kg/tonne)

The addition rates of these reagents are higher than the amounts which are usually used at Pine Point, since the ore contained almost twice the metal content of the ore which is usually produced.

The ground pulp was conditioned for 10 minutes in the presence of the following reagents:

NaIPX	15ml @ 1% per kg.	(0.15 kg/tonne)
$CuSO_4$	15ml @ 10% per kg.	(1.50 kg/tonne)
MIBC	10ml @ 1% per kg.	(0.10 kg/tonne)
CaO	sufficient amount to raise pH to 10.0	

Operating Conditions:

During flotation the following conditions were maintained:

Air flow 3.0 litres per minute (4.0 in scavenger of LCFT)
Impeller speed 1000 R.P.M (1100 in scavenger of LCFT)
pH 10.0, maintained by periodic addition of CaO solution

A1.2 Special Procedures for Locked Cycle Test

Filtration:

The middlings which were generated during the LCFT generally contained large amounts of water and needed to be dewatered prior to recirculation. This was accomplished by vacuum-filtering the sample then re-pulping it in a lesser quantity of water using an ultrasonic bath. In a preliminary test no observable difference was seen between the flotation response of normal sphalerite feed and feed exposed to ultrasonic dispersion.

Acid Leaching:

The second cleaner concentrate from the LCFT was transferred to a plastic pail for leaching. The pulp was kept in suspension with a nylon-coated magnetic stirrer and 20ml of 30% H_2SO_4 was added (approximately 30 kg/tonne). The pulp was left for 90 minutes, after which 10% NaOH solution was used to

neutralize any remaining acid. At Pine Point liquid ammonia is used as a neutralizer; however, ammonia was found to be too obnoxious to use in an unvented laboratory experiment.

A1.3 Analytical Procedures

Analyses of flotation products were made by Atomic Absorption Spectroscopy. Samples of approximately 0.5 grams were dissolved in 10ml of hot concentrated nitric acid. The solutions thus produced were diluted down to a target concentration of approximately 5-10ppm prior to analysis. The concentrations of the samples were read from the absorption curves of a standard solution. The standard was prepared by dissolving 0.1 moles of $PbSO_4$, 0.2 moles of $ZnSO_4$, 0.2 moles of CaO, 0.2 moles of $FeSO_4$ and 0.1 moles of $MgSO_4$ in one litre of 5% nitric acid.

APPENDIX 2

CALCULATION OF MAXIMUM MAGNESIUM REMOVAL IN THE ACID LEACH

The leach which was situated between the second and third cleaners in the locked cycle test removed an unknown amount of magnesium from the second cleaner concentrate. This unknown amount of material affects the recalculated recoveries of magnesium in the rougher and in the first and second cleaners. An estimate of the effects of the acid leach upon the recalculated recoveries of magnesium can be made if it is assumed that:

1) Magnesium cannot be recovered more completely than zinc in any one size fraction of any one flotation stage.
2) The leaching rate of magnesium is inversely proportional to particle size.

Table A2.1 shows an approximate of the maximum amount of magnesium which may have been present in each size class of the second cleaner concentrate prior to leaching.

The first column of the table contains the recalculated recoveries of magnesium in the second cleaner (APPARENT RECOVERY). These recoveries cannot be higher than the recoveries of zinc (ZINC RECOVERY), listed in the second column of the table. If it is assumed that 100 magnesium units were observed in the second cleaner concentrate and tailings then the maximum possible amount of magnesium units which may

TABLE A2.1
MAXIMUM AMOUNT OF MG IN PRE-LEACH CLEANER 2 CONCENTRATE

MAXIMUM MG IN CLEANER 2 CON BASED UPON RECOVERY RATES

MESH SIZE	APPARENT RECOVERY	ZINC. RECOVERY	MAX MG IN CON	MAX % LEACHED
+200	95.27	98.60	333	71
+270	92.93	98.73	550	83
+400	87.60	98.73	964	91
+25UM	85.94	96.96	1086	94
+15UM	57.84	94.30	697	92
+10UM	25.38	82.24	346	93
-10UM	26.04	75.94	233	89

MAXIMUM MG IN CLEANER 2 CON BASED UPON LEACHING RATES

MESH SIZE	MAX % LEACHED	SIZE FACTOR	MAX% DISS	MAX MG IN CON	PERCENT CHANGE
+200	71	25	25	127	33
+270	83	35	35	143	54
+400	91	50	50	175	100
+25UM	94	71	71	227	245
+15UM	92	100	92	723	1150
+10UM	93	100	93	363	1329
-10UM	89	100	89	237	809

have been present in the concentrate prior to leaching is calculated as:

(1-Mg Rec.)/(1-Zn Rec.) - (1-Mg Rec.)

These calculations are shown as (MAX. MG IN CON). The difference between the (APPARENT RECOVERY) and the (MAX. MG IN CON) is equal to the maximum amount of magnesium units which could have been leached from the concentrate. This is converted to a percentage (MAX % LEACHED). The total magnesium units which were present in the second cleaner feed is equal to (MAX. MG IN CON) plus (100 - (APPARENT RECOVERY)).

A second constraint is applied to the calculations in order to comply with the principal that leaching is size-dependant. Ideally, there should be a lower size limit at which all magnesium is removed. At larger sizes the amount of magnesium which is removed from the concentrate should be inversely proportional to particle size. It can be observed in Table 7.26 that magnesium assays in the leached second cleaner concentrate rose in the size classes coarser than approximately 15um. It was therefore considered that 15um was the approximate size limit above which leaching rates should follow the (1/SIZE) progression. Assuming a maximum possible leaching rate of 100% in the +15um size class, the maximum leaching rates in the next four ascending size classes should be approximately 71%, 50%, 35% and 25%, respectively. The maximum leaching rates imposed by this second constraint are

presented as 'SIZE FACTORS' in the table.

The best estimate for the leaching rate of magnesium in the second cleaner is obtained by using the smaller of 'MAX % LEACHED' or the 'SIZE FACTOR' as the maximum percentage of magnesium removal from the concentrate. This is shown as 'MAX % DISSOLUTION' in the table, and represents the maximum possible percentage of magnesium removal in any ore size class which satisfies both constraints. The maximum possible percentage of dissolution can be used to calculate the 'MAX. MG IN CON' and the 'PERCENTAGE CHANGE' between the observed and the estimated results.

Table A2.2 presents an estimate of the effects of the leach upon the recalculated compositions of the rougher and the first cleaner concentrates. It is assumed that in any one size class 100 Mg units are found in the feed to any one flotation stage. For example, recovery of +200 mesh magnesium in the second cleaner was observed to be approximately 95%; therefore, 95 Mg units were found in the concentrate and 5 in the tailings. It was estimated that the actual amount of magnesium in the second cleaner concentrate could have been 33% higher than the amount which was observed (Table A2.1). Thus, the "real" amount of Mg units in the second cleaner concentrate could have been as high as (0.95 * 1.33), or 127. The maximum amount of magnesium which could have been present in the second cleaner tailings is equal to (100 - OBS. MG RECOVERY), or 5. Therefore, the magnesium assay in the +200

TABLE
A2.2

MG LEVELS IN CLEANER CONCENTRATES

SIZE	OBSERVED MAGNESIUM RECOVERY	EST. BEFORE LEACH	OBS. MG IN TAILS	TOTAL MG IN FEED	PERCENT CHANGE
	(CLNR2 CON)		(CLN2 TLS)	(CLN1 CON)	
+200	95	127.00	5	122	32
+270	93	143.00	7	150	50
+400	88	175.00	12	187	87
+25UM	66	227.00	34	261	161
+15UM	58	323.00	42	765	665
+10UM	25	362.00	75	438	338
-10UM	26	237.00	74	311	211
	CLNR1 CON)		(CLN1 TLS)	(RGHP CON)	
+200	76	100	24	124	24
+270	48	72	52	124	24
+400	32	60	68	128	28
+25UM	20	52	80	132	32
+15UM	27	207	73	280	180
+10UM	20	88	80	168	68
-10UM	12	37	88	125	25

TABLE **A2.3**

EFFECTS OF LEACH UPON RECALCULATED RECOVERIES & SEP. EFFICIENCIES

STREAM	SIZE	OBS MG REC	MAX MG REC	OBS SEP EFF	MIN SEP EFF
CLEANER3	+150	91.3	91.3	3.6	3.6
	+200	77.4	77.4	17.9	17.9
	+270	57.2	57.2	18.4	18.4
	+400	50.7	50.7	13.4	13.4
	+25UM	45.4	45.4	8.0	8.0
	+15UM	47.0	47.0	2.4	2.4
	+10UM	26.2	26.2	1.4	1.4
	-10UM	12.6	12.6	1.1	1.1
CLEANER2	+200	95.3	96.2	3.4	2.7
	+270	92.9	95.3	5.6	3.7
	+400	87.6	92.6	9.8	5.0
	+25UM	65.9	87.0	11.2	4.3
	+15UM	57.8	94.5	7.4	1.0
	+10UM	25.4	82.9	4.2	1.0
	-10UM	26.0	76.2	3.1	2.3
CLEANER1	+200	75.7	80.0	30.0	24.0
	+270	47.6	56.1	5.3	4.2
	+400	32.3	46.9	2.9	2.3
	+25UM	20.1	39.4	1.9	1.4
	+15UM	27.1	53.9	3.6	1.3
	+10UM	19.7	52.4	4.7	2.8
	-10UM	12.1	29.6	10.8	8.6

mesh fraction of the second cleaner feed (first cleaner concentrate) could have been as high as (127 + 5), or 32% higher than the calculated value. In a similar manner, since recovery of magnesium in the +200 mesh fraction of the first cleaner was calculated as 76%, the actual amount of magnesium in the first cleaner feed could have been as high as (76 * 1.32) + 24, or 124.

The effects of the leach are less as one progresses back through the circuit. The second cleaner concentrate assays may have differed from the recalculated values by 32%. This difference was 32% for the second cleaner feed (first cleaner concentrate) and 24% for the first cleaner feed (rougher concentrate).

The results presented in the two tables indicate that coarse (+400 mesh) magnesium assays may have been 32% to 100% higher than the recalculated assays in the second cleaner concentrate, 32% to 87% higher than the recalculated values in the second cleaner feed (first cleaner concentrate), and 24-28% higher than the recalculated values for the first cleaner feed (rougher concentrate). The assays of fine (-400 mesh) magnesium may have been 250% to 1300% higher than the recalculated values in the second cleaner concentrate, 100% to 650% higher than the recalculated values in the second cleaner feed (first cleaner concentrate), and 25% to 150% higher than the recalculated values in the first cleaner feed (rougher concentrate). These ranges represent the theoretical maximum

variations which could be experienced between the observed and actual magnesium assays. It is likely that the true variations were somewhat less.

The potential effect of the leach upon the assays of the cleaner concentrates has been shown to be high; however, the recoveries and separation efficiencies of magnesium in the cleaners are less affected by the leach than the recalculated assays of the cleaner concentrate streams. The leach lowers the observed magnesium recoveries and raises the observed separation efficiencies. The true recoveries of magnesium therefore fall between the observed recoveries and the theoretical maxima, while the true separation efficiencies fall between the observed separation efficiencies and the theoretical mimima. These ranges are summarized in Table A2.I.

The major conclusions which were made in the locked cycle test are as follows:

- Recoveries of magnesium are proportional to particle size in all cleaners.
- Separation efficiencies are higher at larger sizes.
- The performance of the third cleaner was superior to that of the first and second cleaners.

It can be seen that the validity of these conclusions is not affected by the acid leach.

APPENDIX I
PROGRAM LISTING FOR PARTICLE SECTIONING MODEL

```
1   REM ********************\
2   REM LOCKED PARTICLE     *
3   REM SECTION SIMULATION  *
4   REM                     *
5   REM                     *
6   REM ********************
7   REM
8   REM
9   REM
10  REM
20  REM ***************************
30  REM   INPUT VARIABLES
40  REM ***************************
50  REM
60  REM
70  GOTO 100
80  FOR L = 1 TO 1000
90  NEXT L
100  HOME : POKE 35,1
110  INPUT "INPUT THE STEP-RATE FOR VOLUME: ;DV
120  INPUT "INPUT THE SECTION SEPARATION: ";DX
130  INPUT "INPUT ROTATION INCREMENT: ";DQR
140  INPUT "INPUT SIZE OF OUTPUT MATRIX: ";MA
150  HOME
160  REM
170  REM
180  REM ************************
190  REM  VERIFY DATA
200  REM ***************************
210  REM
220  REM
230  POKE 35,2
240 C1 =  INT ((MA / DV) + 1E - 5) - (MA   DV): IF C
1    0 THEN  PRINT "M MUST BE A MULTIPLE OF dV": GOTO
 80
250 C2 =  INT ((1 / DX) + 1E - 5) - (1 / DX): IF C2
  0 THEN  PRINT "1/dX MUST BE AN INTEGER": GOTO 80
260 C3 =  INT ((1 / DQR) + 1E - 5) - (1 / DQR): IF C
3  0 THEN  PRINT "1/dQR MUST BE AN INTEGER": GOTO 8
0
270 C4 =  INT ((100 / MA) + 1E - 5) - (100 / MA): IF
 C4   0 THEN  PRINT "100/M MUST BE AN INTEGER": GOTO
 80
280  REM
290  REM
300  REM ************************
310  REM  SET UP INTERVALS
320  REM ************************
330  REM
```

```
340  REM
350 V0 = DV / 2:V1 = .5
360 X0 = DX / 2:X1 = 1 - (DX / 2)
370  REM
380  REM
390  REM ************************
400  REM SUMMARIZE CONDITIONS
410  REM  AND AFFROVE
420  REM ************************
430  REM
440  REM
450  GOSUB 2070
460  PRINT "IS THIS O.K.?";: GET A$: IF A$ = "N" THE
N  GOTO 80
470  REM
480  REM
490  REM ************************
500  REM  DIMENSION MATRIX
510  REM ************************
520  REM
530  REM
540  DIM M(MA + 1,MA + 1)
550  REM
560  REM
570  REM ************************
580  REM  SET VARIABLES
590  REM ************************
600  REM
610  REM
620 PI = 3.141592
630  DEF  FN A(X) =  ATN (((1 - (X   2))    .5) / X)
640 TC = (1 / DOR) * (1 / DV) * (1 / DX)
641 TV = 0
642 TX = 0
643 TQ = 0
650  REM
660  REM
670  REM ************************
680  REM INITIALIZE DISPLAY
690  REM ************************
700  REM
710  REM
720  GOSUB 2250
730  REM
740  REM
750  REM ************************
760  REM VOLUME LOOP
770  REM ************************
780  REM
790  REM
800  FOR V = VO TO V1 + 1E - 5 STEP DV
```

```
810  GOSUB 2250: REM *****PRINT
820 IN =  INT (MA * V) + 1
830  GOSUB 1920: REM *****CALC D
840 QD =  FN A(D)
850  GOSUB 2580: REM  *****PRINT
860  REM
870  REM
880  REM **********************
890  REM SECTION LOOP
900  REM **********************
910  REM
920  REM
930  FOR X = X0 TO X1 + 1E - 6 STEP D(
940  GOSUB 2130: REM  *****PRINT
950 QX =  FN A(X)
960  GOSUB 2440: REM *****PRINT
970 FPRIME =  COS (QX)
980  REM
990  REM
1000  REM **********************
1010  REM  FREE SECTIONS
1020  REM **********************
1030  REM
1040  REM
1050 C1 = QX - QD
1060 FO = C1:FG = 0: IF C1  0 THEN FO = 0:FG =  - 2
1
1070 C2 = 2 * QD: IF C1  0 THEN C2 = 2 * Q(:C1 =  A
BS (C1)
1080 LO = C2
1090 C3 = PI - C2 - C1
1100 FO = FO + C3
1110  REM
1120  REM
1130  REM **********************
1140  REM CONVERT RANGES TO #S
1150  REM **********************
1160  REM
1170  REM
1180 FG =  INT (((FG / PI) / DQR) + .5)
1190 FO =  INT (((FO / PI) / DQR) + .5)
1200  IF FG = 0 THEN  GOTO 1240
1210 Q0 = (DQR / 2) + (FG * DQR)
1220 Q1 = 1 - (DQR / 2) - (FO * DQR)
1230  GOTO 1270
1240 C1 =  INT (((C1 / PI) / DQR) + .5)
1250 C3 =  INT (((C3 / PI) / DQR) + .5)
1260 Q0 = ((DQR / 2) + (DQR * C1)):Q1 = (1 - (DQR /
2) - (C3 * DQR))
1270  GOSUB 2550: REM  *****PRINT
1280  GOSUB 2660: REM  *****PRINT
```

```
1290 M(IN,0) = M(IN,0) + FG
1300 M(IN,MA + 1) = M(IN,MA + 1) + FO
1310  REM
1320  REM
1330  REM ************************
1340  REM  START ROTATION LOOP
1350  REM ************************
1360  REM
1370  REM
1380 LS = 1 + ((Q1 - Q0) / DQR)
1390  IF Q0   Q1 THEN  GOTO 1820
1400  FOR QR = Q0 TO Q1 + 1E - 6 STEP DQR
1410  GOSUB 2770: REM *****PRINT
1420  GOSUB 2900: REM *****PRINT
1430  GOSUB 3000: REM *****PRINT
1440  REM
1450  REM
1460  REM ************************
1470  REM EVALUATE LOCUS PARTCLS
1480  REM ************************
1490  REM
1500  REM
1510 W = X *  COS (QR * PI)
1520 RPRIME =  SIN (QX)
1530 N1 = (D - W)     SIN (PI * QR)
1540 N1 =  ABS (N1)
1550 N = RPRIME - N1
1560 QN =  FN A((RPRIME - N) / RPRIME)
1570 Z = RPRIME *  SIN (QN)
1580 GANGUE = 1 - ((PI - QN) / PI) - (Z * (RPRIME -
N)) / (PI * RPRIME * RPRIME)
1590 GANGUE =  INT (99 * GANGUE + 1)
1600  IF W    D THEN GANGUE = 100 - GANGUE
1610  GOSUB 3700
1620  IF GANGUE   99 OR GANGUE   1 THEN  GOTO 9000
1630  REM
1640  REM
1650  REM ************************
1660  REM  UPDATE % COMPLETION
1670  REM  AND MATRIX
1680  REM ************************
1690  REM
1700  REM
1705 TQ = TQ + 1
1710  GOSUB 3370
1720 U1 =  INT ((GANGUE * MA) / 100) + 1
1730 M(IN,U1) = M(IN,U1) + 1
1740  REM
1750  REM
1760  REM ************************
1770  REM END OF LOOPS
```

```
1780  REM ************************
1790  REM
1800  REM
1810  NEXT QR
1815 TX = TX + 1
1820  NEXT X
1825 TV = TV + 1
1830  NEXT V
1840  GOTO 2750: REM     ****FINAL PRINT
1850  REM
1860  REM
1870  REM ************************
1880  REM   SBR TO CALC. "D"
1890  REM ************************
1900  REM
1910  REM
1920  REM  ROUTINE TO EVALUATE D
1930 D = 0.5
1940 AM = 0.25
1950 SU = (2 * D) - (D * D * D) + (4 * V) - 2
1960  IF  ABS (SU)    1E - 6 THEN  GOTO 1990
1970  IF SU    0 THEN D = D - AM:AM = AM / 2: GOTO 19
50
1980 D = D + AM:AM = AM / 2: GOTO 1950
1990  RETURN
2000  REM
2010  REM
2020  REM ************************
2030  REM SBR TO SHOW CONDITIONS
2040  REM ************************
2050  REM
2060  REM
2070  HOME : POKE 35,10
2080  PRINT 'SIMULATION CONSISTS OF:"
2090  PRINT
2100  PRINT MA;: POKE 36,4: PRINT " COMPOSITION INTE
RVALS"
2110  PRINT 1 / (MA * DV);: POKE 36,4: PRINT " PARTI
CLE COMPOSITIONS PER INTERVAL"
2120  PRINT 1    DX;: POKE 36,4: PRINT " SECTIONS PER
 PARTICLE"
2130  PRINT 1 / DQR;: POKE 36,4: PRINT " ROTATIONS P
ER SECTION"
2140  PRINT
2150  PRINT "TOTAL SIMULATIONS: ";(1    DV) * (1    DX
) * (1 / DQR)
2160  PRINT
2170  RETURN
2180  REM
2190  REM
2200  REM ************************
```

```
2210  REM  SET UP DISPLAY FORMAT
2220  REM **********************
2230  REM
2240  REM
2250  POKE 34,8: POKE 35,24: HOME : PRINT
2260  PRINT "GANGUE FRACTION :"
2270  PRINT "SECTION DISTANCE:"
2280  PRINT "ROTATION ANGLE  :"
2290  PRINT
2300  PRINT "% COMPLETION OF SIMULATION:"
2310  PRINT
2320  PRINT "FREE GANGUE:": PRINT "FREE ORE:": PRINT
 "LOCKED:                TOTAL:"
2330  PRINT : PRINT "          QX:         QD:"
2340  POKE 34,24
2350  RETURN
2360  REM
2370  REM
2380  REM **********************
2390  REM SBR TO PRINT QX
2400  REM **********************
2410  REM
2420  REM
2430  REM
2440 QX$ =  STR$ ( INT ((QX * 10000 + .5) / 10
0))
2450  POKE 1504, ASC ("."): POKE 1505, ASC ("0"): PO
KE 1506, ASC ("0")
2460  FOR K = 1 TO  LEN (QX$): POKE 1501 + K, ASC (
MID$ (QX$,K,1)): NEXT K
2470  RETURN
2480  REM
2490  REM
2500  REM **********************
2510  REM SBR PRINT FREE GNGUE
2520  REM **********************
2530  REM
2540  REM
2550 FG$ =  STR$ (FG)
2560  IF  LEN (FG$)   5 THEN FG$ = " " + FG$: GOTO 2
560
2570  FOR K = 1 TO  LEN (FG$): POKE 1972 + K, ASC (
MID$ (FG$,K,1)): NEXT K
2580  RETURN
2590  REM
2600  REM
2610  REM **********************
2620  REM SBR PRNT FREE ORE
2630  REM **********************
2640  REM
2650  REM
```

```
2660 FO$ =  STR$ (FO)
2670  IF  LEN (FO$)   5 THEN FO$ = " " + FO$: GOTO 2
670
2680  FOR I = 1 TO  LEN (FO$): POKE 1116 + I, ASC (
MID$ (FO$,I,1)): NEXT I
2690  RETURN
2700  REM
2710  REM
2720  REM **********************
2730  REM PRINT  AMOUNT LOCKED
2740  REM **********************
2750  REM
2760  REM
2770 LS =  (Q1 - Q0)   DQR + 1
2780 LS$ =  STR$ (LS)
2790  IF  LEN (LS$)   5 THEN LS$ = " " + LS$: GOTO 2
790
2800  FOR I = 1 TO 5: POKE 1244 + I, ASC ( MID$ (LS$
,I,1)): NEXT K
2810 TT$ =  STR$ (LS + FG + FO)
2820  RETURN
2830  REM
2840  REM
2850  REM **********************
2860  REM PRINT  TOTAL  SECTIONS
2870  REM **********************
2880  REM
2890  REM
2900  IF  LEN (TT$)   5 THEN TT$ = " " + TT$: GOTO 2
900
2910  FOR I = 1 TO 5: POKE 1260 + I, ASC ( MID$ (TT$
,K,1)): NEXT I
2920  RETURN
2930  REM
2940  REM
2950  REM **********************
2960  REM PRINT  QR
2970  REM **********************
2980  REM
2990  REM
3000 D1 =  INT ((QR * 180 / PI) + .5)
3010 D1$ =  STR$ (D1)
3020  IF  LEN (D1$)   3 THEN D1$ = "0" + D1$: GOTO 3
020
3030  POKE 1466, ASC (" ")
3040  FOR I = 1 TO 3: POKE 1466 + I, ASC ( MID$ (D1$
,K,1)): NEXT I
3050  RETURN
3060  REM
3070  REM
3080  REM **********************
```

```
3090  REM PRINT X
3100  REM **********************
3110  REM
3120  REM
3130 D2$ =  STR$ ( INT (1000 * X))
3140  IF  LEN (D2$)   3 THEN D2$ = "0" + D2$: GOTO 3
140
3150  POKE 1238,48
3160  FOR K = 1 TO 3: POKE 1238 + K, ASC ( MID$ (D2$
,K,1)): NEXT K
3170  RETURN
3180  REM
3190  REM
3200  REM **********************
3210  REM PRINT VOLUME% GANGUE
3220  REM **********************
3230  REM
3240  REM
3250 D3$ =  STR$ ( INT (1000 * V))
3260  IF  LEN (D3$)   3 THEN D3$ = "0" + D3$: GOTO 3
260
3270  POKE 1210,46
3280  FOR K = 1 TO 3: POKE 1210 + K, ASC ( MID$ (D3$
,K,1)): NEXT K
3290  RETURN
3300  REM
3310  REM
3320  REM **********************
3330  REM PRINT % COMPLETION
3340  REM **********************
3350  REM
3360  REM
3370 D5 = ((1 / DX) + (1 / DQ)) * TV + (1 / DQ) * TX
 + TQ
3411 D5 =  INT ((10000 * D5 / TC) + .5)
3430 D5$ =  STR$ (D5)
3440  IF  LEN (D5$)   4 THEN D5$ = " " + D5$: GOTO 3
440
3450  FOR K = 1 TO 3: POKE 1731 + K, ASC ( MID$ (D5$
,K,1)): NEXT K
3460  POKE 1734,46
3470  FOR K = 3 TO 4: POKE 1732 + K, ASC ( MID$ (D5$
,K,1)): NEXT K
3480  RETURN
3490  REM
3500  REM
3510  REM **********************
3520  REM SBR TO PRINT QD
3530  REM **********************
3540  REM
3550  REM
```

```
3560 QD$ =  STR$ ( INT ((QD * 10000 / PI) + .5) / 10
0)
3570  POKE 1515, ASC ("."): POKE 1516, ASC ("0"): PO
KE 1517, ASC ("0")
3580  FOR I = 1 TO  LEN (QD$): POKE 1512 + I, ASC (
MID$ (QD$,I,1)): NEXT I
3590  RETURN
3600  REM
3610  REM
3620  REM ************************
3670  REM SBF TO SHOW GANGUE%
3680  REM ****************************
3690  REM
3700 GANGUE$ =  STR$ (GANGUE)
3710  IF  LEN (GANGUE$)   3 THEN GANGUE$ = " " + GAN
GUE$: GOTO 3710
3720  FOR I = 1 TO 3
3730  POKE 1239 + I, ASC ( MID$ (GANGUE$,I,1) : NEXT
 I
3740  RETURN
3743  REM
3744  REM
3745  REM ************************
3746  REM FINAL PRINT ROUTINE
3747  REM ************************
3748  REM
3749  REM
3750  FOR X = 1 TO MA   2
3760  FOR Y = 0 TO MA + 1
3770 M(MA - X + 1,MA - Y + 1) = M(X,Y)
3780  NEXT Y
3790  NEXT X
3800  PR# 1
3810  POKE 34,0
3820  FOR X = 0 TO MA + 1
3830  FOR Y = 0 TO MA + 1
3840  PRINT M(X,Y);"  ";
3850  NEXT Y
3860  PRINT
3870  NEXT X
3880  PR# 0
3890  END

]RUN
```

REFERENCES

Agar, G.E., and Kipkie, W.B., Predicting Locked Cycle Flotation Results from Batch Data. CIM Bulletin, V.71, No. 799, p.119, Nov., 1978

Agar, G.E., Stratton-Crawley, R., and Bruce, T.J., Optimizing the Design of Flotation Circuits. CIM Bulletin, V.77, No.824, Dec. 1984

Baranger, W.A., Geolog. of the Lead-Zinc Deposits (Pine Point): North. Bimonthly Publication of the Northern Administration Branch, Dept. of Northern Affairs and National Resources, Ottawa, V.11, No.3, pp.18-22, 1964

Campbell, N., The Lead-Zinc Deposits of Pine Point. CIM Bulletin, V.59, No.652, pp.957-980, 1966

Campbell, N., Tectonics, Reefs and Stratiform Lead-Zinc Deposits of the Pine Point Area, Canada. Economic Geology, Monograph 3, pp.59-70, 1967

Cormodé, D.A., Reduction in Dolomite Contamination in Pine Point Zinc Concentrate. Proceedings of the 10th Annual Operators' Conference of the CMP Division of the CIM, pp.24-38, 1977

Dunsmore, H.E., Diagenetic Processes of Lead-Zinc Emplacement in Carbonates. IMM Trans. Sect. B, V.82, pp.168-173, 1973

Dutrizak, J.E., The End of Horizontal Zinc Retorting in the United States. CIM Bull., V.76, No.850, pp.99-101, 1983

Finkelstein, N.P., and Allison, S.A., The Chemistry of Activation, Deactivation and Depression in Flotation of Zinc Sulphide: A Review, in Flotation, A.M. Gaudin Memorial Volume, published by AIME, New York, V.1, pp.414-457, 1976

Frenay, J., Experimental Study of Sulphuric Acid Leaching of a Mangangese Carbonate Ore, Ind. Miner., V.3, No.77, pp.235-244, 1977

Fritz, P., The Oxygen and Carbon Isotopic Composition of Carbonates from the Pine Point Lead-Zinc Ore Deposits. Econ. Geol. , V.67, pp.451-471, 1969

Gerdemann, P.E., and Myers, W.E., Relationships of Carbonate Facies Patterns to Ore Genesis in the Southeast Missouri Lead District. Econ. Geol. , V.67, pp.420-433, 1972

Gorman, J.E., Fagel, R.F., and Nenninger, E.H., Preleaching Zinc Concentrates at Amax's Sauget Refinery. E/MJ , pp.65-69, Aug. 1976.

Jackson, S.A. and Folinsbee, R.E., The Pine Point Lead-Zinc Deposits, N.W.T., Canada. Introduction to the Paleoecology of the Presqu'ile Reef. Econ. Geol. , V.64, No.7, pp.711-717, 1969

Jones, R.E., Circuit Consolidation at Pine Point Mines Ltd., Pine Point, N.W.T., Proceedings of the 15th Annual Operators' Conference of the CMP Division of the CIM , pp.261-277, 1982

McLimans, R.K., Barnes, H.L. and Ohmoto, H., Sphalerite Stratigraphy of the Upper Mississippi Valley, Zinc-Lead District, Southwest Wisconsin, Econ. Geol. , V.67, No.3, pp351-361, 1980

Roedder, E. The Non-Colloform Origin of "Colloform" Textures Sphalerite Ores. Econ. Geol , V.67, pp.451-471, 1968

Roedder, E., and Dwornik, E.J., Sphalerite Color Banding: Lack of Correlation with Iron Content, Pine Point, N.W.T., Canada. Am. Miner. , V.53, pp.1523-1529, 1968

Schweitzer, A., Beneficial Results Obtained Applying a Zinc Regrind at the Magmont Concentrator, Mining Engineering , V.35, No.4, pp.354-356, Apr. 1983

Small, H., The Paleoenvironment of the Pine Point Lead-Zinc District, Econ. Geol. , V.70, pp27-47, 1975

Sverjensky, D.A., The Origin of a Mississippi Valley-Type Deposit in the Vibernum Trend, S.E. Missouri, Econ. Geol. , V.76, pp.1848-1872, 1981

Trahar, W.J., A Rational Interpretation of the Role of Particle Size in Flotation, Int. J. Miner. Process., V.8, pp.289-327, 1981